

**A COMPREHENSIVE EXPERIMENTAL AND  
COMPUTATIONAL ANALYSIS OF PRESSURE DROP  
IN PIPES AND FITTINGS**

**BORU VE BAĞLANTILARDA ÇOK AMAÇLI  
DENEYSEL VE HESAPLAMALI BASINÇ DÜŞÜMÜ  
ANALİZİ**

**VEDA DUMAN**

A THESIS OF MASTER OF SCIENCE  
Prepared in the NUCLEAR ENGINEERING DEPARTMENT  
According To Regulations of  
The Institute for Graduate Studies in Pure and Applied Sciences of  
Hacettepe University

2010

To the Directory of the Institute for Graduate Studies in Science and Engineering.

This study has been accepted as a thesis for the degree of **MASTER OF SCIENCE in NUCLEAR ENERGY ENGINEERING** by our Examining Committee.

Head :.....  
Assoc. Prof. Dr. C. Niyazi Sökmen

Advisor :.....  
Asst. Prof. Dr. Şule Ergün

Member :.....  
Assoc. Prof. Dr. Murat Köksal

Member :.....  
Assoc. Prof. Dr. C. Ayhan Yilmazer

Member :.....  
Asst. Prof. Dr. Cemil Kocar

This is to certify that the Board of Directors of the Institute for Graduate Studies in Science and Engineering has approved this thesis on ...../...../.....

Prof. Dr. Adil DENİZLİ  
Director  
The Institute for Graduate Studies  
in Science and Engineering

# **A COMPREHENSIVE EXPERIMENTAL AND COMPUTATIONAL ANALYSIS OF PRESSURE DROP IN PIPES AND FITTINGS**

**Veda Duman**

## **ABSTRACT**

The objectives of this thesis are to design and construct an experimental setup which includes basic fluid mechanics applications, to conduct and simulate the associated experiments. The constructed experimental setup will be used in the undergraduate education at the lab sessions of the Thermal-Hydraulics Laboratory. Hence, preparation of the experiment manuals will be used in the lab sessions is also an aim of this study. In the design and sizing of the setup, FLOWNEX which is a computational fluid dynamics (CFD) code for macro systems was used. Moreover, RELAP which is a best estimate code was used to simulate the experiments performed in this study.

The experimental data was obtained and compared with similar data available in literature. The results of the experiments are consistent with the literature. The results of the RELAP simulations were obtained and compared with the experimental data. The results of the RELAP simulations are in good agreement with the experimental results.

As an important result of this study, experience on experimental methods was gained for further research projects.

**Keywords:** Flow in pipes, Hydraulic loss coefficient, Friction factor, Parallel Flow, FLOWNEX, RELAP

# **BORU VE BAĞLANTILARDA ÇOK AMAÇLI DENEYSEL VE HESAPLAMALI BASINÇ DÜŞÜMÜ ANALİZİ**

**Veda Duman**

## **ÖZ**

Bu tezin amaçları, temel akışkanlar mekaniği uygulamalarını içeren bir deney düzeneğinin tasarımını yapmak ve bu deney düzeneğini oluşturmak, ilgili deneyleri yapmak ve bu deneyleri bilgisayar yazılımları ile modellemektir. Oluşturulan deney düzeneği, lisans eğitiminde yer almak üzere Isıl-Akışkanlar Mekaniği Laboratuvarı'nda kullanılacaktır. Bu sebeple, bu çalışmanın bir diğer amacı da laboratuvar da kullanılacak deney föylerinin hazırlanmasıdır. Deney düzeneğinin tasarımında ve boyutlandırılmasında makro sistemler için hesaplamalı akışkanlar dinamiği (HAD) kodu olan FLOWNEX kodu kullanılmıştır. Buna ek olarak, deneylerin modellemeleri nükleer güç santrallerinin modellenmesinde kullanılan RELAP kodu ile yapılmıştır.

Yapılan deneylerin sonuçları literatürdeki verilerle kıyaslanmıştır. Deney sonuçları literatür ile uyumludur. RELAP ile yapılan modellemelerin sonuçları ise deney sonuçları ile kıyaslanmıştır. Modelleme sonuçları deneysel sonuçlar ile uyum içerisindedir.

Bu çalışmanın önemli bir sonucu olarak gelecekte yapılacak olan deneysel çalışmalar için deneyim kazanılmıştır.

**Anahtar Kelimeler:** Borularda akış, hidrolik kayıp katsayısı, sürtünme katsayısı, paralel akış, FLOWEX, RELAP

## **ACKNOWLEDGMENT**

I would like to express my sincere gratitude to my dear advisor, Asst. Prof. Dr. Şule Ergün for the continuous support of my MS thesis, for her patience, motivation, and enthusiasm. Her guidance helped me not only in all time of laboratory work and writing of this thesis, but also in all the hardest times the last two years. I could not have imagined having a better advisor and mentor for my MS study.

In the second place, I would like to thank Assoc. Prof. Dr. C. Niyazi Sökmen for his innovative ideas for setup design and analysis. This work cannot be finished without his invaluable contributions.

I also would like to thank the rest of my thesis committee: Assoc. Prof. Dr. Murat Köksal, Assoc. Prof. Dr. Ayhan Yilmazer and Asst. Prof. Dr. Cemil Kocar, for their encouragement and insightful comments.

I thank my family: my parents Eda and Kenan Duman and my dear sister Sevda Duman Yalçın for supporting me throughout my life.

Last but not the least; I would like to thank my friend Mehmet Türkmen and all members of Nuclear Engineering Department of Hacettepe University.

# CONTENTS

|  | <u>Page</u> |
|--|-------------|
| ABSTRACT.....  | i           |
| ÖZ.....  | ii          |
| ACKNOWLEDGMENTS.....   | iii         |
| CONTENTS.....  | iv          |
| LIST OF FIGURES.....   | viii        |
| LIST OF TABLES.....  | x           |
| 1. INTRODUCTION .....  | 1           |
| 2. THEORETICAL BACKGROUND .....  | 4           |
| 2.1. FLOW IN PIPES.....  | 4           |
| 2.1.1. Entrance of Pipe .....  | 9           |
| 2.1.2. Laminar Flow .....  | 10          |
| 2.1.3. Transient Flow .....  | 15          |
| 2.1.4. Turbulent Flow .....  | 16          |
| 2.2. MACROSCOPIC BALANCES FOR ISOTHERMAL SYSTEMS .....                     | 20          |
| 2.2.1. The Macroscopic Mass Balance .....                                  | 21          |
| 2.2.2. The Macroscopic Momentum Balance.....                               | 21          |
| 2.2.3. The Macroscopic Mechanical Energy Balance (Bernoulli Equation)..... | 22          |
| 2.3. LOSS COEFFICIENTS .....   | 24          |
| 2.3.1. Hydraulics of Loss Coefficients.....                                | 24          |
| 2.3.2. Estimation of Friction Losses.....                                  | 25          |
| 2.3.3. Flow through Valves .....   | 28          |
| 2.3.4. Flow through Elbows .....   | 29          |
| 2.3.5. Flow through C-Shape Bend.....                                      | 31          |
| 2.3.6. Flow through S-Shape Bend.....                                      | 32          |
| 2.3.7. Flow through Enlarging Pipes .....                                  | 33          |
| 2.4. FLOW THROUGH PARALLEL PIPES .....                                     | 35          |
| 2.5. MAIN COMPONENTS OF FLOW IN PIPES .....                                | 36          |
| 2.5.1. Pumps .....   | 36          |
| 2.5.2. Valves [8].....   | 40          |

|        |  |    |
|--------|--|----|
| 2.6.   | MEASUREMENT TECHNIQUES .....   | 41 |
| 2.6.1. | Flow Rate Measurement.....   | 41 |
| 2.6.2. | Pressure Measurement .....   | 44 |
| 2.6.3. | Calibration of Measurement Devices .....   | 46 |
| 2.7.   | DATA ACQUISITION SYSTEMS (DAQs) .....  | 47 |
| 2.7.1. | Data Logger .....  | 47 |
| 2.7.2. | Data Acquisition.....  | 48 |
| 3.     | DESIGN OF THE EXPERIMENTAL SET UP .....  | 50 |
| 3.1.   | SIMULATIONS WITH FLOWNEX .....   | 52 |
| 3.1.1. | Section 1.....   | 55 |
| 3.1.2. | Section 2.....   | 55 |
| 3.1.3. | Section 3.....   | 56 |
| 3.2.   | PRESSURE DROP CALCULATION CODE (MATHEMATICA) .....   | 57 |
| 3.3.   | PUMP.....  | 58 |
| 3.3.1. | Selection of Pump.....   | 58 |
| 3.3.2. | Specifications of the Selected Pump .....  | 60 |
| 3.4.   | DIMENSIONS OF THE SET UP.....  | 64 |
| 3.5.   | SELECTION OF THE MEASUREMENT TECHNIQUES.....   | 65 |
| 4.     | EXPERIMENTAL SET UP .....  | 66 |
| 4.1.   | GENERAL LAYOUT .....   | 66 |
| 4.1.1. | Section 1: Determination of Friction Factor for Flow in Straight Pipes ....                | 67 |
| 4.1.2. | Section 2: Analysis of the Parallel Flow .....   | 68 |
| 4.1.3. | Section 3: Determination of the Hydraulic Loss Coefficient for Fittings...68               |    |
| 4.2.   | FLUID PROPERTIES .....   | 68 |
| 4.3.   | PRESSURE DROP MEASUREMENT POINTS .....   | 69 |
| 4.4.   | DATA ACQUISITION DEVICE: LABJACK .....   | 70 |
| 4.5.   | COMPUTER PROGRAM FOR CONTROL OF THE PUMP AND<br>DISPLAYING THE MEASUREMENTS: PROFILAB..... | 73 |
| 4.5.1. | The Use of the Software Application.....   | 73 |
| 5.     | PROCEDURES OF MEASUREMENTS AND ANALYSES .....  | 79 |
| 5.1.   | FLOW RATE MEASUREMENT PROCEDURES .....   | 79 |
| 5.1.1. | Measurements with the Magnetic Flow Meter.....   | 79 |
| 5.1.2. | Measurements with the Water Meter .....  | 80 |

|        |   |     |
|--------|---|-----|
| 5.2.   | PRESSURE DROP MEASUREMENT PROCEDURES.....                         | 80  |
| 5.2.1. | Description of Experiments in Section 1 .....                     | 81  |
| 5.2.2. | Description of Experiments in Section 2 .....                     | 81  |
| 5.2.3. | Description of Experiments in Section 3 .....                     | 82  |
| 5.3.   | RELAP ANALYSES.....   | 83  |
| 5.4.   | REPEATABILITY ANALYSES.....                                       | 84  |
| 6.     | DATA AND RESULTS .....  | 88  |
| 6.1.   | FLOW RATE MEASUREMENT.....  | 88  |
| 6.1.1. | Measurement with Magnetic Flow Meter .....                        | 88  |
| 6.1.2. | Measurement with Water Meter.....                                 | 89  |
| 6.2.   | PRESSURE DROP MEASUREMENT .....                                   | 90  |
| 6.2.1. | Section 1.....  | 90  |
| 6.2.2. | Section 2.....  | 95  |
| 6.2.3. | Section 3.....  | 99  |
| 6.3.   | RELAP SIMULATIONS OF TEST SECTIONS.....                           | 105 |
| 6.3.1. | Section 1.....  | 105 |
| 6.3.2. | Section 2.....  | 108 |
| 6.3.3. | Section 3.....  | 109 |
| 6.4.   | EXPERIMENT MANUALS.....   | 112 |
| 7.     | CONCLUSIONS .....   | 113 |
|        | REFERENCES.....   | 115 |
|        | APPENDIX .....  | 1   |
|        | APPENDIX A. FLOWNEX [16] .....                                    | 1   |
|        | A.1. GENERAL INFORMATION.....                                     | 1   |
|        | A.1.1. Solver Properties .....                                    | 1   |
|        | A.1.2. List of applications that can be modeled with FLOWNEX..... | 2   |
|        | A.1.3. Fluids in FLOWNEX .....                                    | 2   |
|        | A.1.4. Components in FLOWNEX.....                                 | 2   |
|        | A.1.5. Advanced heat transfer capabilities of FLOWNEX .....       | 3   |
|        | A.2. GOVERNING EQUATIONS.....                                     | 3   |
|        | A.2.1. Mass Equation in FLOWNEX (1-Dimensional) .....             | 5   |
|        | A.2.2. Momentum Equation in FLOWNEX (1-Dimensional).....          | 5   |
|        | A.2.3. Energy Equation in FLOWNEX (1-Dimensional) .....           | 6   |



APPENDIX B. RELAP (Reactor Excursion and Leak Analysis Program) [17] .....8

    B.1. GENERAL INFORMATION.....8

    B.2. GOVERNING EQUATIONS .....9

        B.2.1. Mass Equation in RELAP .....10

        B.2.2. Momentum Equation in RELAP .....10

        B.2.3. Energy Equation in RELAP .....12

APPENDIX C. THE MEASUREMENT ERROR ANALYSIS .....13

APPENDIX D. THE EXPERIMENT MANUALS .....17

    D.1. MANUAL FOR EXPERIMENT #1 .....17

    D.2. MANUAL FOR EXPERIMENT #2 .....25

    D.3. MANUAL FOR EXPERIMENT #3 .....32

    D.4. MANUAL FOR EXPERIMENT #4 .....42

## LIST OF FIGURES

|   |    |
|---|----|
| Figure 2.1. Reynolds experiment.....  | 6  |
| Figure 2.2. Fluid flows in a vertical pipe .....  | 8  |
| Figure 2.3. Two adjoining layers of a fluid .....   | 8  |
| Figure 2.4. Flow at the pipe entrance .....   | 9  |
| Figure 2.5. Entrance region, fully developed flow in a pipe system .....  | 10 |
| Figure 2.6. Laminar flow in a circular pipe .....   | 11 |
| Figure 2.7. Flow through a vertical pipe .....  | 12 |
| Figure 2.8. The results of measurements which present laminar, transient and turbulent flow transitions <b>[4, Figure 8.11]</b> ..... | 16 |
| Figure 2.9. The behaviors of laminar and turbulent flow.....  | 17 |
| Figure 2.10. Parts of fluid velocity .....  | 18 |
| Figure 2.11. Typical turbulent flow velocity profile .....  | 20 |
| Figure 2.12. Macroscopic flow system .....  | 21 |
| Figure 2.13. The Moody Chart - Friction factor as a function of Reynolds number and relative roughness <b>[4]</b> .....               | 27 |
| Figure 2.14. Well rounded, flanged, 90 <sup>0</sup> elbow (up) .....  | 29 |
| Figure 2.15. Hydraulic loss coefficients for the 90 <sup>0</sup> elbow (up) <b>[10]</b> .....   | 30 |
| Figure 2.16. Well rounded, flanged 90 <sup>0</sup> elbow (down).....  | 30 |
| Figure 2.17. Hydraulic loss coefficients for 90 <sup>0</sup> elbows (down).....   | 31 |
| Figure 2.18. C-shape bend.....  | 31 |
| Figure 2.19. Hydraulic loss coefficients for C-shape bend.....  | 32 |
| Figure 2.20. S-shape bend.....  | 32 |
| Figure 2.21. Hydraulic loss coefficients for S-shape bend.....  | 33 |
| Figure 2.22. Flow in Slowly Enlarging Pipes.....  | 33 |
| Figure 2.23. Flow through parallel pipes .....  | 35 |
| Figure 2.24. Classification of pumps <b>[8]</b> .....   | 36 |
| Figure 2.25. Multi-jet flow meter .....   | 43 |
| Figure 2.26. Magnetic flow meter .....  | 43 |
| Figure 2.27. Working principle of magnetic flow meter .....   | 44 |
| Figure 2.28. Bourdon Gauge .....  | 45 |
| Figure 2.29. Differential pressure transmitter (DP cell) <b>[11]</b> .....  | 46 |
| Figure 2.30. Pressure transducer .....  | 46 |
| Figure 2.31. Data Acquisition Process .....   | 49 |
| Figure 3.1. Model design of the setup .....   | 51 |
| Figure 3.2. The modeling pump in early simulations with FLOWNEX .....   | 54 |
| Figure 3.3. The modeling with the pump defined in FLOWNEX component library....   | 54 |
| Figure 3.4. FLOWNEX simulation of section 1 .....   | 55 |
| Figure 3.5. FLOWNEX simulation of section 2 .....   | 56 |
| Figure 3.6. FLOWNEX simulation of section 3 .....   | 57 |
| Figure 3.7. Pressure drop over the set-up.....  | 59 |
| Figure 3.8. System curves of the set-up.....  | 60 |
| Figure 3.9. Pump used in the setup <b>[13]</b> .....  | 61 |
| Figure 3.10. Structure of the pump used <b>[13]</b> .....   | 61 |
| Figure 3.11. Pump head vs Flow rate <b>[13]</b> .....   | 62 |

|  |     |
|--|-----|
| Figure 3.12. Net Positive Suction Head of Pump vs Flow rate [13]   | 63  |
| Figure 3.13. Shaft Power of Pump vs Flow rate [13]   | 63  |
| Figure 3.14. Dimensions of the Experimental Setup  | 64  |
| Figure 4.1. The experimental setup for basic fluid mechanics applications  | 67  |
| Figure 4.2. Pressure drop measurement points   | 69  |
| Figure 4.3. Data acquisition box (Lab Jack) [14]   | 71  |
| Figure 4.4. General view of software   | 74  |
| Figure 4.5. Pump run techniques: constant volumetric flow rate & manually control                                  | 76  |
| Figure 4.6. The calibration constants window   | 76  |
| Figure 4.7. I/O Window   | 77  |
| Figure 5.1. Repeatability of friction factor determination (copper pipe)   | 85  |
| Figure 5.2. Repeatability of hydraulic loss coefficient of elbow (down)  | 86  |
| Figure 5.3. Repeatability of contraction coefficient   | 87  |
| Figure 6.1. Magnetic Flow Meter: Volumetric Flow rate vs Pump RPM  | 88  |
| Figure 6.2. Magnetic Flow Meter: Volumetric Flow rate vs Pump Outlet Pressure                                      | 89  |
| Figure 6.3. Water Meter: Volumetric Flow rate vs Pump RPM  | 90  |
| Figure 6.4. Water Meter: Volumetric Flow rate vs Pump Outlet Pressure  | 90  |
| Figure 6.5. Section 1: Friction factor of the stainless steel pipe   | 92  |
| Figure 6.6. Section 1: Friction factor of the copper pipe  | 93  |
| Figure 6.7. Section 1: Friction factor of the PVC pipe   | 94  |
| Figure 6.8. Friction Factor Chart  | 95  |
| Figure 6.9. Estimated total volumetric flow rate for parallel flow sampling 1                                      | 97  |
| Figure 6.10. Fractional volumetric flow rates in branches for sampling 1   | 97  |
| Figure 6.11. Estimated total volumetric flow rate for parallel flow sampling 2                                     | 98  |
| Figure 6.12. Fractional volumetric flow rates in branches for sampling 2   | 99  |
| Figure 6.13. Hydraulic loss coefficients of the 90° elbow (up)   | 100 |
| Figure 6.14. Hydraulic loss coefficients of the 90° elbow (up) (cont.)   | 101 |
| Figure 6.15. Hydraulic loss coefficients for 90° elbow (down)  | 102 |
| Figure 6.16. Hydraulic loss coefficients of C-shape bend   | 102 |
| Figure 6.17. Hydraulic loss coefficients of S-shape bend   | 103 |
| Figure 6.18. Expansion coefficients of gradually enlarging pipe  | 104 |
| Figure 6.19. Hydraulic loss coefficients of gate valve   | 104 |
| Figure 6.20. Results of RELAP analyses for the estimation of friction factor of the stainless steel pipe           | 106 |
| Figure 6.21. Results of RELAP analyses for the estimation of friction factor of the copper pipe                    | 107 |
| Figure 6.22. Results of RELAP analyses for the estimation of friction factor of the PVC pipe                       | 108 |
| Figure 6.23. Estimated total volumetric flow rate (RELAP)  | 108 |
| Figure 6.24. Results of RELAP analyses for the hydraulic loss coefficient determination of the 90° elbow (down)    | 109 |
| Figure 6.25. Results of RELAP analyses for the hydraulic loss coefficient determination of the 90° elbow (up)      | 110 |
| Figure 6.26. Results of RELAP analyses for the hydraulic loss coefficient determination of the gradual enlargement | 111 |
| Figure C.1. Percentage errors in flow rate measurement [12]  | 14  |

## LIST OF TABLES

|  |    |
|--|----|
| Table 2.1. Comparison of Laminar and Turbulent Flows .....                                   | 17 |
| Table 2.2. Terms of the Macroscopic Mechanical Energy Balance Equation .....                 | 22 |
| Table 2.3. Expansion coefficients for $\frac{D}{d} = 2, \theta = 60^\circ$ <b>[10]</b> ..... | 34 |
| Table 2.4. Classification of Flow Meters .....   | 42 |
| Table 3.1. FLOWNEX components .....  | 53 |
| Table 3.2. Technical specifications of pump <b>[13]</b> .....                                | 62 |
| Table 3.3. Length and internal diameter of pipes .....                                       | 65 |
| Table 4.1. Water properties .....  | 68 |
| Table 4.2. Measurement points, locations and purpose of measurement .....                    | 70 |
| Table 4.3. DAQ Specifications .....  | 72 |
| Table 4.4. Displays and sources of data .....  | 74 |
| Table 5.1. Properties of the differential pressure measuring equipments .....                | 80 |
| Table 5.2. Experiments selected for RELAP analyses .....                                     | 83 |
| Table 6.1. Roughness of the pipes .....  | 94 |
| Table C.1. Measurement errors of the DP cells .....  | 13 |

## 1. INTRODUCTION

The laboratory applications are important and essential parts of the engineering education. They provide opportunity of the unbounded observations about the nature behind the theories. Since the early years of the engineering education, the experimental studies have great importance [20]. Experiments can be performed in education laboratories for several reasons such as to confirm a theory, to teach measurement methods and etc. [21]. In addition to educational purposes, one of the most important roles of the experiments is introducing new theories. Although computer simulations have been used to model physical applications, they are limited for estimation of the real world because they have developed by using number of assumptions. Hence, for the verification of these simulation codes, performing experiments is needed.

In this study, an experimental setup of basic fluid mechanics applications was designed, constructed and the associated experiments were performed and finally these experiments were simulated. For design and sizing of the setup, FLOWNEX, which is a system computational fluid dynamics (CFD) code, was used. The experiments were simulated by using RELAP (Reactor Leak and Excursion Program) which is a best estimate code used to simulate nuclear power plants .

The first step of this study was designing an experimental setup of the basic fluid mechanics experiments. Design process began with the selection of the applications which were going to be taken into consideration in this study. First of all, observation on the hydraulic losses on flow through pipes was chosen as the basic theme of this study. The basic hydraulic loss mechanisms such as friction losses, losses on bends, valves and branches were included in the experimental setup. In addition to hydraulic loss mechanisms, a section was added to the setup for the observation of the parallel flow. Second of all, various pressure and flow rate measurement techniques were decided to use. Theoretical information about hydraulic losses in pipe flow and measurement techniques is given in Chapter 2.

In Chapter 3, the details of the designing of the experimental setup were explained. Once the experiments that would be performed were determined, the pipe materials were selected. Since stainless steel is widely used material in nuclear power plants, it was used in the setup as a pipe material. Moreover, for the friction loss experiments copper and PVC pipes were also used.

For sizing of the setup FLOWNEX analyses were performed. Determination of the size of the components such as pump and determination of the dimensions of the pipes were bounded to each other. Thus, sizing of the setup was completed by following an iterative method. As explained in Chapter 3, FLOWNEX simulations were performed for the setup and appropriate flow rate values stated and then sizing of the pump was completed with the help of another computer code which was developed for this study by using Mathematica code.

The measurement techniques were chosen when the sizing of the setup was completed. By using the estimated flow rate and pressure drop values, the appropriate measurement techniques were stated. Magnetic flow meter and a multi-jet flow meter were chosen for flow rate measurements while differential pressure cells and bourdon type manometer were chosen for pressure measurements. Eventually, the setup was built when the measurement techniques had been selected.

In Chapter 4, the details of the experimental setup are given. The setup has three main sections. Each section has a different aim and covers different theory. In the first section, friction losses on a straight pipe can be investigated for three different pipes which are stainless steel, copper and PVC pipes. In the second section, experiments on parallel flow can be performed. In the third, experiments on estimation of the hydraulic loss coefficients for various fittings can be conducted.

The measurement procedures for the experiments, RELAP analyses and repeatability analyses were explained in Chapter 5. The measurement procedures can be divided into two categories according to the measured identity. The categories are flow rate measurement and pressure drop measurement. The experiments performed in each section of the setup are defined in this chapter, also.

The data obtained from the experiments, results obtained from analyses and simulations are presented in Chapter 6 while Chapter 7 is the conclusion part. Detailed information about FLOWNEX and RELAP are given in Appendices A and B, respectively. Finally, the measurement error analyses are explained in Appendix C and experiment manuals prepared for the lab sessions of the Thermal Hydraulics Laboratory are given in Appendix D.

## 2. THEORETICAL BACKGROUND

### 2.1. FLOW IN PIPES

Flow in pipes is a varied and fascinating subject. Although the simpler cases of flow in pipes are well understood, there are many complicated cases which still have to be researched. The study of flow in pipes is not important only to understand the physical and mechanical phenomena but also it has a practical importance. Pipe flow forms in nuclear facilities as in other fields of industry. Pipes lie all around a nuclear facility and pipe flow has a significant role in heat exchangers. So it is important to understand hydraulic and mechanical properties of flow in pipes.

The material which flows in a pipe can be a gas or a liquid. Not only gas or liquid materials but solid materials can be carried in pipes with the help of them as well. In the case of steady or slowly varying flow, liquid generally is assumed to be incompressible while in surge situations the compressibility of the liquid has to be taken into account and also the pipe elasticity. Conveying of solid materials in pipe is more complicated than of gas or liquid. Solid materials can be conveyed in pipes by pulverization and support by air or a liquid. In general, liquid is forced to flow in pipes by using a fan or a pump. Pipe systems include a number of pipes connected to each other by fittings or elbows, valves to adjust the flow rate and pumps to supply pressure required to circulate liquid in the system. [1]

When the fluid flows into a pipe, some forces become effective on the fluid. The major forces acting on the fluid are pressure forces, forces acted by system components, gravitational force and viscous friction forces. One of the most important events occurring because of fluid motion into the pipe is pressure drop across the pipe. Pressure drop across the pipe strongly depends on the friction between fluid and the pipe wall.

Analytical solutions for fluid flow in pipes depend on principles of continuity, conservation of linear momentum and conservation of energy. Analytical solutions of pipe flow give compatible results with experiments only for limited cases such as fully-developed laminar flow. Experimental data and empirical correlations become



significant for other flow types. Although same conditions are tried to be provided for two experiments, results of these experiments cannot be perfectly identical. As a result of this fact, it must be accepted that the calculations of some identities by using empirical correlations will have error of almost 10 percent. This is a standard value for calculations with empirical correlations. [2]

Measuring the velocity of fluid in a pipe is important for further calculations. To achieve this, velocity profile is tried to be obtained first. In a pipe, velocity is zero at pipe wall and it reaches to its maximum value at the center of the pipe. Due to the fact that velocity varies through the cross section of the pipe, average velocity is used for the calculations. Average velocity can be determined by the principle of conservation of mass as follows:

$$\dot{m} = \rho V_{avg} A = \int \rho u(r) dA \quad (2.1)$$

In this equation,  $\dot{m}$ ,  $\rho$ ,  $V_{avg}$ ,  $A$  and  $u(r)$  are total mass flow rate, density of fluid, average velocity of fluid, cross-sectional area of pipe and velocity profile of the fluid in the circular pipe.

Determination of fluid properties is also important for calculations. If there is no heat source in the system, fluid properties can be assumed constant. Although there is no heat source in the system, friction between pipe and fluid may cause small increase in temperature. This increase does not affect the calculations significantly, so it can be neglected.

In literature there are two main kinds of flow defined. In the early 1880's Osborne Reynolds (1842-1912) showed nature of the two types of flow clearly by his experiments. His experiment depends on observation and he used very simple experimental set-up to demonstrate flow types. Briefly, his experiment set-up contains a straight circular glass tube with smoothly rounded, flared inlet was placed in a large tank which is also glass and filled with water. The other inlet is placed through the end of the tank. Water flow rate at the outlet of the tank is controlled by a valve at the end. He fixed glass tube to keep the level at the surface constant. A highly colored solution

coming from a small reservoir is discharged into the inlet of glass tube. Schematic representation of experiment is given in Figure 2.1.

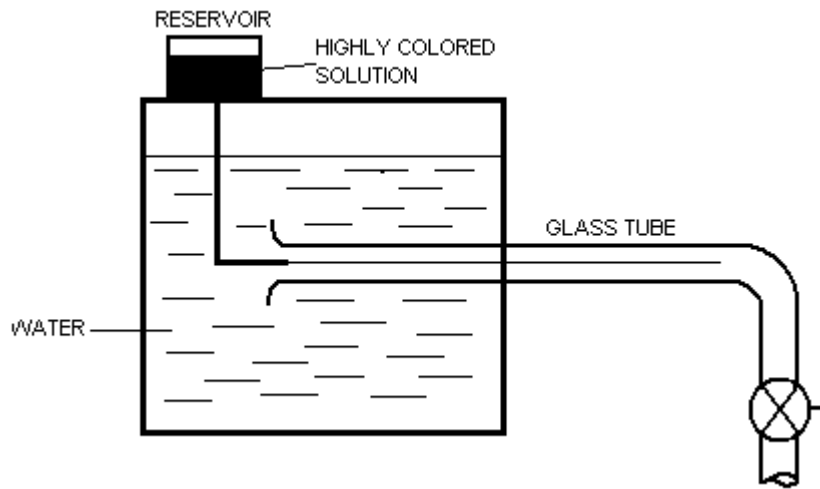


Figure 2.1. Reynolds experiment

Fluid entered the tube through tube center. Reynolds observed behavior of stream along the tube by changing the flow rate of the fluid. He defined Reynolds Number and concluded his experiments that flow type depends on a critical value of Reynolds Number. At the lower values of this number, flow is **laminar** and at the higher values flow is **turbulent**. [3]

The flow is in the form of straight lines in laminar flow, and it shows a chaotic behavior in turbulent case. In addition to laminar and turbulent flow types there is also transition flow in which flow does not completely show chaotic behavior but it is not in the form of straight lines either.

Reynolds defined a dimensionless number, still called with his name even one century has passed since the definition and it is used to determine the type of flow. Reynolds Number is defined as;

$$Re = \frac{\rho V_{avg} D}{\mu} \quad (2.2)$$

In this equation,  $\rho$ ,  $V_{avg}$ ,  $D$  and  $\mu$  are the density of fluid, average velocity of fluid in the pipe, circular pipe diameter and dynamic viscosity of fluid, respectively. In other words, Reynolds number is the ratio of inertia force to the viscous force. Reynolds number is dimensionless so it's a general representation to determine the flow type for any fluid or any pipe or any systems.

Reynolds number is main identifier of the flow type. Reynolds number includes both velocity of fluid and the viscosity term. Velocity is not adequate information to determine the flow type, since flow type also varies with the fluidity of the fluid.

According to the Reynolds' experiments, following Reynolds number ranges were determined to define the flow types [4]:

$$\begin{cases} \text{Re} < 2300 & \text{Laminar Flow} \\ 2300 \leq \text{Re} \leq 4000 & \text{Transient Flow} \\ \text{Re} \geq 4000 & \text{Turbulent Flow} \end{cases}$$

Viscosity of a fluid is generally defined as the fluidity of fluids. This term is used to demonstrate the behavior of the fluids through flow. Water and oil are good examples to explain the nature of this term. These two fluids have almost same density values; however their flow behaviors are different. The difference is due to the shear stress occurring between the fluid particles and it is represented with Greek symbol,  $\tau$ .

Figure 2.2 represents the vertical flow in a pipe. The velocity of the fluid is given with  $u$  and it varies with distance  $y$ . The curve in the figure is used to present velocity profile. The velocity gradient in  $-y$  direction can be given with  $\partial u / \partial y$ .

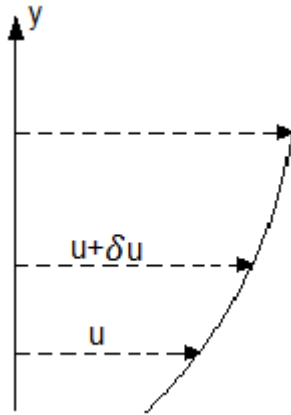


Figure 2.2. Fluid flows in a vertical pipe

If fluid motion is analyzed with closer view then motion of two adjoining layers of fluid can be identified as given in Figure 2.3.

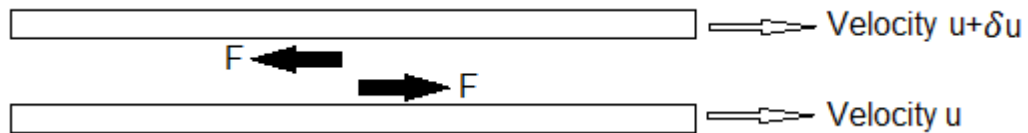


Figure 2.3. Two adjoining layers of a fluid

Newton postulated that, for the straight and parallel motion of a given fluid, the tangential stress between two adjoining layers is proportional to the velocity gradient in a direction perpendicular to the layers [3]. This information can be summarized with Eq.2.3.

$$\tau = \frac{F}{A} = \mu \frac{\partial u}{\partial y} \quad (2.3)$$

The proportionality constant is defined as absolute or dynamic viscosity. It is a property of the fluid and a scalar quantity. The actual value of viscosity varies with from fluid to fluid and with temperature.

( $\tau$  =shearing stress,  $\partial u/\partial y$  =velocity gradient,  $\mu$  = dynamic viscosity)

### 2.1.1. Entrance of Pipe

When fluid suddenly flows into the pipe, velocity profile of fluid is disturbed at the pipe entrance because of shear forces near the pipe wall. Due to the no slip boundary condition at the pipe wall, velocity of flow particles touching to the pipe wall is almost zero. Moreover, friction between fluid layers cause decrease in velocity of other layers with the effect of layer near the pipe wall. The volume passing through every section of pipe per unit time is same so velocities of layers near the axis of the pipe increase.

[1]. Figure 2.4 shows the velocity profile at the entrance of the pipe.

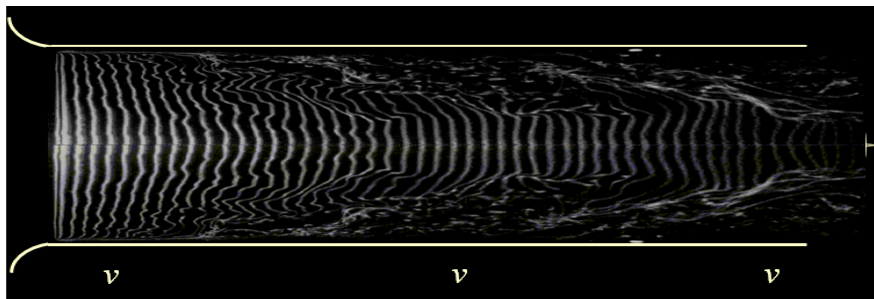


Figure 2.4. Flow at the pipe entrance

At this point, another important definition is “boundary layer”. This term represents a boundary in which viscous effects are important. Boundary layer has an imaginary boundary surface from which viscous effects lose their importance, friction forces are negligible and velocity profile does not change with the distance along the pipe. The boundary layer has grown in thickness until pipe is completely filled. [1]

Figure 2.5 represents the development of flow through a pipe from inlet to the length at which flow becomes fully developed. The entrance region, shown in figure, flow is also known as *developing flow*. The flow after the entrance region is called *fully developed flow*. In fully developed flow, flow is simpler to describe than is in the developing flow because velocity is a function of only the distance from the pipe centerline. In case of a change in pipe characteristics, such as a change in pipe diameter or geometry, flow is no more fully developed, it is developing flow.

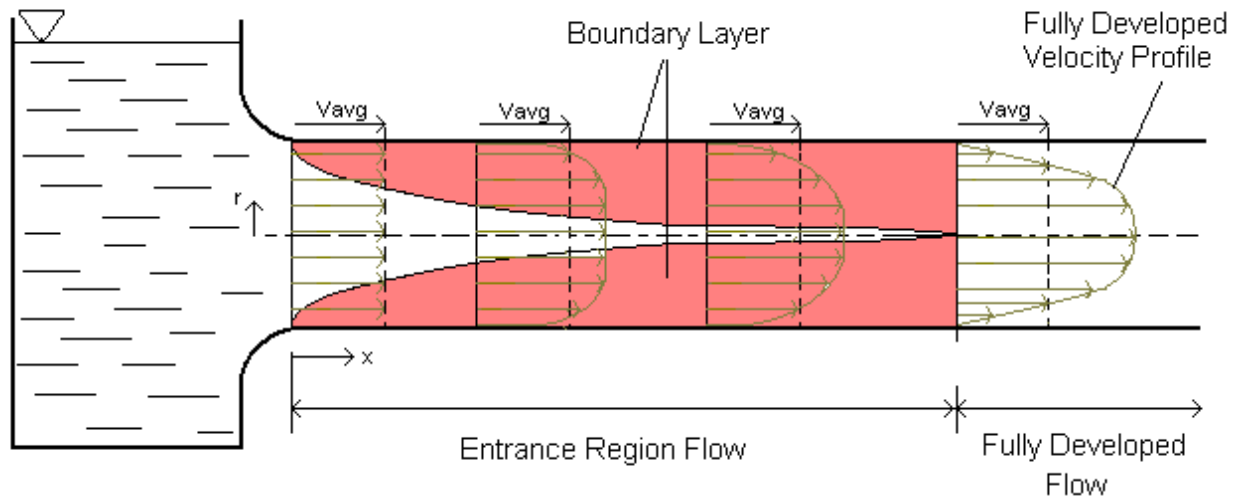


Figure 2.5. Entrance region, fully developed flow in a pipe system

The shape of the velocity profile and length of the entrance region depend on the flow type. In laminar fully developed flow, velocity profile of fluid is parabola.

In the case of laminar flow, typical length of entrance region is defined as [5];

$$\frac{l_e}{D} = 0.06 Re \quad (2.4)$$

In the case of turbulent flow, typical length of entrance region is defined as [5];

$$\frac{l_e}{D} = 4.4 Re^{1/6} \quad (2.5)$$

The entrance length in turbulent flow is smaller than is in laminar flow and its dependency on Reynolds number is quite less. In practice, entrance effects are assumed to become negligible at a distance from the entrance which is about 10 times bigger than the pipe diameter for commercial pipes.

### 2.1.2. Laminar Flow

As discussed earlier, type of flow is dependent on Reynolds Number. As the results of Reynolds' experiments, when the flow's Reynolds Number is smaller than 2300, its type is called as "Laminar Flow". The main characteristic of laminar flow is that the streamlines are straight lines which are parallel to the pipe axis. A representation of

laminar flow in the horizontal pipe with a length at which the entrance effects can be negligible is given with Figure 2.6.

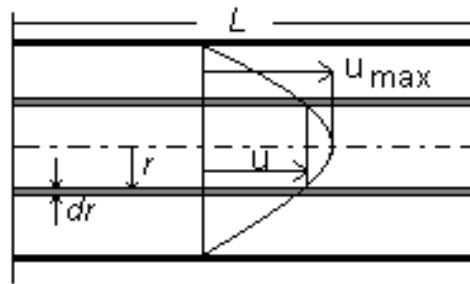


Figure 2.6. Laminar flow in a circular pipe

In fully developed flow region, the velocity profile is same at any cross-section of the pipe. It is possible to derive equations for velocity profile for fully developed steady laminar flow if fluid is incompressible (constant  $\rho$ ). The velocity profile can be determined by conservation of momentum and law of continuity. By this way, a relationship between friction factor and velocity profile and pressure drop and losses can be determined using this information.

Consider the momentum balance for flow in a vertical circular pipe. A thin shell of fluid as shown in Figure 2.7 is selected with a thickness of  $\Delta r$  and the length of  $L$ . Flow direction is positive in  $z$  direction. **[6]**

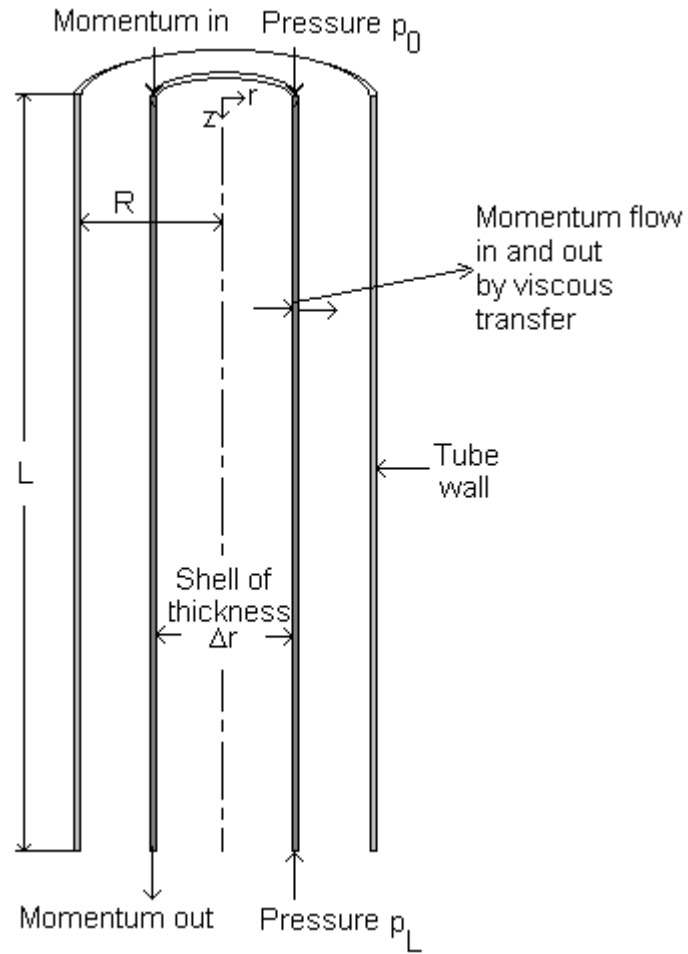


Figure 2.7. Flow through a vertical pipe

Thus, momentum balance in z-direction can be written as follows:

$$\left\{ \begin{array}{c} \text{rate of momentum in} \\ \text{flow area} \end{array} \right\} - \left\{ \begin{array}{c} \text{rate of momentum out} \\ \text{flow area} \end{array} \right\} = 0$$

**Contributors of rate of momentum in flow area:**

- at  $r$  :  $(2\pi r L \tau_{rz})|_r$
- at  $z=0$  :  $(2\pi r \Delta r v_z)|_{z=0}$  ( $v_z$  is the velocity at z-direction)
- gravity force acting on shell :  $(2\pi r \Delta r L) p_0$
- pressure force acting on  $z=0$  :  $(2\pi r \Delta r L) p_0$



- pressure force acting on  $z=L$  :  $(2\pi r\Delta r)p_L$

**Contributors of rate of momentum out flow area:**

- at  $r+\Delta r$  :  $(2\pi rL\tau_{rz})|_{r+\Delta r}$
- at  $z=L$  :  $(2\pi r\Delta r v_z)(\rho v_z)|_{z=L}$

**Momentum Balance [6]:**

$$(2\pi rL\tau_{rz})|_r - (2\pi rL\tau_{rz})|_{r+\Delta r} + (2\pi r\Delta r v_z)(\rho v_z)|_{z=0} - (2\pi r\Delta r v_z)(\rho v_z)|_{z=L} + (2\pi r\Delta rL)\rho g - (2\pi\Delta r)p_L = 0 \quad (2.6)$$

Velocity profile is known steady and fluid is incompressible, balance equation will be in the form of:

$$2\pi L[(r\tau_{rz})|_r - (r\tau_{rz})|_{r+\Delta r}] + 2\pi r\Delta rL\rho g + 2\pi r\Delta r(p_0 - p_L) = 0 \quad (2.7)$$

If Eq.2.7 is arranged then Eq.2.8 can be obtained.

$$\frac{(r\tau_{rz})|_{r+\Delta r} - (r\tau_{rz})|_r}{\Delta r} = \left( \frac{p_0 - p_L}{L} + \rho g \right) r \quad (2.8)$$

If the limit of both sides as  $\Delta r \rightarrow 0$  is taken, final form of the momentum balance equation is:

$$\frac{d}{dr}(r\tau_{rz}) = \left( \frac{p_0 - p_L}{L} + \rho g \right) r \quad (2.9)$$

or

$$\frac{d}{dr}(r\tau_{rz}) = \left( \frac{P_0 - P_L}{L} \right) r \quad (2.10)$$

where  $P = p - \rho gz$ .

Integration of both sides gives:

$$\tau_{rz} = \left( \frac{P_0 - P_L}{2L} \right) r + \frac{C}{r} \quad (2.11)$$

C must be equal to zero since  $\tau_{rz}$  must be finite.

$$\tau_{rz} = \left( \frac{P_0 - P_L}{2L} \right) r \quad (2.12)$$

Due to the Newton's law of viscosity definition of shear stress in this situation is

$$\tau_{rz} = -\mu \frac{dv_z}{dr} \quad (2.13)$$

The negative sign comes from the nature of the flow which the velocity decreases from the pipe centerline to the pipe wall. If we put Eq.2.13 into 2.12 following equation will be obtained.

$$\frac{dv_z}{dr} = - \left( \frac{P_0 - P_L}{2\mu L} \right) r \quad (2.14)$$

The velocity distribution is to be determined easily from above equation.

$$v_z = \left( \frac{P_0 - P_L}{4\mu L} \right) r^2 + C_1 \quad (2.15)$$

By applying the boundary condition,  $v_z = 0$  at  $r = R$  :

$$v_z = \frac{(P_0 - P_L)R^2}{4\mu L} \left[ 1 - \left( \frac{r}{R} \right)^2 \right] \quad (2.16)$$

If velocity profile is known then maximum velocity in the pipe, average velocity in the pipe or volume flow rate in the pipe is to be determined. The maximum velocity is at the center of the pipe where  $r=0$ :

$$v_{z,\max} = \frac{(P_0 - P_L)R^2}{4\mu L} \quad (2.17)$$

Especially average velocity in the pipe has a quite importance and can be determined as follows:

$$\langle v_z \rangle = \frac{\int_0^{2\pi} \int_0^R v_z r dr d\theta}{\int_0^{2\pi} \int_0^R r dr d\theta} = \frac{(P_0 - P_L)R^2}{8\mu L} = \frac{v_{z,\max}}{2} \quad (2.18)$$

Average velocity of fluid is always equal to the half of the maximum velocity if flow is laminar. [6]

### 2.1.3. Transient Flow

As the velocity of fluid is increased, laminar flow begins to disturb and transition to turbulence occurs. But if water is replaced with honey and large enough pressure is provided to reach the same velocity with water, it will be observed that flow type is still laminar. Viscosity of honey is higher than of water.

When transition point is tried to be identified, Reynolds number is the constraint. If Reynolds number is below the value of 2300, flow is always laminar. If the experiments conducted as pipes are smooth and there are no disturbances to the velocity higher values of Reynolds number can be obtained for transition to turbulence. Besides, for every flow which has a Reynolds number smaller than 2300 flow type is laminar even it is disturbed. Transition begins at some point but not end immediately and complete turbulent flow cannot be seen at this point. Because of some mechanical and thermal-hydraulic factors, including the surface roughness, heat transfer, vibration, noise and other disturbances transient flow is observed over a range of Reynolds numbers. This range begins at 2300 and ends at approximately 4000. This region is called as the transient region. [1]

Figure 2.8 shows the transition from laminar to turbulent flow with the change in Reynolds number and as time changes in flow measurement. As figure represents, when Reynolds number is between 2000 and 4000, the Reynolds number changes with velocity at a slower rate, through the transitional region. [4]

While Reynolds number exceeds the value of 2300, intermittent spots or bursts of turbulence appear. As the Reynolds number increase, the entire flow field becomes turbulent and remains turbulent as long as the Reynolds number is greater than 4000.

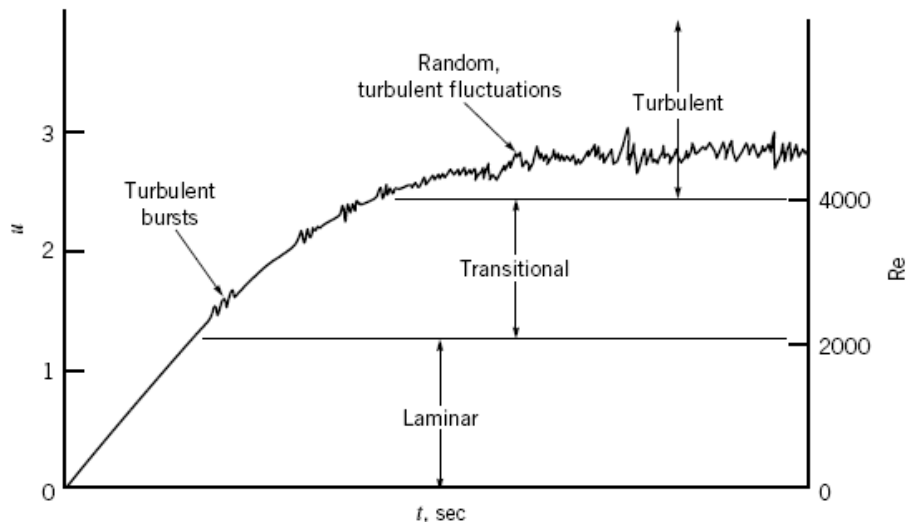


Figure 2.8. The results of measurements which present laminar, transient and turbulent flow transitions [4, Figure 8.11]

#### 2.1.4. Turbulent Flow

Nature of the turbulent flow is irregular and random. Flow shows chaotic behavior in this region. The characteristics of important properties of the flow such as pressure drop depends on the existence of fluctuations and randomness indicated. Although it is hard to analyze, turbulent flow is desirable in some situations. For example, there are heat exchangers in nuclear power plants. Heat exchangers are needed to be modeled with enormous dimensions to cover up the losses in heat transfer if the flow would be laminar [1]. The turbulent fluctuations create additional momentum and energy transfer mechanisms. Figure 2.9 shows the behavior of laminar and turbulent flow. The left hand side of the figure shows the straight behavior of laminar flow and the chaotic behavior of the turbulent flow.

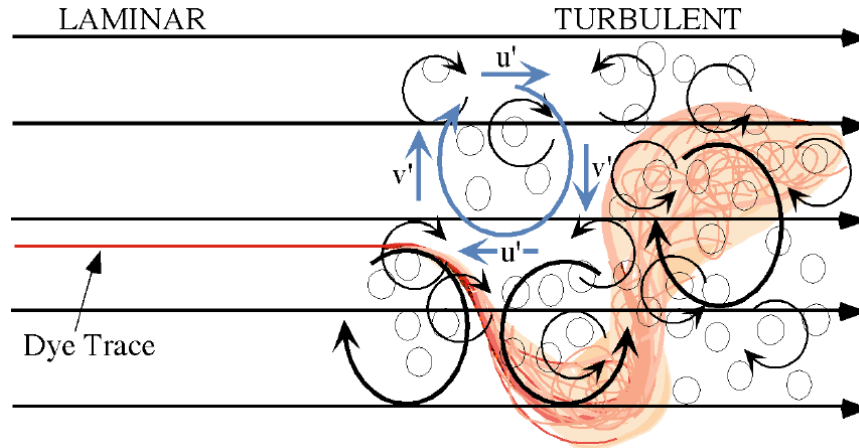


Figure 2.9. The behaviors of laminar and turbulent flow

In Table 2.1, the basic differences between laminar and turbulent flow are represented. Velocity profiles, mean velocities and pressure drop characteristics of two flow types are compared.

Table 2.1. Comparison of Laminar and Turbulent Flows

| <b>Fully Developed Laminar Flow</b>  | <b>Fully Developed Turbulent flow</b>  |
|--|--|
| <ul style="list-style-type: none"> <li>• Velocity profile is invariably parabolic</li> <li>• <math>\frac{\bar{u}}{u_{\max}} = 0.5</math> (always)</li> <li>• The slope of velocity profile at surface is much smaller under same conditions.</li> <li>• As mean velocity increases the resistance to flow is slightly increases.</li> <li>• The resistance is less sensitive to roughness of the pipe</li> <li>• The pressure drop per unit length is less than turbulent flow.</li> </ul> | <ul style="list-style-type: none"> <li>• Velocity profile is not completely independent of Reynolds number</li> <li>• <math>\frac{\bar{u}}{u_{\max}}</math> is about 0.8 to 0.82 for very large Reynolds number values.</li> <li>• The slope of velocity profile at surface is much greater under same conditions.</li> <li>• As mean velocity increases, the resistance to flow is increases more rapidly.</li> <li>• The resistance is more sensitive to roughness of the pipe</li> <li>• As a result the pressure drop per unit length is greater.</li> </ul> |

Velocity of fluid in turbulent region is three-dimensional because of fluid particle rotations and also time dependence. In this case, velocity of fluid is assumed having two parts. First part of velocity is the mean part and second one is the fluctuating part. The longitudinal velocity  $u(t)$  and the vertical velocity  $v(t)$  can be formulated as follows:

$$u(t) = \bar{u} + u' \quad (2.19)$$

$$v(t) = \bar{v} + v' \quad (2.20)$$

$\bar{u}$  is the mean velocity and it is defined as time averaged form of the instantaneous velocity.  $u'$  is the fluctuating part of the velocity. All components of the velocity are presented in Figure 2.10.

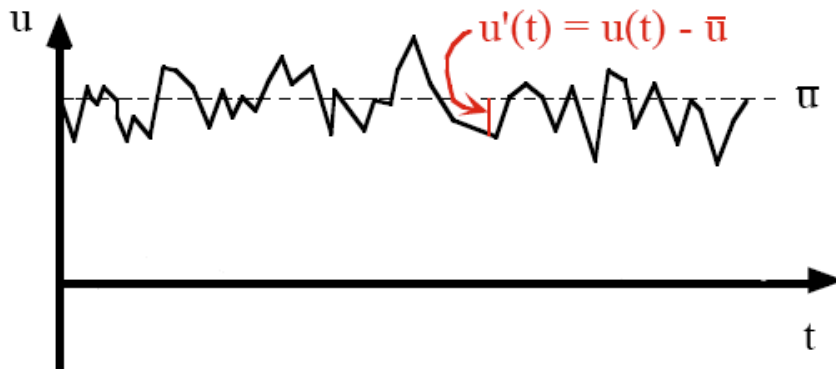


Figure 2.10. Parts of fluid velocity

Average value of fluctuating part is zero. Chaotic motion of fluid particles plays an important role on pressure drop and these motions are taken into account in the average velocity for analyses.

Shear stress also has a turbulence component. According to the definition of shear stress, its representation for horizontal pipe flow is given with Eq. 2.21.

$$\tau = \mu \frac{d\bar{u}}{dx} \quad (2.21)$$

Experimental studies show that actual value of shear stress is greater than the value obtained by using Eq.2.21. The turbulence fluctuations cause this difference. As a result shear stress is the sum of two components as follows [6]:

$$\tau = \tau_{lam} + \tau_{turb} \quad (2.22)$$

The turbulent shear stress is defined as

$$\tau_{turb} = -\rho \overline{u'v'} \quad (2.23)$$

Turbulent shear stress is always greater than zero. This term is also called as Reynolds stress. Experiments showed that the laminar shear stress is dominant in the region very near the pipe wall. In contrast, turbulent shear stress is 100 to 1000 times greater than the laminar shear stress in the region away from the wall. The accurate modeling of turbulent flow is strongly depends on accurate modeling of turbulent shear stress.

Another way to analyze the turbulent flow is using eddy viscosity term which is dependent on turbulent flow conditions and also position in the pipe. By using eddy viscosity, turbulent shear stress can be formulated with Eq.2.24.

$$\tau_{turb} = \rho l_m^2 \left( \frac{d\bar{u}}{dy} \right)^2 \quad (2.24)$$

$l_m$ , is the mixing length and defined as the length of the distance between two regions with two different velocities. Determination of  $l_m$  is quite complicated since varies from region to region.

Turbulent velocity profile cannot be obtained by integrating the force balance equation because of the lack of accurate prediction of the shear stress. Determination of turbulent velocity profile is based on both empiric and experimental analyses. A typical velocity profile in turbulent flow is given in Figure 2.11.

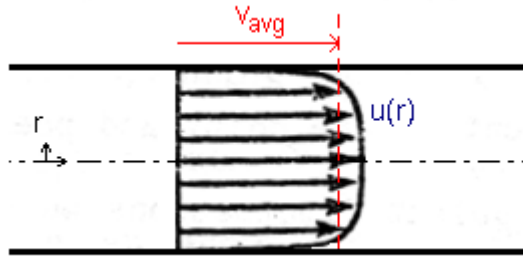


Figure 2.11. Typical turbulent flow velocity profile

A number of semi-empirical formulas exist but the most often-used and relatively easy to use correlation is the empirical power law velocity profile. [6]

$$\frac{\bar{u}}{V_c} = \left(1 - \frac{r}{R}\right)^{\frac{1}{n}} \quad (2.25)$$

where  $V_c$  is the centerline velocity, and  $n$  is an empirical constant which is a function of Reynolds number. The one-seventh power law ( $n=7$ ) is the most reasonable approximation for many practical flows. [6]

## 2.2. MACROSCOPIC BALANCES FOR ISOTHERMAL SYSTEMS

Analyzing the macroscopic balances of flow systems is required to size experimental setups and to model and investigate the flow behavior. Therefore macroscopic balances are performed in this study. The macroscopic balances can be written for the flow systems and the balance between the inlet and the outlet is determined. Moreover, they are widely used in the analysis of engineering flow systems. The derivation of macroscopic balances of mass, momentum and mechanical energy is presented in this section. Figure 2.12 represents the flow system for which the balance equations are derived.



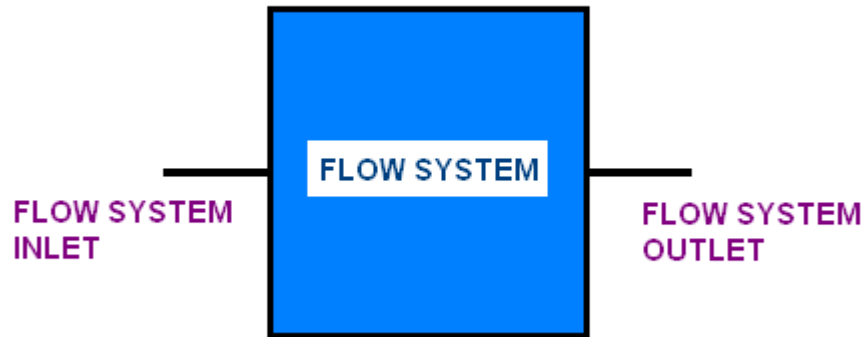


Figure 2.12. Macroscopic flow system

### 2.2.1. The Macroscopic Mass Balance

Mass balance in macroscopic flow systems based on the fact that the mass entering to the system is equal to the mass leaving the system. This conclusion can be reached by writing the conservation of mass equation. [6]

$$\frac{d}{dt} m_{\text{total}} = \rho_{\text{in}} \langle \bar{v}_{\text{in}} \rangle S_{\text{in}} - \rho_{\text{out}} \langle \bar{v}_{\text{out}} \rangle S_{\text{out}} \quad (2.26)$$

Here  $\rho$  is density,  $\bar{v}$  is average velocity and  $S$  is the flow area of the pipe. Product of those three identities gives the definition of mass flow rate.

If flow is in steady state condition which means that the total mass of flow does not change with time, then left-hand side of the Eq.2.26 is zero. In conclusion, mass flow rate at the inlet is equal to the one at the outlet.

### 2.2.2. The Macroscopic Momentum Balance

The conservation of momentum equation is also derived for this system. [6]

$$\frac{\partial}{\partial t} P_{\text{total}} = \rho_{\text{in}} \langle \bar{v}_{\text{in}}^2 \rangle S_{\text{in}} - \rho_{\text{out}} \langle \bar{v}_{\text{out}}^2 \rangle S_{\text{out}} + \{ p_{\text{in}} S_{\text{in}} - p_{\text{out}} S_{\text{out}} \} - \{ F \} + \{ m_{\text{total}} g \} \quad (2.27)$$

First two terms on the right-hand side of the Eq.2.27 represent the rate of momentum influx and efflux by virtue of the bulk-fluid motion. The third term is the difference

between pressure forces acting at inlet and outlet, respectively. Fourth term,  $-\{F\}$ , is the net force acting on fluid applied by solid surface. Final term is the gravity.

If flow system is at steady state force condition then steady state momentum balance can be rewritten as in Eq.2.28.

$$F = \rho_{in} \langle \overline{v_{in}^2} \rangle S_{in} - \rho_{out} \langle \overline{v_{out}^2} \rangle S_{out} + \{p_{in} S_{in} - p_{out} S_{out}\} + \{m_{total} g\}$$

(2.28)

### 2.2.3. The Macroscopic Mechanical Energy Balance (Bernoulli Equation)

The general form of the energy balance equation for a stationary volume element through which fluid flows is represented as follows [6]:

$$\frac{\partial}{\partial t} \left( \frac{1}{2} \rho v^2 \right) = - \left( \nabla \cdot \frac{1}{2} \rho v^2 v \right) - (\nabla \cdot \rho v) - p(-\nabla \cdot v) - (\nabla \cdot [\tau \cdot v]) - (-\tau : \nabla v) + \rho(v \cdot g) \quad (2.29)$$

The terms used in Eq.2.29 are defined in the Table 2.2.

Table 2.2. Terms of the Macroscopic Mechanical Energy Balance Equation

|                        |                            |   |
|------------------------|----------------------------|---|
| <b>Left –hand side</b> |                            | Rate of increase in kinetic energy per unit volume              |
| <b>Right-hand side</b> | <i>1<sup>st</sup> term</i> | Net rate of input of kinetic energy by virtue of bulk flow      |
|                        | <i>2<sup>nd</sup> term</i> | Rate of work done by pressure of surroundings on volume element |
|                        | <i>3<sup>d</sup> term</i>  | Rate of irreversible conversion to internal energy              |
|                        | <i>4<sup>th</sup> term</i> | Rate of work done by viscous forces on volume element           |
|                        | <i>5<sup>th</sup> term</i> | Rate of irreversible conversion to internal energy              |
|                        | <i>6<sup>th</sup> term</i> | Rate of work done by gravity force on volume element            |

This equation is integrated over volume and written for steady and incompressible flow system. [6]

$$\Delta \frac{1}{2} \langle \bar{v} \rangle^2 + g\Delta h + \left( \frac{P_{out} - P_{in}}{\rho} \right) + \frac{W}{\dot{m}} + \frac{E_v}{\dot{m}} = 0 \quad (2.30)$$

Where  $\dot{m}$  is the mass flow rate,  $g\Delta h$  is gravitational force acting on the system,  $W$  is the rate at which the system performs mechanical work on its surroundings and  $E_v$  is the total loss from resistance to flow. This equation is also known as Bernoulli equation when  $W$  and  $E_v$  are equal to zero.

In consideration of this thesis, definition of  $E_v$  has a great importance.  $E_v$  has two components in practical applications. First component is the total loss on all sections of straight conduits and second one is the total loss on all fittings, valves and etc. The equation given above is frequently used for the turbulent flow calculations in a system composed of various kinds of piping and additional resistances such as our experimental set-up. Eq.2.30 can be represented in a form of pressure difference along the system. The total pressure difference due to the total loss on system can be defined as in Eq.2.31. [6]

$$\Delta p = \rho g \left( \sum_i \left( \frac{1}{2g} \langle \bar{v} \rangle^2 \frac{L}{D} f \right)_i + \sum_i \left( \frac{1}{2g} \langle \bar{v} \rangle^2 e_v \right)_i \right) \quad (2.31)$$

$f$  is the friction factor and  $e_v$  is the hydraulic loss coefficient. They will be discussed in the following section.

The mechanical balance equation is important for the system design especially the pump sizing. By analyzing system gains and losses, system requirements can be determined.

## 2.3. LOSS COEFFICIENTS

### 2.3.1. Hydraulics of Loss Coefficients

The pressure loss coefficient of fittings,  $K$ , is defined with the Darcy equation (Eq.2.32),

$$K = \frac{h_f}{V^2/2g} \quad (2.32)$$

$K$  is the loss coefficient,  $h_f$  is the fitting head loss,  $V$  is the average upstream velocity at the inlet of the fitting and  $g$  is the gravitational acceleration. The head loss of a fitting is to be determined by using the Bernoulli's equation between two points of fitting at which we want to determine the losses. General form of Bernoulli equation for horizontal (no elevation change) fittings can be written as follows:

$$\frac{P_1}{\gamma} + \frac{V_1^2}{2g} = \frac{P_2}{\gamma} + \frac{V_2^2}{2g} + \sum_i \frac{f_i L_i}{D_i} \frac{V_i^2}{2g} + h_f \quad (2.33)$$

$P$  is the pressure,  $\gamma$  is the specific weight which is defined as weight per unit volume and its relation with density is given as;

$$\gamma = \rho g \quad (2.34)$$

Also in Eq.2.33,  $f$  is the Darcy-Weisbach friction loss coefficient of the pipe connected to the fitting,  $D$  is the diameter of pipe and  $L$  is the length of pipe between the pressure measurement points. Average velocity in fittings can be estimated by using the measured flow rate and using the pipe cross sectional area. All other parameters are known, and then by measuring pressure difference between two points, head loss of fitting can be determined. The key information to determine head loss in fitting is the Darcy-Weisbach friction loss coefficient. In this study, Moody chart is going to be used to estimate the friction factor.

### 2.3.2. Estimation of Friction Losses

In the pipe flow, friction occurs at the pipe wall. As a result of that some head loss exists and this loss is defined by Darcy-Weisbach equation.

$$h_f = f \frac{L V^2}{D 2g} \quad (2.35)$$

Here,  $h_f$  is the loss of head due to friction, L and D are the length and internal diameter of the pipe and V the mean velocity of flow. The factor  $f$  is the friction factor and it is a dimensionless quantity.

Although the pressure drop for laminar flow is independent of pipe roughness, it is necessary to take into account the effect of roughness of the pipe for the turbulent flow. First of all friction factor is a function of Reynolds number and relative roughness [6].

$$f = \phi \left( \text{Re}, \frac{\varepsilon}{D} \right) \quad (2.36)$$

Here,  $\varepsilon$  is the roughness of the pipe and the ratio of the roughness and the pipe diameter is the relative roughness.

For fully developed laminar flow this function can be simplified as in Eq.2.36 since the friction is independent from the relative roughness for the laminar flow [4].

$$f = \frac{64}{\text{Re}} \quad (2.37)$$

For turbulent flow Re and relative roughness dependence of friction factor is more complicated that it cannot be determined by theoretical analysis; therefore sets of experiments are performed and by using curve fitting applied to the data, Reynolds number and relative roughness dependence of f is represented with correlations or by graphical plots.

The experiments conducted for friction factor determination included artificially roughened pipes. Pressure drops along pipes were measured for known flow rate values and data was fitted to functions representing the effects of the Reynolds

number and relative roughness. These tests were firstly conducted at 1933 and improved over the years. Tests were repeated numerous times for a wide range of Reynolds numbers and relative roughness. [7]

The most widely used study on friction factor representation belongs to Lewis F. Moody. His studies are represented in November, 1944. His aim with publishing this study was not to offer something new; instead he aimed to embody some conclusions in convenient form for engineers to use. In other words, he was interested in the conditions which practically exist. He conducted experiments with commercial pipes and he obtained results in a range of Reynolds numbers which includes laminar, transitional and turbulent flow regimes. These experiments did not take into account extreme conditions such as flows with very high velocities, with very low velocities or flow in open channels in which friction factor depends on Mach number, Froude's number or Weber number. He explained that the friction factor in the Darcy's equation is a function of only two dimensionless parameters which are relative roughness and Reynolds number in the practical applications with ordinary velocities.

Moody correlated the original experiment results in terms of the relative roughness of commercially available pipe materials. He represented his studies with a chart which is called with his name "Moody Chart" (Figure 2.13). This chart includes friction factor values in wide range of Reynolds number and relative roughness.

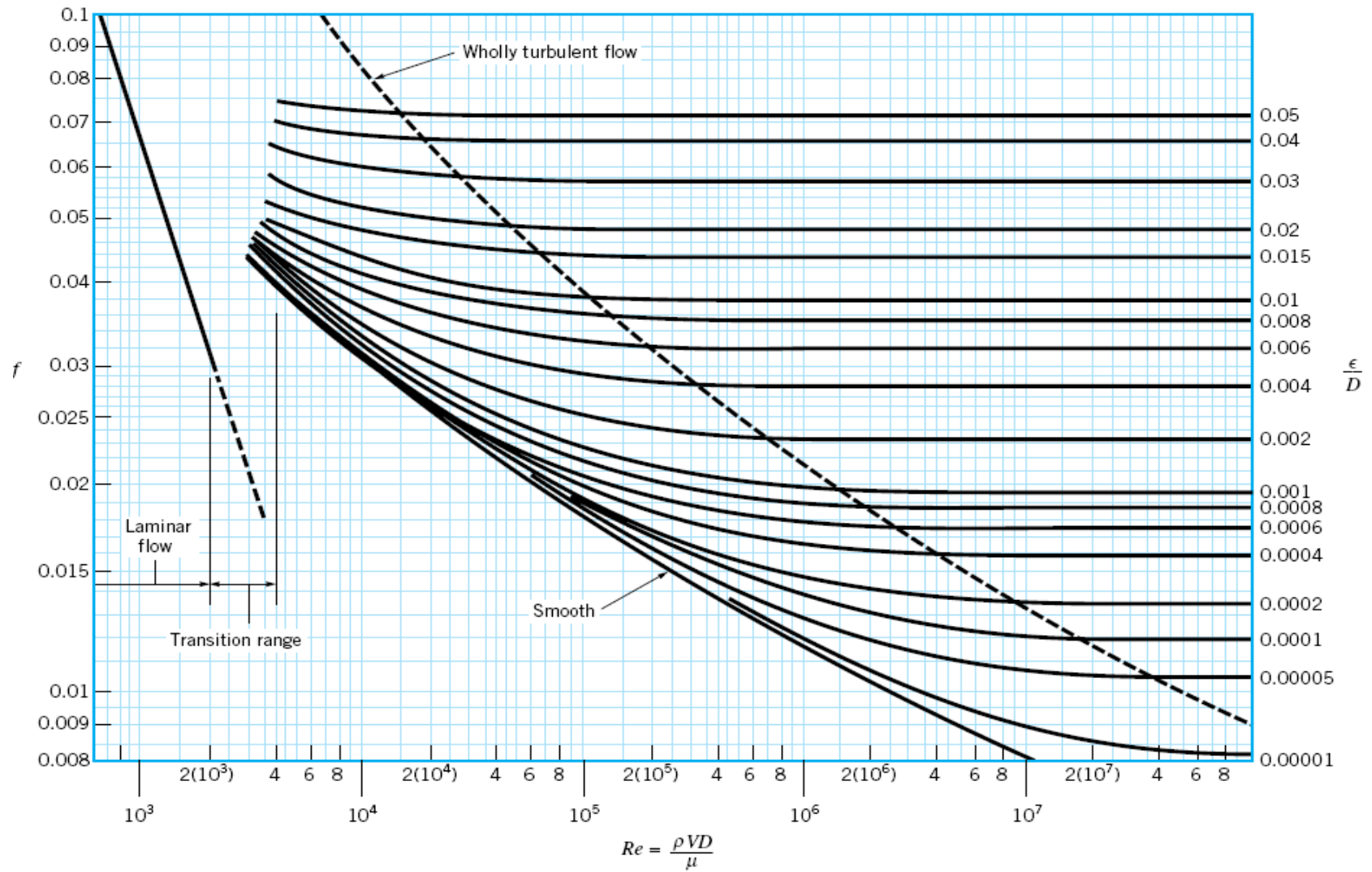


Figure 2.13. The Moody Chart - Friction factor as a function of Reynolds number and relative roughness [4]

The Moody chart is valid for all steady, fully developed, incompressible pipe flows. Also Colebrook formula is valid for all non-laminar part of the chart and friction factor can be determined from this formula by solution with iterative methods.

$$\frac{1}{\sqrt{f}} = -2.0 \log \left( \frac{\varepsilon / D}{3.7} + \frac{2.51}{\text{Re} \sqrt{f}} \right) \quad (2.38)$$

### 2.3.3. Flow through Valves

Besides friction, the most common head loss is generated by valves. Valves are used to regulate the flow rate. Opening or closing a valve causes change in geometry of flow. Changes in the geometry of flow create losses associated with the flow through the valve. Valves are significant contributor to the flow resistance. For instance, when the valve is completely closed, the resistance to the flow is infinite. [8]

Specifying the loss coefficient is the most common method to determine pressure drop or head loss across a component. Hydraulic loss coefficients of components strongly depend on the geometry of flow also on the fluid properties. Since obtaining the information of geometry of flow in fittings, such as valves, is not possible, head loss information is given in dimensionless form and strongly depends on the experimental data. [9]

In many practical applications hydraulic loss coefficient is independent of Reynolds number; it is only function of geometry. For various kinds of valves practically used, hydraulic loss coefficients are estimated by the experiments and the results are tabulated. Head losses across a valve can be determined by using Eq.2.39. As presented in this equation, in order to evaluate the head loss across a valve, hydraulic loss coefficient must be known.

$$h_1 = K \frac{V^2}{2g} \quad (2.39)$$



### 2.3.4. Flow through Elbows

The elbow (or bend) is used to change the direction of the flow in pipe [8]. The elbow which is used to change the direction of the flow is named by using the angle between the previous direction of the flow and the current flow direction. 90° elbows are used in this study.

For rounded elbows inlet and outlet cross sectional areas are same. Thus, velocity does not change from inlet to outlet. All elbows used in this study are well rounded elbows.

For well rounded elbows, loss at the entrance of the pipe can be neglected [8].

$$h_l = K \frac{V^2}{2g} \quad (2.40)$$

In Eq.2.40,  $h_l$  is the head loss through the elbow and it is essential information to determine hydraulic loss coefficient of the elbow ( $K$ ).

The study of Idelchik shows that hydraulic loss coefficient behavior changes with the change in flow direction. There are two kinds of 90° elbows depending on the direction of the flow. [10]

In the first kind, the flow direction changes from vertical-upward to the horizontal. To refer these elbows throughout this thesis, “the 90° elbow (up)”, as an acronym, is used to name them. Figure 2.14, illustrates the 90° elbow (up).

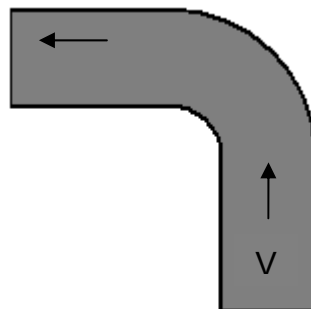


Figure 2.14. Well rounded, flanged, 90° elbow (up)

The results of the experiments conducted by Idelchik to determine the hydraulic loss coefficient for a 90° elbow (up) are represented as the function of Reynolds number

and the relative roughness. The Figure 2.15 represents these results and it shows that behavior of the hydraulic loss coefficients for this type of elbow changes with the Reynolds number. The loss coefficient decreases with Reynolds number then it starts to increase at an observable Reynolds number range.

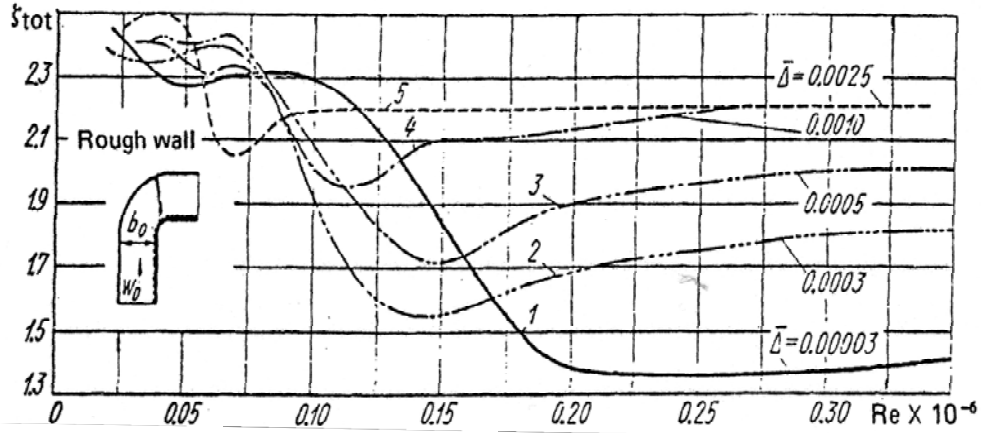


Figure 2.15. Hydraulic loss coefficients for the 90° elbow (up) [10]

The second 90° elbow changes the flow direction from horizontal to vertical-downward. To mention these elbows throughout this thesis, “90° elbow (down)” is used to name them. Figure 2.16 illustrates the 90° elbow (down).

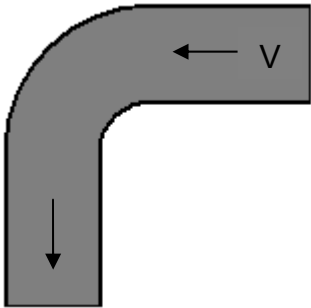


Figure 2.16. Well rounded, flanged 90° elbow (down)

Figure 2.17 represents the results of experiments performed by Idelchik to represent the hydraulic loss coefficient for 90° elbows (down) [10]. As shown in the figure, hydraulic loss coefficient of the elbow decreases as the Reynolds number increases.

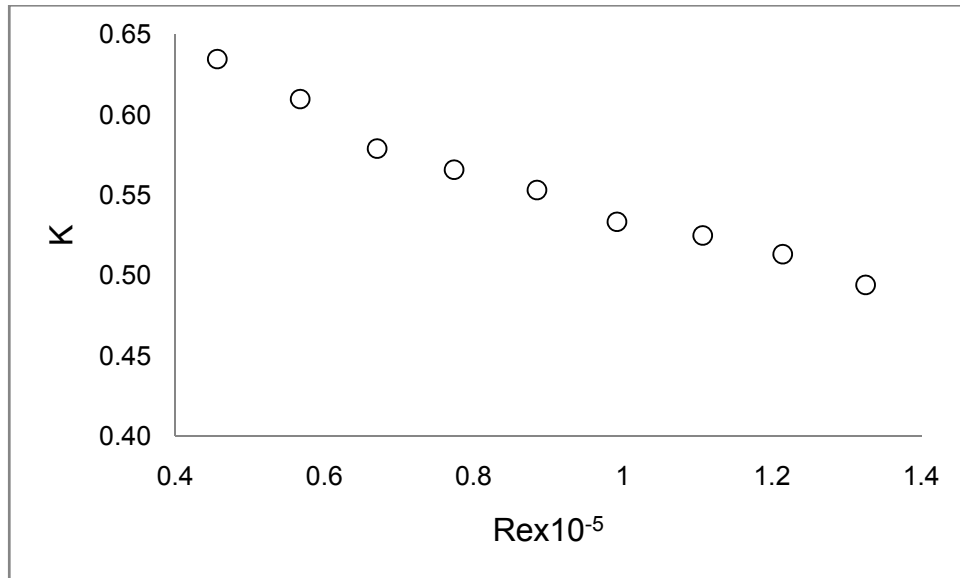


Figure 2.17. Hydraulic loss coefficients for 90° elbows (down)

### 2.3.5. Flow through C-Shape Bend

C-shape bend is an 180° bend which changes direction of the flow to the opposite direction of the inlet direction. This fitting is obtained by adding two 90° elbow with a small pipe as shown in Figure 2.18.



Figure 2.18. C-shape bend

The results of experiments which were conducted by Idelchik to determine the hydraulic loss coefficients of C-shape bend [10] are presented in Figure 2.19.

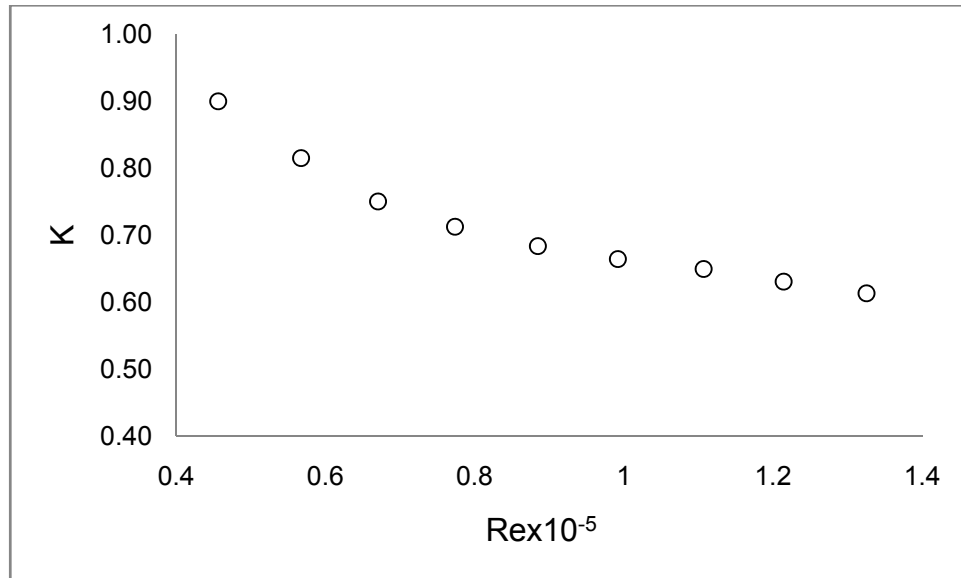


Figure 2.19. Hydraulic loss coefficients for C-shape bend

### 2.3.6. Flow through S-Shape Bend

S-shape bend or gooseneck type bend is a fitting which does not change the direction of the flow but elevation of the flow. This fitting is obtained by adding two  $90^\circ$  elbow with a small pipe. Figure 2.20 represents the S-shape bend.

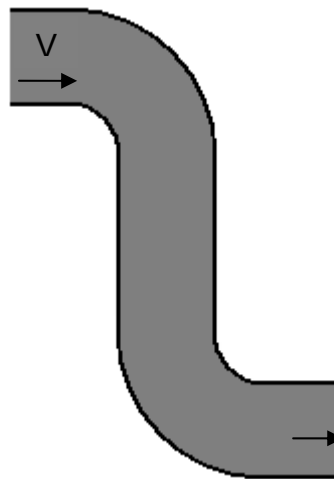


Figure 2.20. S-shape bend

The results of experiments which were conducted by Idelchik to determine the hydraulic loss coefficients of S-shape bend [10] are shown in Figure 2.21. The hydraulic loss coefficient decreases as the Reynolds number increases, as the figure indicates.

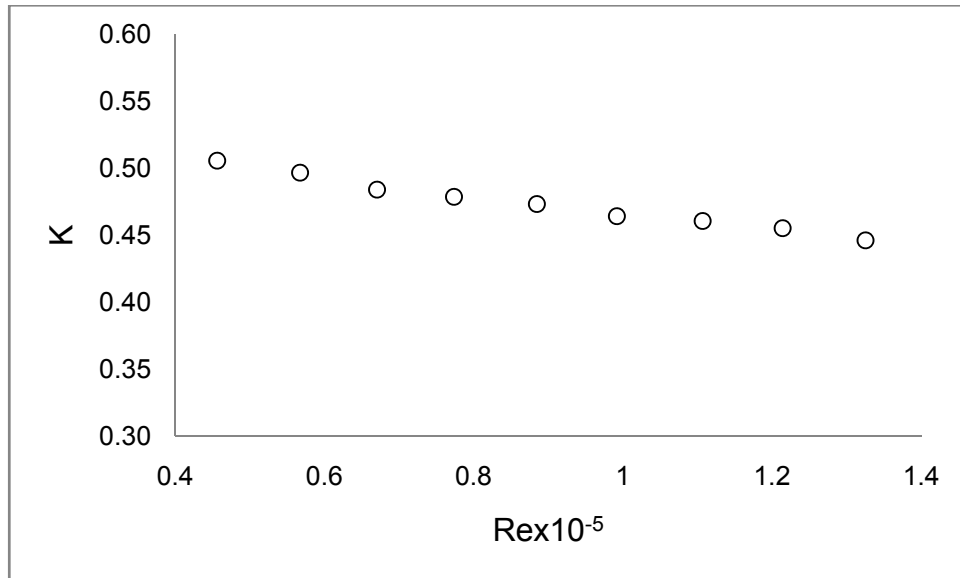


Figure 2.21. Hydraulic loss coefficients for S-shape bend

### 2.3.7. Flow through Enlarging Pipes

When enlargement in pipe diameter occurs, cross sectional area through which fluid flows increases then pressure changes. If sudden enlargement with sharp edges is used, loss due to change in diameter will be greater than that of slowly enlarging pipes [8]. Figure 2.22 illustrates a gradually enlarging pipe. In the figure,  $d$  is the diameter at the inlet and  $D$  is the diameter of the outlet and  $\theta$  is the angle of the gradual enlargement.

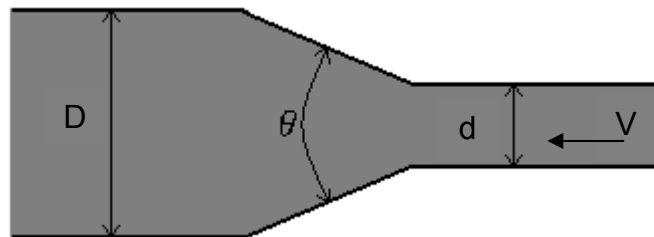


Figure 2.22. Flow in Slowly Enlarging Pipes

The expansion coefficient for enlarging pipes  $K_{exp}$  can be estimated by using Eq.2.42. In this equation,  $h_1$  is the head loss through the enlargement.

$$h_1 = K_{exp} \frac{V^2}{2g} \quad (2.41)$$

The contributors of the head loss (or gain) through the enlargement are head loss due to pressure difference, velocity head and head loss due to friction loss as given in Eq.2.42.

$$h_l = \frac{\Delta p}{\gamma} + \frac{Q^2}{2g} \left( \frac{1}{A_1^2} - \frac{1}{A_2^2} \right) - \sum f \frac{L}{D} \frac{V^2}{2g} \quad (2.42)$$

In Eq.2.42,  $Q$  is the volumetric flow rate while  $A_1$  and  $A_2$  are initial and final flow areas after enlargement, respectively.

The expansion coefficients due to gradual enlargement in pipe diameter depend on inlet to outlet diameter ratio ( $D/d$ ), Reynolds number and  $\theta$ . The results of the expansion coefficient experiments conducted by Idelchik are classified due to inlet to diameter ratio, first. The results are reported as a function of Reynolds number and angle of the gradual enlargement [10]. In Table 2.3, the results of Idelchik's experiments on the expansion coefficient of gradually enlarging pipes for  $D/d = 2$  and  $\theta = 60^\circ$  are listed.

Table 2.3. Expansion coefficients for  $\frac{D}{d} = 2, \theta = 60^\circ$  [10]

| Reynolds number | $K_{\text{exp}}$ |
|-----------------|------------------|
| 50000           | 0.386            |
| 100000          | 0.286            |
| 200000          | 0.268            |
| $\geq 400000$   | 0.272            |

## 2.4. FLOW THROUGH PARALLEL PIPES

The flow through parallel pipes is a common application among flow systems. The parallel flow can be defined as the flow which divides and subsequently merges again when three or more pipes are connected as shown in Figure 2.23.

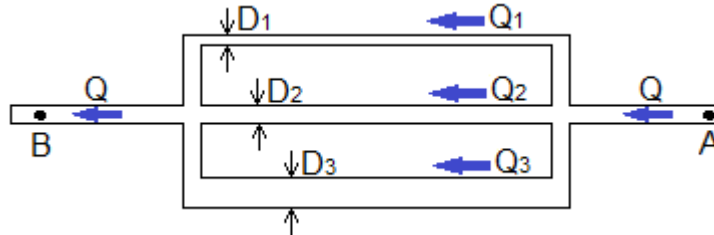


Figure 2.23. Flow through parallel pipes

As shown on the figure, the sum of volumetric flow rates at each parallel line is equal to the total volumetric flow rate. Therefore continuity equation for this flow can be represented with Eq.2.43.

$$Q = Q_1 + Q_2 + Q_3 \quad (2.43)$$

The separation of volumetric flow rate depends on the flow area of the each parallel pipe and elevation of pipes because of the effect of gravity.

The steady state energy equation (Bernoulli's equation), between points A and B, may be rewritten as given below;

$$\frac{p_A}{\gamma} + \frac{V_A^2}{2g} + z_A - h_l = \frac{p_B}{\gamma} + \frac{V_B^2}{2g} + z_B \quad (2.44)$$

The head loss due to friction and pipe fitting elements are included in  $h_l$ . [4]

## 2.5. MAIN COMPONENTS OF FLOW IN PIPES

### 2.5.1. Pumps

A pump is required to circulate water through the pipes and fittings in our system. A pump is defined as a device which converts mechanical power into fluid power. The mechanical power is usually provided by shaft rotation which is obtained by a prime mover attached to the shaft. However, the stated prime mover is usually an electric motor for commercial pumps, in practice, diesel or fuel engines may be used for some industrial applications. Pumps can be divided into two main groups, positive displacement and rotodynamic pumps.

Figure 2.24 shows the classification of pumps.

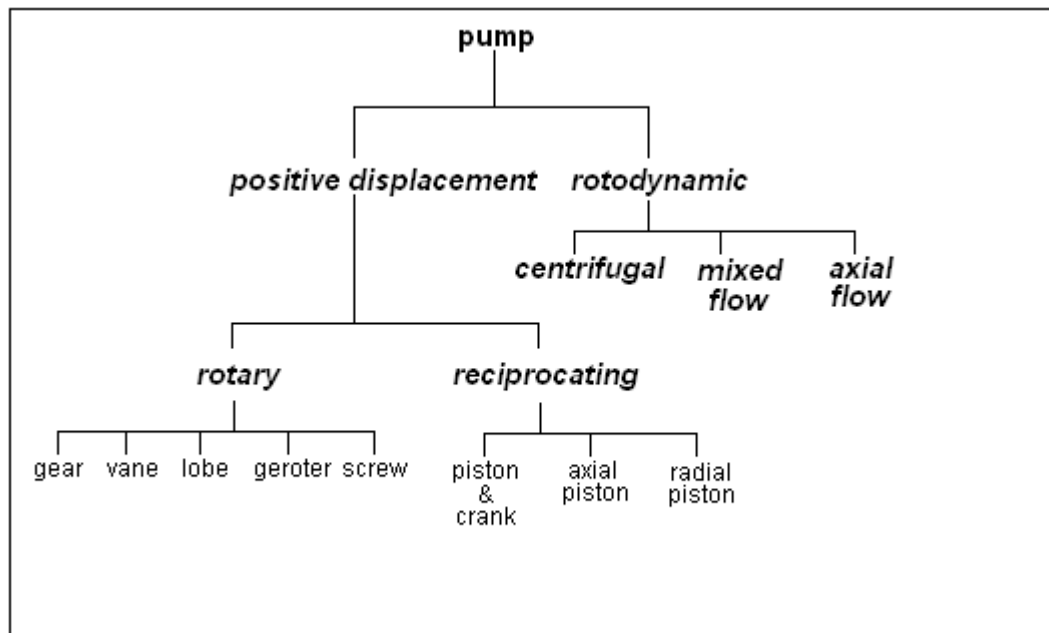


Figure 2.24. Classification of pumps [8]

In reality, pumps may be used with any type of fluids but we use the word 'pump' for the incompressible fluids (liquids) and 'compressor' for the compressible fluids (gases). Fluid of our system is water so we will use the word pump in further sections.

#### 2.5.1.1. Positive Displacement Pumps [8]

The working principle of these pumps is that enclosing a certain quantity of liquid at inlet and physically transferring it through the pump to the outlet which is at



the higher pressure. The amount of the liquid transferred per revolution of the pump shaft is constant. In practice, there is an internal leakage loss (back flow from outlet to inlet) which increases as the outlet pressure increases since the flow rate reduces. As it is shown in Figure 2.24, there are two types of positive displacement pumps.

#### **2.5.1.2. Reciprocating positive displacement pumps**

These pumps use a piston which reciprocates in a cylinder. A flexible rubber diaphragm is used, in general, instead of a piston. They provide relatively low discharge pressures. [8]

#### **2.5.1.3. Rotary**

There are five types of rotary pumps. The gear type pumps are the most widely used rotary pumps. The fluid is carried around the outside of a pair of meshing gears between the inlet and outlet. The vane type rotary pumps use adjacent vanes to carry the fluid. The lobe pump uses the same principle with gear type but a pair of rotating lobes used to carry the fluid instead of gears and the lobes do not contact each other. There are also gerotor and screw type rotary positive displacement pumps. [8]

#### **2.5.1.4. Rotodynamic pumps**

These types of pumps rely on hydro dynamic action to achieve fluid pumping. They do not produce as high pressures possible as the positive displacement pumps. But the delivery pressure can be increased by multi-staging. Although delivery pressure is smaller, their simple design makes them much cheaper. In addition, they are capable of handling high volume fractions. Some of the other advantages of rotodynamic pumps can be listed as being suitable for use with slurries, corrosive liquids and liquid with the inclusion of abrasive particles. In case the pump inlet is above liquid level, a foot valve or check valve is fitted at the inlet of the pump. The liquid discharge controlling is also important. It may be controlled by throttling the discharge line which has no damaging effect in case of short period runs. The prolonged use of these pumps with throttling may result in rise in liquid temperature. The shaft power may be converted into internal energy of liquid with a rise in temperature and there can be a risk of overheating. A second way to control

discharge, which is using variable speed drive, is more efficient but also more costly. [8]

There are three types of rotodynamic pumps, centrifugal, axial and mixed flow pumps. Hence pump chosen for our set-up is a centrifugal pump and the working principles of axial, centrifugal and mixed flow pump are mentioned below. [8]

#### **2.5.1.5. Axial flow pumps**

These pumps consist of an impeller or series of impellers which rotate inside a casing and cause the fluid to move in an axial direction from inlet to outlet. They are similar to the propeller of a helicopter. These kinds of pumps have the smallest dimensions of an all rotodynamic machines. For instance, small fans in computers are typical example of axial flow pumps. Disadvantages of axial flow pumps are that developing a low head, having steeply decreasing efficiency curves and limited suction capacity, being prone to cavitation. [8]

#### **2.5.1.6. Centrifugal Pumps**

These pumps come out of an impeller rotating inside a spiral casing. They use simply a principal of centrifugal force that whenever a body rotates in a circular path, centrifugal force is generated. The fluid enters the pumps axially through the suction pipe via the eye of the impeller. Then the fluid is discharged from the impeller, radially. The casing collects and slows down the fluid and eventually discharges it through the delivery flange. The centrifugal force drives the fluid outward from the centre of rotation and also cause pressure rise [8]. Multi staging may be used to produce high pressures. Multi staging is carried out by arranging numbers of impellers in series on a common shaft. The working principle is that when fluid leaves one impeller it is directed through the inlet of the next impeller. By this way head is increased for the same volume, so that the total head produced is the sum of the heads generated in each stage [4].

#### **2.5.1.7. Mixed flow pumps**

These pumps are used for operating in between the centrifugal pumps, explained next, with high head-low flow rate and the axial flow pumps with low head-

high flow rate. They are basically used for medium head-medium flow rate applications. The impeller is designed for both axial and radial flow directions. They can provide high pressures by multi staging and efficiency of this pumps is high (almost 90 percent). [8]

#### **2.5.1.8. Basic principles of pump selection**

When engineers designs a system of pipes and fittings, the main concern is reaching the goal, such as distribution of fluid through a pipe network at required flow rate and pressure, with minimum costs. Cost of building an experiment is also the main constraint of an experiment design. To reduce the costs, a number of system analyses for different pipe diameters or different pressures are performed and optimum result is obtained. For this reason, computer codes are used to simplify the calculation procedures and also for saving time.

All pipe network analysis are depends on two basic principles.

- The conservation of mass of the system: If the pipes are put in series then flow rate in all pipes has to be same. On the other hand, in case of parallel pipes, total flow rate is equal to the sum of flow rate in each parallel branch.
- The mechanical energy balance of the system: This balance is written for each system, individually. The actual head, has to be gained by fluid from the pump, is to be determined by the balance of mechanical energy.

#### **2.5.1.9. Determination of Required Pump Power**

As discussed in the previous part, two basic principles have to be concerned for pump selection. Required pump power can be simply determined by analyzing the system taking into consideration whole losses on system (mechanical energy balance). For this reason, energy equation is written for the system. Therefore total work, per unit mass, done by the fluid in the pump (or the actual head gained by fluid from the pump) is obtained. Eventually, the required pump power is stated using the information of total work, per unit mass, done by the fluid and mass flow rate of flow.

### **2.5.2. Valves [8]**

Valves are the devices used for performing on-off function (open/close) and throttle function (control the rate of flow). Valves which are designed to perform throttle function can be used as on-off valve, on position when fully opened and off position when fully closed. On the contrary, on-off type valves cannot be used as throttle type valve. Valves are widely used in fluid systems. Selection of valve type depends on following constraints:

- Function required
- Application method (manual or by remote control)
- Nature of fluid
- Pressure and temperature of fluid
- Nature of process
- Nature of environment
- Cost including maintenance, expected life

There are several types of valves such as gate, globe, needle, diaphragm, ball, butterfly, check valves. Here is the further information about some of these types.

#### **2.5.2.1. Gate valve**

It is a sliding gate which moves up and down in guides. Because the straight-through configuration, gate valves cause a low flow loss in the fully open position. It is relatively cheap to manufacture and widely used type. They are readily available in a wide range of sizes such as from 6mm to 600mm. the type of valves are used to operate only in fully open or fully closed positions (no use for throttling otherwise valve could be damaged).

#### **2.5.2.2. Globe valve**

This type is used for manual throttling control. The fluid forced through two sharp changes of direction hence the flow loss is much higher than that of the same size gate valve in the fully opened position. It is widely used for throttling because it may be used at any intermediate position between fully closed and fully opened positions.

### **2.5.2.3. Needle valve**

Needle type valve is used when fine control of flow rate at low flow rates is required. It is virtually a globe valve with a tapered stem rather than a disc. The flow area gradually changes as the valve is opened. Eventually, fine control of the flow is provided. Needle valve is used in relatively small sizes because of very high head loss through it.

### **2.5.2.4. Diaphragm valve**

Diaphragm valves are suitable for fluids containing abrasive particles. They utilize a synthetic rubber diaphragm which seals against a weir or seat. The resilience of the diaphragm allows for a tight seal on closure even when a solid particle is embedded in it. Design of these valves takes preventing permanent damage into account in case of abrasive particles present in the flow.

### **2.5.2.5. Check valve**

The check valves are used to force the flow in one direction only, in other words they are used to avoid reverse flow. The working principle of them is very simple such as the flow goes in the correct direction valve opens, closed otherwise.

## **2.6. MEASUREMENT TECHNIQUES**

### **2.6.1. Flow Rate Measurement**

#### **2.6.1.1. Types of Flow Meters**

Since almost all theoretical information is based on the velocity of fluid in the system, one of the most important measurements performed in fluid mechanics experiments is the measurement of the rate of flow. To measure the flow rate of fluids a number of methods and devices have been developed over years. Some of the flow meters measure the flow rate roughly and some of them provide more sensitive measurements. The flow meter selection depends on the requirement of the degree of measurement sensitivity.

There are numerous types of flow meters for piping systems and Table 2.4 shows the classification of flow meters.

Table 2.4. Classification of Flow Meters

| <b>Differential Pressure</b>  | <b>Positive Displacement</b>                                      | <b>Velocity</b>  | <b>Mass</b>         |
|---|---|--|---------------------|
| Orifice Plate<br>Venturi Tube<br>Flow Tube<br>Flow Nozzle<br>Pitot Tube<br>Rotameters<br>etc. | Reciprocating Piston<br>Over Gear<br>Nutating Disk<br>Rotary Vane | Single-jet<br>Multi-jet<br>Turbine<br>Vortex Shedding<br>Momentum Exchange<br>Electromagnetic<br>Ultrasonic, Doppler<br>etc. | Coriolis<br>Thermal |

As shown in Table 2.4, in general, main types of flow meters can be classified as the differential pressure, positive displacement, and velocity and mass meters. Differential pressure devices (also known as head meters) include orifices, venturi tubes, flow tubes, flow nozzles, pitot tubes and variable-area meters.

Positive displacement meters include piston, oval-gear, nutating-disk, and rotary-vane types. Velocity meters consist of single-jet, multi-jet, turbine, vortex shedding, electromagnetic, and sonic designs. Mass meters include Coriolis and thermal types.

The experimental set-up built for this study includes two types of the flow meters which are both velocity based. First one is the multi-jet fluid flow meter and it shows the total volume of fluid that goes through it.

Figure 2.25(a) shows a typical multi-jet flow meter. Multi-jet flow meters are very accurate in small sizes. They have an impeller which placed horizontally on a vertical shaft. They use multiple parts surrounding an internal chamber, to create a jet of water against an impeller (Figure 2.25(b)). Rotation speed of the impeller is proportional to the flow velocity. Multi-jet meters generally have bronze alloy bodies and outer casings, with internal measuring parts made from thermoplastics and stainless steel. Multi-jet meters are very accurate in low flow rates and they provide long-term flow measurement.

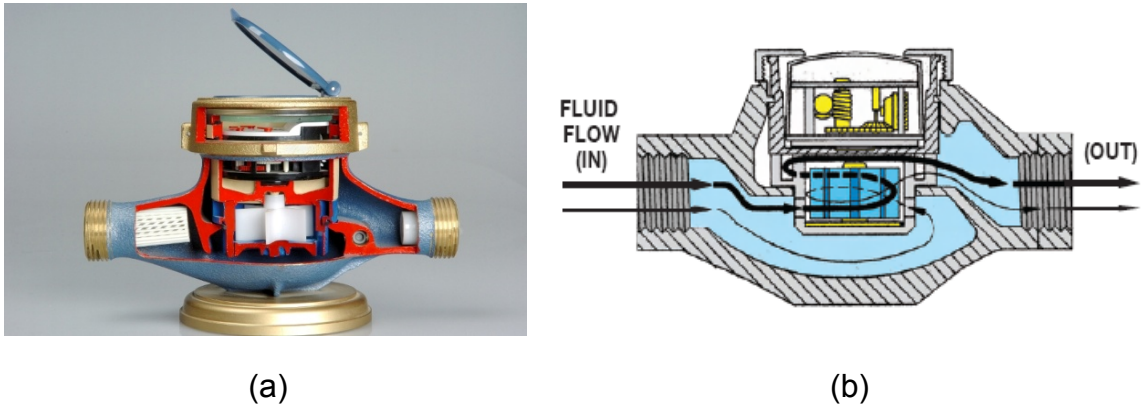


Figure 2.25. Multi-jet flow meter

Second flow rate measurement device is an electromagnetic flow meter. This device is technically a velocity type water meter. It uses magnetic properties to determine the water flow velocity. The magnetic flow meter used in this setup is shown in Figure 2.26.



Figure 2.26. Magnetic flow meter

One of the attractive properties of the magnetic flow meters is that they do not obstruct the flow. Thus, the pressure drop across the magnetic flow meter is equal to the pressure drop through a pipe. The operation of a magnetic flow meter is based on Faraday's law of induction. A magnetic field is applied to the metering tube, which results in a potential difference proportional to the flow velocity perpendicular to the

flow direction. A voltage is induced when a conductor moves through a magnetic field. The liquid serves as the conductor. Applied voltage is directly proportional to the flow velocity and is fed to the measuring amplifier by a pair of electrodes. Across the cross-section of the pipe the flow volume is calculated.

A schematic presentation of a magnetic flow meter is given in Figure 2.27. In the figure,  $U_e$  is the induced voltage and it is equal to the product of magnetic induction ( $B$ ), distance between electrodes ( $L$ ) and flow velocity ( $v$ ).

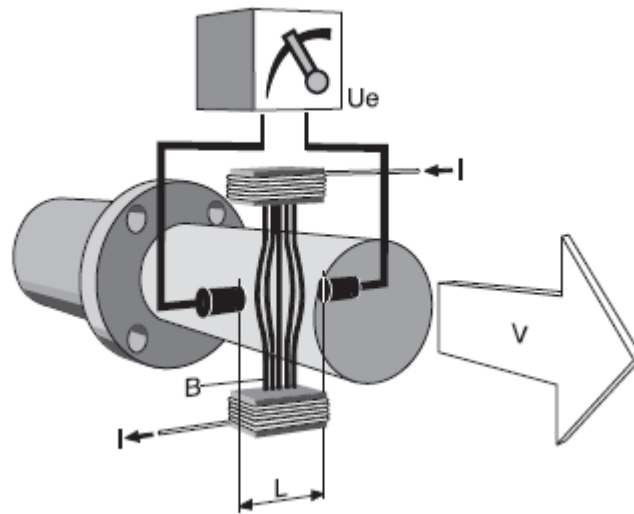


Figure 2.27. Working principle of magnetic flow meter

There are two main advantages of the magnetic flow meters. First, they can measure difficult and corrosive liquids and slurries. Secondly, they can measure forward and reverse flows with high accuracy.

## 2.6.2. Pressure Measurement

### 2.6.2.1. Types of Pressure Measuring Equipment

Measurement of pressure is very important for fluid mechanics applications since pressure is the most important characteristic of a fluid field. There are a lot of techniques and devices to measure the pressure. There are two basic definitions in pressure measurement. First one is absolute pressure which is measured relative to a perfect vacuum. Second one is the gage pressure and it is defined as the pressure measured relative to the local atmospheric pressure.



Basic pressure measurement devices are manometers. Manometers are devices which are used to measure pressure by using vertical or inclined liquid columns. There are many types of manometers such as piezometers tube, u-tube manometer, inclined tube manometers.

In addition to manometers, there are mechanical and electronic pressure measuring devices. The experimental set-up includes two techniques for pressure measurement. In the first technique, a mechanical pressure measuring device, pressure gage, is used (Figure 2.28). Using pressure gages is the more direct and common method in industry. Pressure gauges are fitted with a bent tube of oval section which tends to straighten as pressure is applied to it. One end of the tube is fixed and the movement of the other end is magnified and transmitted to a pointer which rotates over a calibrated scale [8]. The gauge is calibrated to read zero at atmospheric conditions and measures above atmospheric pressure.



Figure 2.28. Bourdon Gauge

As the second technique, differential pressure cells (DP cells) are used (Figure 2.29). The main advantage of DP cells is that they are convenient for the data acquisition performed using computer. In this regard, a differential pressure cell is used to measure pressure drop and gives off an electrical signal (0-5V) or current (4-20mA) that is proportional to the pressure reading. The DP cells are widely used in industry [11].



Figure 2.29. Differential pressure transmitter (DP cell) [11]

For many applications in which pressure measurement is performed, the pressure is measured with a device that converts the pressure into an electrical output. For instance, this type of a device is required when continuous pressure monitoring is desired. These devices are called the pressure transducers and there are many kinds of designs (Figure 2.30). [4]



Figure 2.30. Pressure transducer

### 2.6.3. Calibration of Measurement Devices

Calibration is a measurement process that assigns value to the response of an instrument relative to reference or to a designed measurement process. The purpose of calibration is to eliminate or reduce the difference between the measurement device and the reference base. Instrument calibration is necessary to eliminate or reduce bias in an instrument's readings over a range for all continuous values. For this purpose reference standards with known values for selected points are used for cross check. A series of measurements performed and a calibration curve is obtained using reference values. Calibration curve is attained by establishing a functional relationship between the standard values and corresponding measurements. The calibration procedure is same for situations both instruments which reads in the same unit as the reference standards and instruments which reads in different units than the reference standards.

The calibration method can be summarized in following steps:

- Selection of reference standards with known values to cover the range of interests
- Measurements on the reference standards with the instrument to be calibrated
- Functional relationship between the measured and standard values (usually a least squares fitting is used to fit the data) called a *calibration curve*
- Correction of all measurements by the inverse of the calibration curve

In the experimental setup built for this study, there are two types of measurement instruments, pressure and flow rate measurement devices.

Flow rate measurement device, magnetic flow meter, gives off an electrical signal (0-5V) or current (4-20mA) and these values are proportional to the flow rate reading [12]. The calibration of the device has been made by the manufacturer and its calibration constant given as 4.32 in the user's manual of the device. This value is used in the data acquisition software. The second type flow measurement device, water meter, does not require any correction so the value of calibration constant is 1.

The pressure measurement devices, DP cells and pressure transducers, have also been calibrated with the standard values by the manufacturer. All of pressure measurement devices, used in this study, give off electrical output signal (0-5V) or current (4-20mA). The reference standard values are fitted to the range of electrical output signals.

## **2.7. DATA ACQUISITION SYSTEMS (DAQs)**

### **2.7.1. Data Logger**

Data logger is an electronic device that records data over time or depending on the location. This relation can be obtained by placing in instrument or sensors or via external instruments and sensors. Generally, they are connected to a digital processor or computer. The primary components are microprocessors, internal memory to store the data and sensors. They are typically small battery powered and portable devices.

Some data loggers such as the one included in our experimental setup, interface with a personal computer and utilize software to activate the data logger and view and analyze the collected data. On the other hand some of them have their own local interface device i.e. keypad or LCD.

The kinds of data loggers vary with the purpose of their usage. While some types are used for general purposes such as large range of measurement applications, some types are used for measuring only a specific data in one environment. In general, it is common to program the data loggers. In contrast, data loggers have many applications in which they remain as static machines because they are designed as they have limited number or unchangeable parameters. Electronic data loggers have replaced chart recorders in many applications. There are many benefits of using data loggers. The most outstanding one is the ability of automatically collecting the data on a 24 hour basis.

By the technological developments, data logging has improved in time and gain some new features with a new name called data acquisition. The terms data logging and data acquisition have the same meaning. On the other hand data logging have some disadvantages compared to the data acquisition such as;

- Data loggers have slower sample rates. (Typical maximum sample rate is 1 Hz)
- Data acquisition has the more programming flexibility.

### **2.7.2. Data Acquisition**

Data acquisition (DAQ) is the sampling of real world physical conditions and conversion of the resulting samples into digital numeric values that can be manipulated by a computer in computer data processing. DAQ involves the conversion of analog signals and wave forms into digital values. After the processing of these digital signals, desired information is obtained (

Figure 2.31. Data Acquisition Process). There are three main components of DAQ.

- Sensors that convert physical parameters to electric signals.

- Signal conditioning circuitry
- Analog to digital converters

Depending on the application, acquired data can be displayed, analyzed or recorded. DAQ applications are generally controlled by the commercial DAQ software. Specialized programming languages used for data acquisition include EPICS for building large scale data acquisition systems such as ProfiLab which, is used in our experimental setup, offers a graphical programming environment.

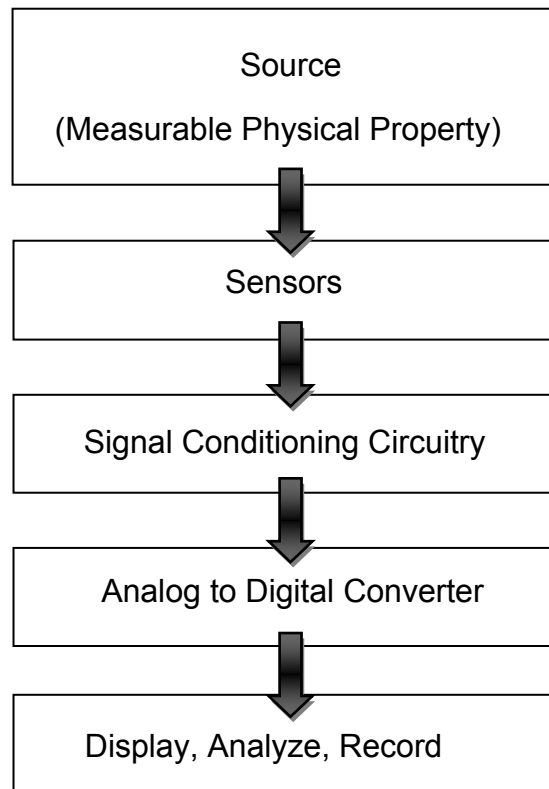


Figure 2.31. Data Acquisition Process

### **3. DESIGN OF THE EXPERIMENTAL SET UP**

The study has begun with the design of the experimental setup. After the selection of the theories which were going to be included in the setup was chosen, an appropriate experimental setup was designed and modeled. A model design was constructed and analyzes were performed to state the final dimensions and choose appropriate main components such as pump from the available commercial products. The main constraint for the selection of the appropriate components was expected flow ranges. Flow ranges were set with the maximum value of 150 thousand. Moreover, there were financial limitations which were dominant constraint for selection of the measurement equipments. The design of the setup includes several steps which are material selection, sizing of the setup by using theories and also computer simulation, selection of the measurement techniques and equipments.

The first step of the setup design is selection of the material. The main material used for pipes in the setup is stainless steel. Stainless steel is chosen because of being the widely used pipe and component material in nuclear power plants. In addition to the stainless steel, copper and PVC pipes are used in the setup section of friction factor behavior is observed.

Design of the experimental setup was based on basic laws of fluid mechanics and computer simulation of the design with computational fluid dynamic code FLOWNEX. A basic design of the setup was generated at first. The basic design is shown in Figure 3.1. The components named with numbers are water tank, pump, water meter and magnetic flow meter, respectively.

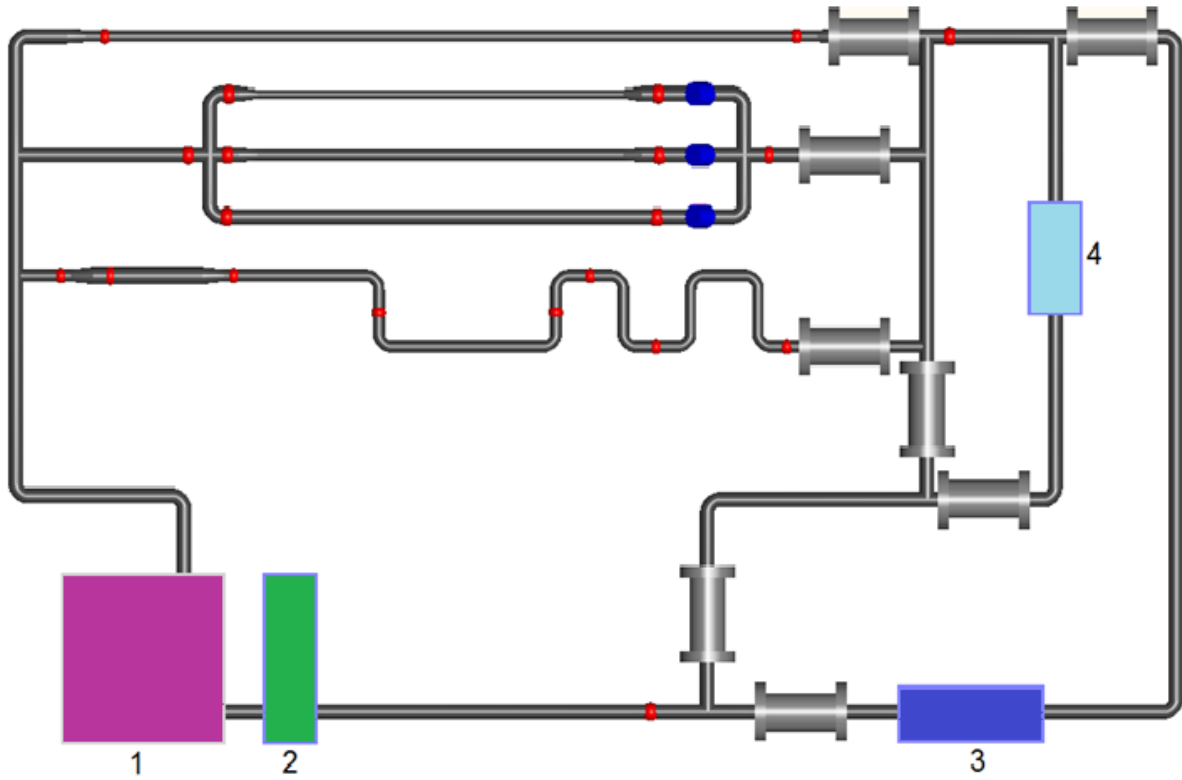


Figure 3.1. Model design of the setup

Subsequently, calculations were performed to size the components of the setup. Sizing of the components was an iterative process. Calculations oriented the sizes and requirements of the flow such as pump power. First analyses were performed using FLOWNEX for each section. Final results and pump requirements were obtained by using the developed code which is based on the law of fluid mechanics. This code was developed using Mathematica program.

### **3.1. SIMULATIONS WITH FLOWNEX**

FLOWNEX is the code which is used for sizing of the experimental setup. The model problem is demonstrated with the appropriate components of the FLOWNEX and set of runs are performed for selected cases of the flow. FLOWNEX simulations are based on macroscopic balance equations for mass, momentum and energy. FLOWNEX solves one dimensional conservation equations as explained in Appendix A. Each section of the experimental setup model is simulated. Eventually, the required pump power, pressure range for water circulation through sections and appropriate flow rate values are determined for the setup. Three sections are modeled individually and combined resultant values are used for sizing.









A model design of the experimental setup is developed with including experiments wanted to be performed. The model design is used in FLOWNEX analyses which were used to determine dimensions of the components, size of the pump for the flow rates which are appropriate for the selected experiments and pipe dimensions.

The components are selected from the FLOWNEX libraries and their dimensions and elevations are entered. The working range of the mass flow rate is determined by selecting the Reynolds number as to be under the 150 thousand. Set of runs for various mass flow rates are performed.

The components used in the simulation of all sections are basic pipes, pipes, 90 degree elbows, gate valves, globe valves, a water reservoir and nodes used to define inlet and outlet conditions of the components. Also pump component is used to model the actual pump used in the setup. The Table 3.1 shows the components symbols, input types and outputs used for this study in FLOWNEX.



Table 3.1. FLOWNEX components

| Component          | Symbol  | Inputs   | Outputs  |
|--------------------|---|--|--|
| Basic Pipe         |    | <ul style="list-style-type: none"> <li>• Dimensions</li> <li>• Roughness</li> </ul>  | Average velocity, Reynolds number, static pressure and temperature, total pressure drop (inlet-outlet), total mass and volumetric flow rate, properties of water, elevation                  |
| Pipe               |    | <ul style="list-style-type: none"> <li>• Dimensions</li> <li>• Roughness</li> <li>• Method of friction factor determination</li> <li>• Number of increments</li> </ul> | Average velocity, Reynolds number, friction factor, static pressure and temperature, total pressure drop (inlet-outlet), total mass and volumetric flow rate, properties of water, elevation |
| Elbow              |    | <ul style="list-style-type: none"> <li>• Elbow degree</li> <li>• Radius</li> <li>• Diameter (<math>r/d=1.25</math>)</li> <li>• Roughness</li> </ul>                    | Average velocity, Reynolds number, total pressure drop, static pressure and temperature, total mass and volume of flow, elevation  |
| Gate Valve         |    | <ul style="list-style-type: none"> <li>• Valve diameter</li> <li>• Inlet diameter</li> <li>• Outlet diameter</li> <li>• Fraction open</li> </ul>                       | Average velocity, static pressure and temperature, total pressure drop (inlet-outlet), total mass and volumetric flow rate, properties of water, valve resistance coefficient                |
| Node               |  | <ul style="list-style-type: none"> <li>• Elevation</li> </ul>  | Average velocity, static pressure and temperature, total pressure drop (inlet-outlet), total mass and volumetric flow rate, properties of water  |
| Boundary Condition |  | <ul style="list-style-type: none"> <li>• Fixed mass source (outlet of the pump)</li> <li>• Fixed pressure (defined for reservoir)</li> </ul>                           | Pressure, temperature  |
| Reservoir          |  | <ul style="list-style-type: none"> <li>• Elevation</li> </ul>  | None   |
| Pump               |  | <ul style="list-style-type: none"> <li>• The pump operation curve (pump head (m) vs volumetric flow rate (l/s)) given in Figure 3.4.</li> </ul>                        | None   |

The components are linked considering the flow direction. The selection of fluid and its properties is the next step following the components selection. The fluid for the designed experimental setup is ordinary water and its properties are defined in FLOWNEX fluid libraries. Constant properties of the water are used for simulations

because there is no heat addition to the fluid in the setup and the differences in pressure and temperature are small enough to assume water properties constant.

The demonstrations of the sections include two steps, component selection and modeling of the pump. The pumps which operational curves and properties have already been defined in FLOWNEX components libraries are larger than the required pump for this setup. They are industrial pumps and the flow rate values are high for the small diameter pipes such as pipes used in this study. As a result, a basic pipe between two nodes is used for modeling a pump simply in early simulations of whole sections (Figure 3.2). The node at the inlet of the pipe is used as a pressure boundary and a constant mass flow rate is given to the node at the outlet of the pipe.

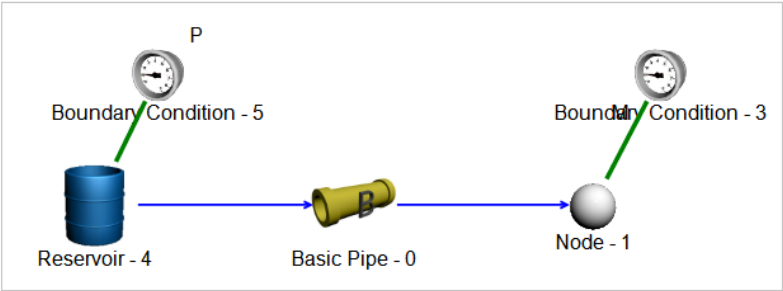


Figure 3.2. The modeling pump in early simulations with FLOWNEX

By simulations and further calculations with developed code, general pump characteristics are determined and an appropriate pump is provided. The actual pump performance curve (Figure 3.11) is used for further simulations. A new pump is defined in the FLOWNEX component library with its performance curve and components arrangement in simulations are modified as given in Figure 3.3.

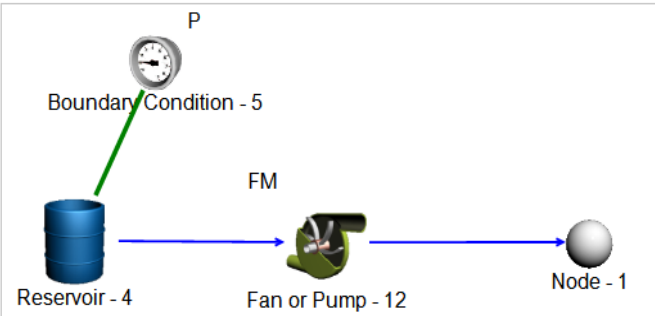


Figure 3.3. The modeling with the pump defined in FLOWNEX component library

### 3.1.1. Section 1

The first section of the setup was designed to observe pressure loss due to friction and determine friction factor of the pipes made of various materials. The model of this section was comprised with the components given in Table 3.1. The FLOWNEX model of the section 1 is given in Figure 3.4. The dimensions of the components are entered.

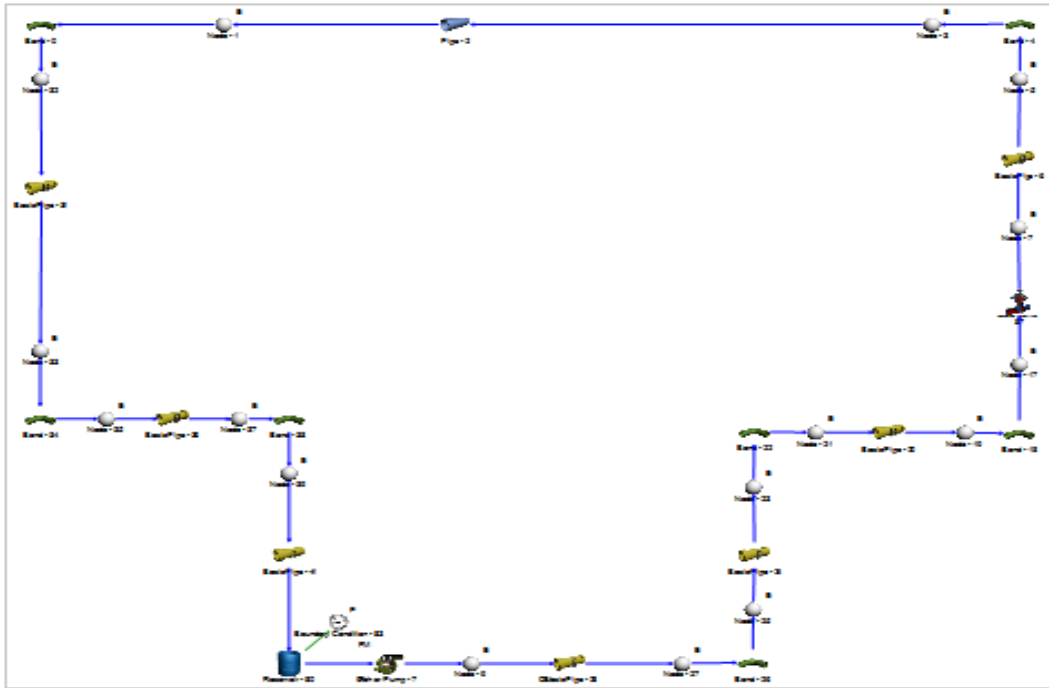


Figure 3.4. FLOWNEX simulation of section 1

Set of runs are performed for various mass flow rate values. The observed results for this section are total pressure drop along the pipe (blue), pressure gradients on each component and pressure drop on the whole section. The results are represented with “*result layers*”.

### 3.1.2. Section 2

The second section of the setup was designed to analyze the main pressure loss characteristics and observe parallel flow. Total pressure loss in this section is sum of friction losses, losses on valves and losses on elbows. The appropriate FLOWNEX

components given in Table 3.1 are used for simulation of section 2. The FLOWNEX model of the section 2 is given in Figure 3.5.

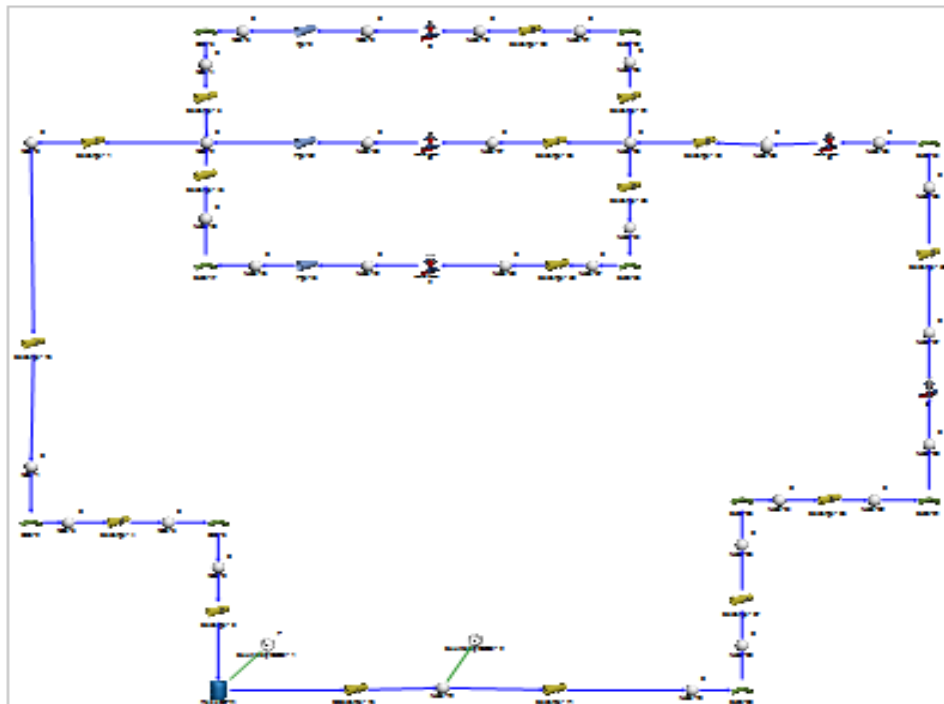


Figure 3.5. FLOWNEX simulation of section 2

Analyses are performed for various mass flow rate values and different valve positions of the parallel flow control valves. The observed results for this section are total pressure drop along the parallel pipes (blue), mass flow rate separation in parallel flow branches, and total pressure drop between parallel flow section and pressure gradients on each component.

### 3.1.3. Section 3

The third section of the setup was designed to observe pressure loss due losses on elbows and losses on enlarging pipe, mainly. In addition, losses due to friction still have contribution on head loss. The model of this section is comprised with the components given in Table 3.1. The FLOWNEX model of the section 3 is given in Figure 3.6.

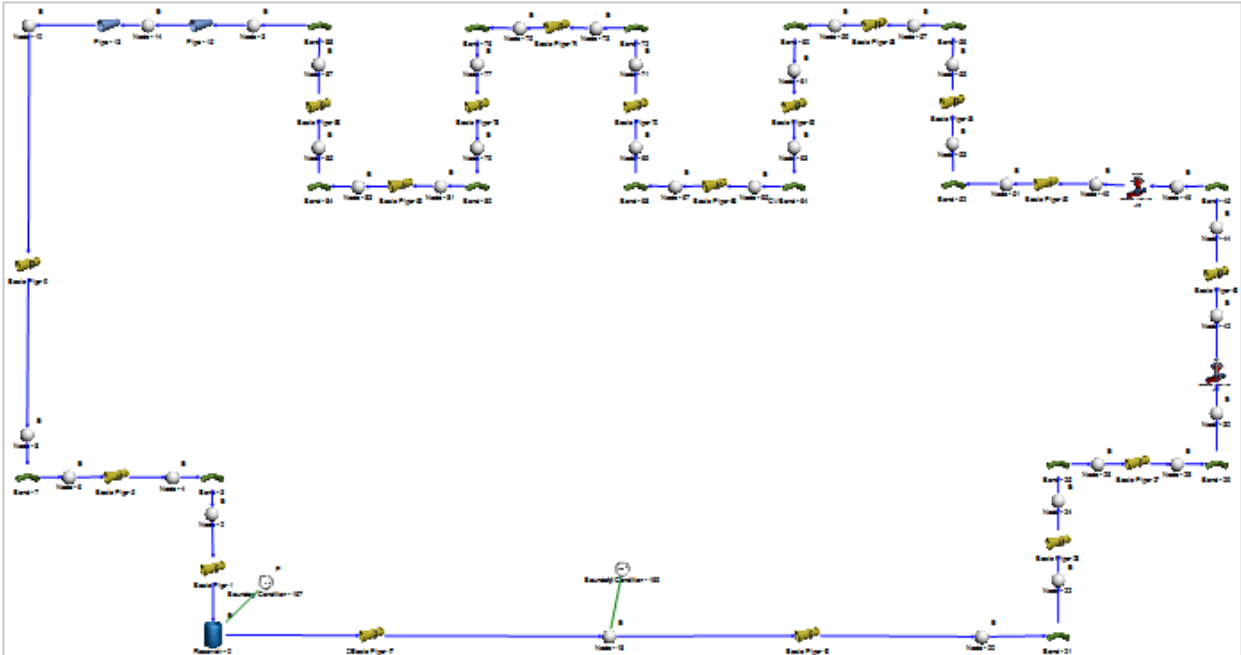


Figure 3.6. FLOWNEX simulation of section 3

Analyses are performed for various mass flow rate values. There are several measurement points on this section on the setup. Pressure difference between any two measurement points can be taken as output of the simulation. The observed results of this section are total pressure drop along the whole section, pressure loss between selected two nodes and pressure gradients on any component of the section.

### 3.2. PRESSURE DROP CALCULATION CODE (MATHEMATICA)

The appropriate mass flow rate values and dimensions of the components were obtained by the simulations of the experimental setup with FLOWNEX. Subsequently, a code was developed with using Mathematica program. The aim of this program was to determine requirements of the pump which will be used to circulate water through the experimental setup. This code obtains required pump head by evaluating the total pressure drop along each section with small increments in mass flow rate.

### 3.3. PUMP

#### 3.3.1. Selection of Pump

The pump selection is based on the determination of system requirements to circulate the fluid through the system. The characteristics of the experimental setup are determined and analyzed. The energy equation is applied to the setup. The setup is a closed system. The fluid is collected at the water container and it is pumped from the container to the system again. Flow is incompressible and steady state. For this flow conditions, macroscopic mechanical energy balance can be written as in Eq.2.31. By using Eq.2.31 and Eq.2.32, Bernoulli equation is obtained for this system.

$$\frac{P_1 - P_2}{\gamma} = \sum f \frac{L}{D} \frac{V^2}{2g} + h_t \quad (3.1)$$

Over all pressure drop through the system is determined first and required pump head is estimated with Eq.3.2.

$$h_p = \frac{\Delta p}{\gamma} \quad (3.2)$$

The pressure drop across this setup is determined for each section of the setup. The results are given in Figure 3.7. As can be seen from figure, the highest pressure drop values are obtained in the section 2 which is the observation of the parallel flow.

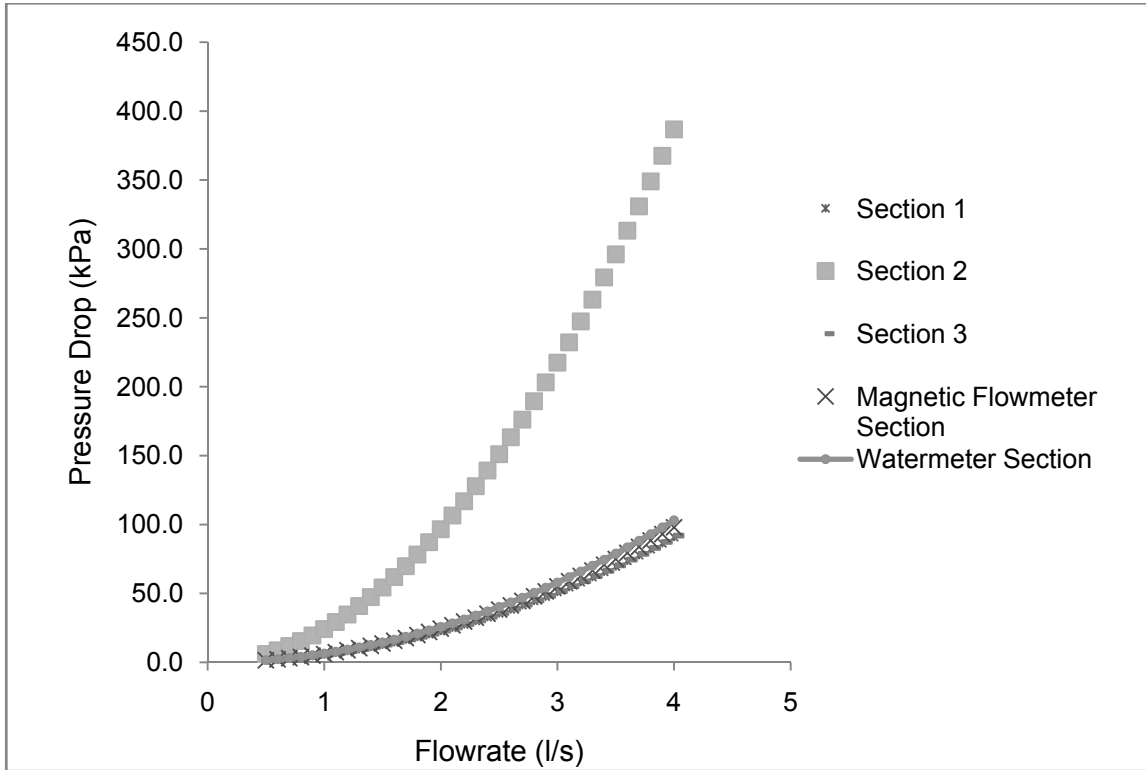


Figure 3.7. Pressure drop over the set-up

By performing calculations with Eq.3.1, required pump head is obtained for all sections of the setup individually. Figure 3.8 represents the required pump head values via change in volumetric flow rate. This curve is called as “*the system curve*”.

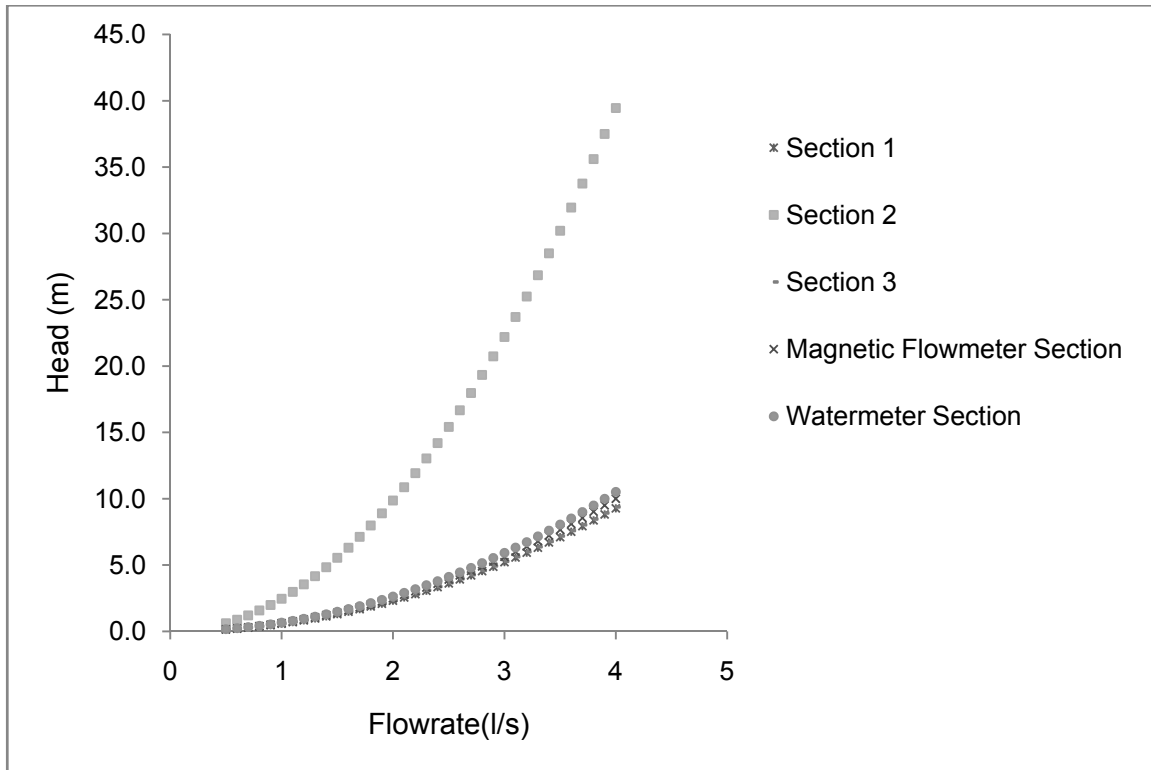


Figure 3.8. System curves of the set-up

Figure 3.8 shows that with having the highest pressure drop values, maximum pump head requirement is obtained in Section 2. The maximum pump head requirement is used for selection of the pump.

### 3.3.2. Specifications of the Selected Pump

The pump used in the set-up is a multistage centrifugal pump (Figure 3.9). The pump design includes impellers that are made of stainless steel and vertically joined in series with in-line design. The in-line design represents that the inlet and outlet pressure glands are in a line.





Figure 3.9. Pump used in the setup [13]

Technical drawing of the pump is given with Figure 3.10. The pump stands on a grey cast iron pump footplate which serves as a fixing base. The pump contains 20 stages to produce high pressures. The stage casings are in multiple modular constructions. As usual in multistage centrifugal pumps, the impellers are fitted on one shaft. All parts of pump contacting with the fluid, for instance stage casings, impellers, pressure casings and pump base with flanges, are made of chromium nickel steel. The pump and motor shafts are linked together by a clutch. The pump is also suitable for use with drinking water. The speed of pump is controlled by computer via frequency converter.

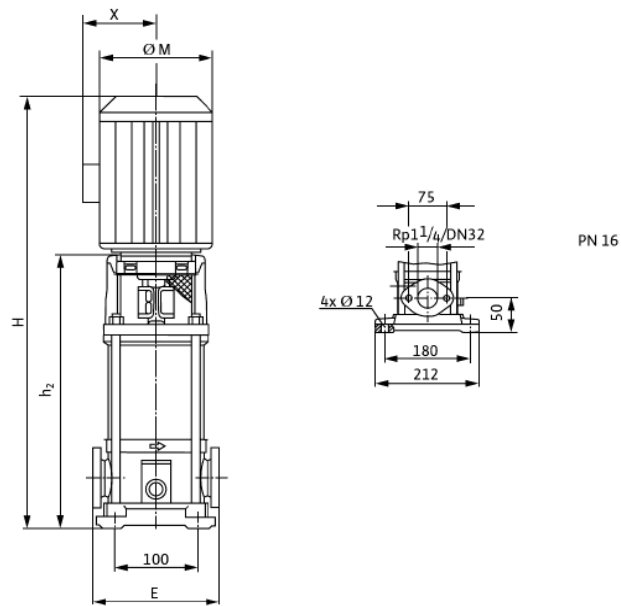


Figure 3.10. Structure of the pump used [13]

The pump is connected to a water storage tank and top of the tank is opened to the atmosphere. So pressure at the inlet of the pump is atmospheric pressure (1.01bars). Technical specifications of the pump are given in the Table 3.2.

Table 3.2. Technical specifications of pump [13]

|  |  |
|--|--|
| Permissible temperature range for use with drinking water                                | -15 <sup>0</sup> C to +90 <sup>0</sup> C |
| Maximum ambient temperature  | 40 <sup>0</sup> C                        |
| Maximum permissible working pressure<br>at the inlet<br>at the outlet for a 2 pole motor | 10 bar<br>16 bar                         |
| Mains voltages<br>EM: for P <sub>2</sub> ≤ 1.5 kW  | 1~230V ± 10%, 50Hz                       |
| Speed                    2 pole version  | 2900 RPM                                 |

Performance curves of the pump are presented in Figures 3.11 through 3.13. These curves are used to determine operational conditions of the setup. Each figure shows specific values of the pump against the various flow rate values.

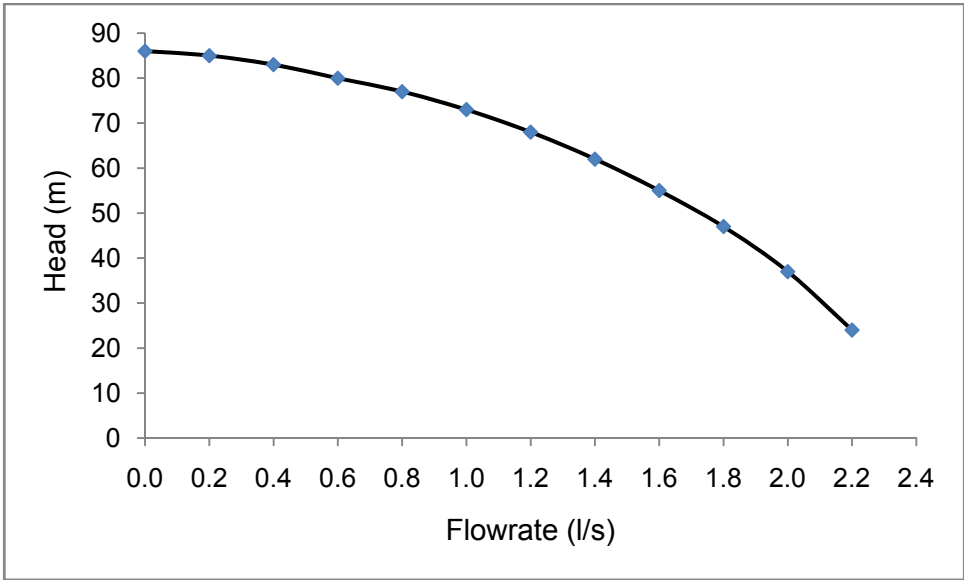


Figure 3.11. Pump head vs Flow rate [13]

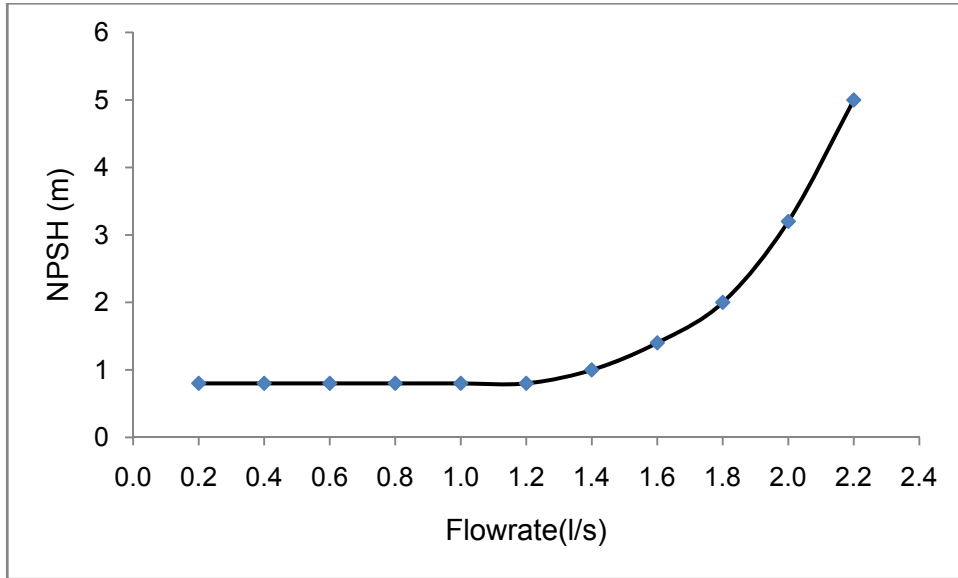


Figure 3.12. Net Positive Suction Head of Pump vs Flow rate [13]

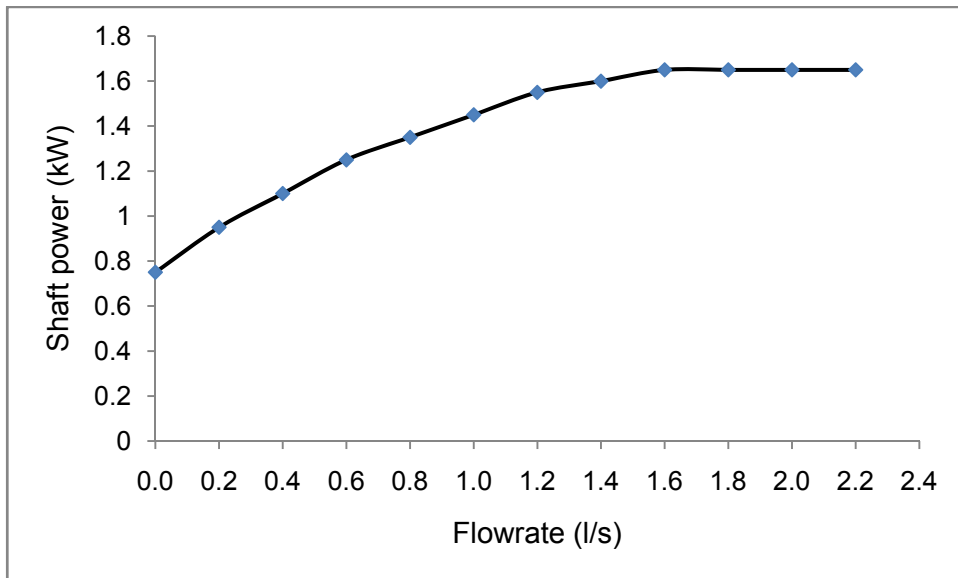


Figure 3.13. Shaft Power of Pump vs Flow rate [13]

### 3.4. DIMENSIONS OF THE SET UP

The sizing of the setup was completed by performing the analyses explained in previous sections. The final dimensions of the setup are given in Figure 3.14. Pipe diameters and lengths at the test sections are presented on this figure.

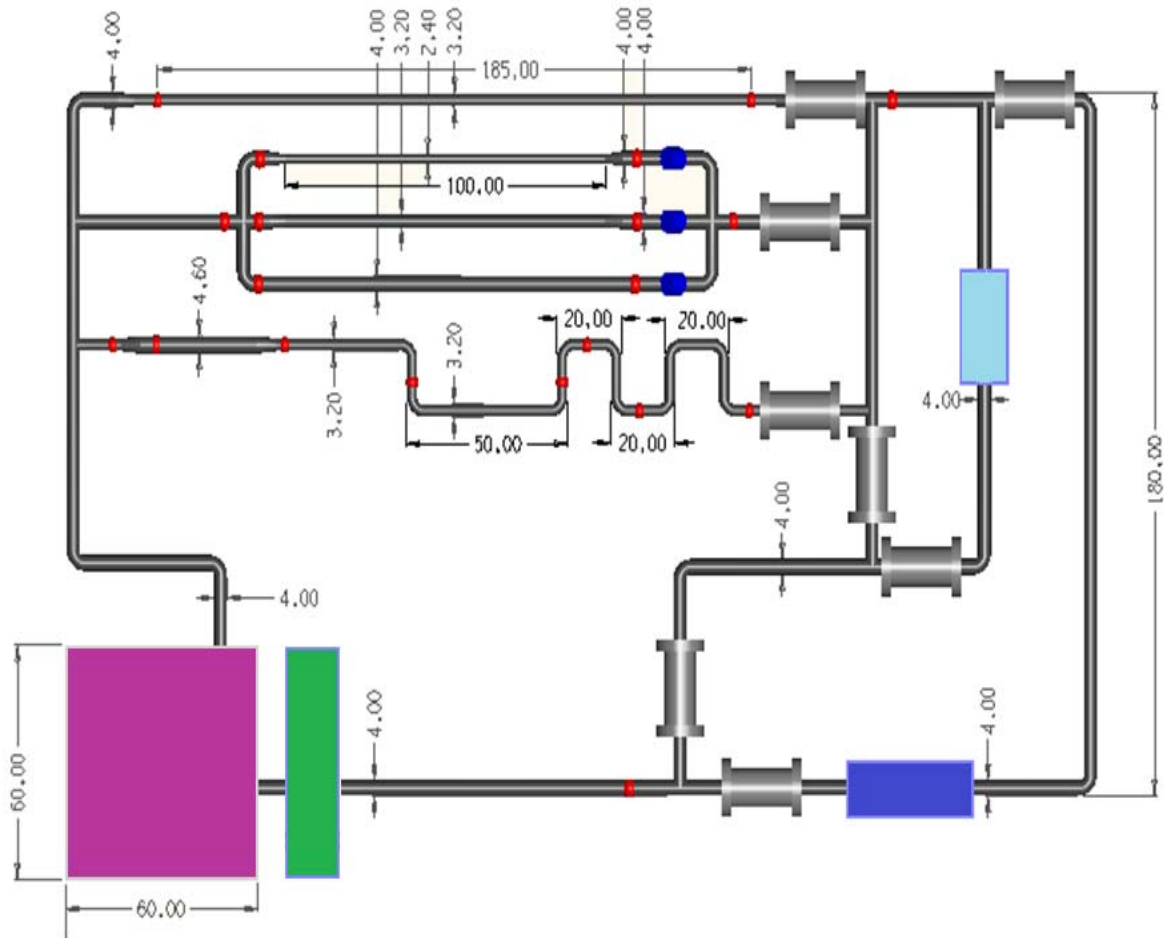


Figure 3.14. Dimensions of the Experimental Setup

The total height of the setup is 1.80 meters and total width is 3 meters. The highest level of the setup is easily reachable for an average height of a person. Table 3.3 shows the length and internal diameter of pipes. The length parameter becomes more important in the sections that friction losses are analyzed.

Table 3.3. Length and internal diameter of pipes

|                            |                  | Internal Diameter (cm) | Length (cm) |
|----------------------------|------------------|------------------------|-------------|
| Section 1                  |                  | 3.2                    | 185         |
| Section 2                  | Upper part       | 2.4                    | 100         |
|                            | Middle part      | 3.2                    | 100         |
|                            | Lower part       | 4.0                    | 100         |
| Section 3                  | Elbow part       | 3.2                    | -           |
|                            | Enlargement part | 4.6                    | -           |
| Magnetic Flow meter Branch |                  | 4.0                    | -           |
| Watermeter Branch          |                  | 4.0                    | -           |

### 3.5. SELECTION OF THE MEASUREMENT TECHNIQUES

The pump characteristics are stated by the calculations with the selected mass flow rate values as explained above. After the pump selection, the most important step is to decide the measurement techniques, the measurement devices and their specifications. The results of FLOWNEX runs are used for these specifications. Working ranges of the measuring devices are stated by the results for the components concerned for the experiment. This experimental setup is designed for educational purposes. Hence, the main concern in measurement technique selection is variety of techniques. The main limitation for the measurement device selection is cost. The appropriate measuring devices for the measurements which will be performed are assigned with an optimum cost.

## **4. EXPERIMENTAL SET UP**

### **4.1. GENERAL LAYOUT**

Experimental studies are fundamental and essential for engineering applications and education. Theoretical information can be revised and developed with the help of well conducted basic experiments. Hence, the creativity of the researcher or student is to be improved. The experimental setup, which is used in this study, is designed for measurement of pressure drop in pipes and fittings. Moreover, determination of hydraulic loss coefficient is strictly related with pressure drop measurements. Furthermore, basic measurement techniques of pressure and flow rate are to be examined with this setup.

The experimental setup built for this study is shown in Figure 4.1. Main components of the set up are pump (circulates water through setup), water tank, leaf and differential pressure manometers, two types of flow meters, pipes, valves and elbows. In this study, the selected fluid is liquid water. Also for flow conditions, appeared in our experimental set-up, liquid can be assumed incompressible. Since pressure variations are small enough to be appropriate for this assumption in all sections of the set-up. Furthermore, all pipes in the set-up are circular pipes.



Figure 4.1. The experimental setup for basic fluid mechanics applications

The experimental setup is separated into three sections of which aims are varied. There are also two larger circulation loops. These loops are added to the setup to measure the flow rate. A magnetic flow meter is placed on the first loop and a water meter is placed on the second loop which is the largest loop.

#### **4.1.1. Section 1: Determination of Friction Factor for Flow in Straight Pipes**

The main goal of this section is to get experience with pressure drop measurement along straight pipes. Also, friction factors of pipes manufactured with different materials are to be determined with the information of pressure drop.

Stainless steel, copper and polyvinyl chloride (PVC) pipes are used in this section. All pipes are equal in diameter and length. In this section, the set up permits to replace pipes for measurements. Pressure drop can be measured for each pipe and the friction factor of each pipe can be determined.

The main contributor of pressure drop across a pipe is the loss due to friction between fluid and pipe wall. As discussed in estimation of friction losses part, friction factor determination is to be performed by using the information of pressure drop. Estimation technique and procedures will be explained in the following section.

#### **4.1.2. Section 2: Analysis of the Parallel Flow**

Second section of setup aims to observe flow in branched pipes and characteristics of parallel flow. There are three valves at the entrance of each parallel pipe to regulate the mass flow rate of each line. The diameters of pipes are different from each other and diameter values are to be taken into account while calculation of the fraction of mass flow rate at lines. The main goal of this section is to measure the pressure drop across the pipes in case of parallel flow and to compare results of measurements with theoretical calculations.

#### **4.1.3. Section 3: Determination of the Hydraulic Loss Coefficient for Fittings**

The main goal of this section is determination of losses on fittings. For this reason, a number of fittings placed on the section and pressure drop through each are measured. Through the information of pressure drop on fitting, hydraulic loss coefficient of fitting can be determined. The fittings can be examined in this section are 90° elbows, C-shape and S-shape turns, gradual enlargement in pipe diameter. In addition, hydraulic loss coefficient of a gate valve is also examined in this section.

### **4.2. FLUID PROPERTIES**

The fluid used in the setup is liquid water. The water is chosen because it is the most common used fluid in the thermal hydraulic applications since it is cheap and has the easiest supply conditions. Water properties which used in the analyses are shown in Table 4.1. Properties listed in the table are taken from common literature.

Table 4.1. Water properties

|                             |                         |
|-----------------------------|-------------------------|
| Property                    |                         |
| Temperature                 | 20° C                   |
| Density ( $\rho$ )          | 998.6 kg/m <sup>3</sup> |
| Dynamic viscosity ( $\mu$ ) | 1.002 mPa.s             |



### 4.3. PRESSURE DROP MEASUREMENT POINTS

Technical drawing of the setup is presented in the Figure 4.2. Control of the flow direction is provided with gate valves placed in eight different locations. The name of the gate valves are their numbers and numbers are shown on the figure. Flow is controlled to let the fluid flow through only one test section of the setup. There are twenty pressure measurement points on the setup to connect the differential pressure cells. Twentieth pressure measurement point is not used for DP cell measurements, it is only to observe the pump outlet pressure with Bourdon type manometer and it is directly connected to a display.

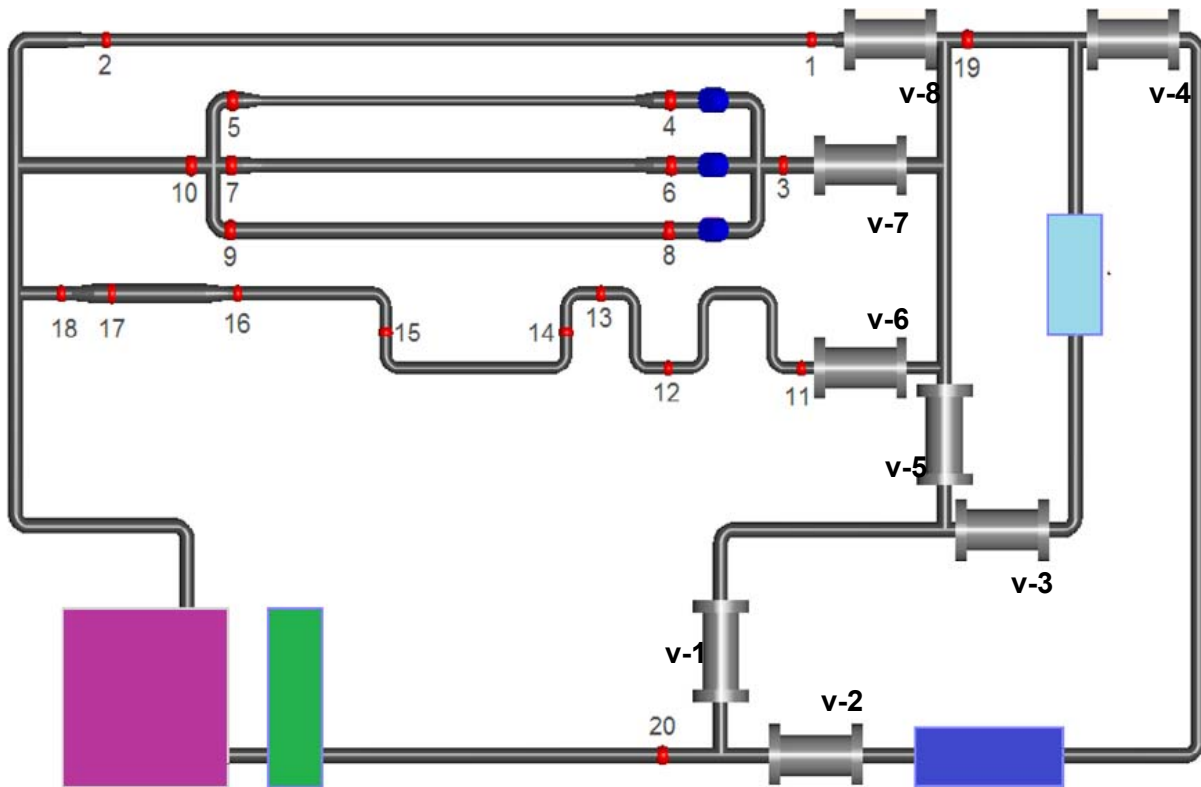


Figure 4.2. Pressure drop measurement points

In Table 4.2, pressure drop measurements are summarized. Pressure measurement points which are used to measure the pressure drop on the related component are listed. Measurement locations are used to name the each measurement. Measurement procedures are explained in Chapter 5.

Table 4.2. Measurement points, locations and purpose of measurement

| Section | Measurement Location | Measurement Points | Component                        | Purpose  |
|---------|----------------------|--------------------|----------------------------------|--|
| 1       | 1/1                  | 1-2                | Straight Pipe                    | Friction loss coefficient estimation                   |
| 2       | 2/1                  | 4-5                | Straight Pipe                    | Parallel flow observation                              |
|         | 2/2                  | 6-7                | Straight Pipe                    | Parallel flow observation                              |
|         | 2/3                  | 8-9                | Straight Pipe                    | Parallel flow observation                              |
|         | 2/4                  | 3-10               | 3 -Parallel Braches              | Parallel flow observation                              |
| 3       | 3/1                  | 11-12              | C-shape turn with two 90° elbows | Estimation of hydraulic loss coefficient of 90° elbows |
|         | 3/2                  | 12-13              | S-shape turn with two 90° elbows | Estimation of hydraulic loss coefficient of 90° elbows |
|         | 3/3                  | 13-14              | 90° elbow (turn to up)           | Estimation of hydraulic loss coefficient of 90° elbow  |
|         | 3/4                  | 15-16              | 90° elbow (turn to down)         | Estimation of hydraulic loss coefficient of 90° elbow  |
|         | 3/5                  | 16-17              | Enlargement in flow area         | Estimation of contraction coefficient                  |
|         | 3/6                  | 19-1               | Gate valve                       | Estimation of hydraulic loss coefficient of valves     |

#### 4.4. DATA ACQUISITION DEVICE: LABJACK

The DAQ device used in this experimental setup is LabJack with model U3 (Figure 4.3). Working principle of a typical DAQ is explained in the previous section and some of the features of the LabJack U3 are explained in detail in this section.

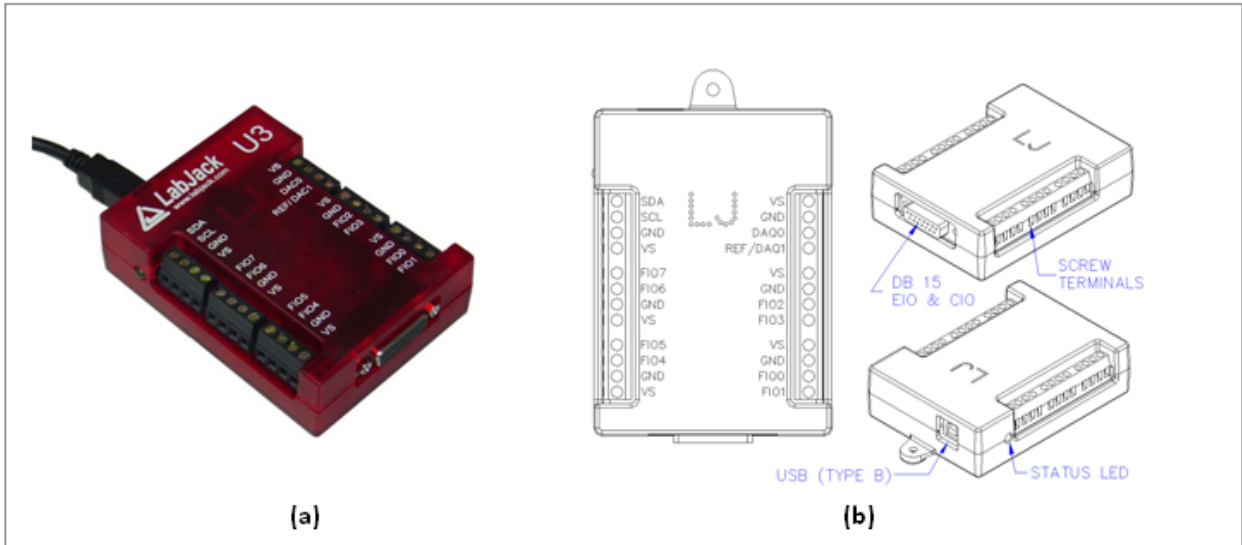


Figure 4.3. Data acquisition box (Lab Jack) [14]

First of all, the U3 model is the most affordable DAQ device. U3 model has two versions as low voltage and high voltage versions. The low voltage version is used in the setup. Main features of this device are summarized as given below [14]:

- 16 Flexible I/O (Digital Input, Digital Output, or Analog Input)
- 2 Timers
- 2 Counters (32-Bits Each)
- 12-bit Analog Inputs
- 2 Analog Outputs
- Capable of Command/Response Times Less Than 1 Millisecond
- USB 2.0/1.1 Full Speed Interface
- Powered by USB Cable
- Drivers Available for Windows, Linux, Mac and Pocket PC
- Rated for Industrial Temperature Range (-40 to +85 Degrees C)

Single ended measurements can be taken of any line compared to ground or differential measurements (two ended measurements) can be taken of any line to any other line. Both of the options are used in the setup. While single ended measurements is used for the flow rate measurement data taken of the Magnetic flow Fmeter, differential measurement is used for the pressure drop data from the D/P

cells. The analog inpt resolution is 12-bits and command /response (software timed) analog input reads typically take 0.6-4.0 ms depending on the number of channels and communication configuration. It has two analog outputs. Each analog output can be set to a voltage between 0 and 5 volts with 10 bits of resolution. It has 16 digital channels and 12 of them are available from measurement lines and 4 from the connector. Each digital line can be individually configured as input, output-high or output –low. [14]

Some of the technical specifications of this device are given in Table 4.3. DAQ Specifications and further specifications are available in user manual.

Table 4.3. DAQ Specifications

| Parameter  | Conditions  | Min             | Typical  | Max                 | Units   |
|--|---|-----------------|--|---------------------|---|
| <b>General</b><br>Supply voltage<br>Supply current<br>Operating Temperature  |   | 4.0<br><br>-40  | 5.0<br>50  | 5.25<br><br>85      | Volts<br>mA<br>C  |
| <b>Vs Outputs</b><br>Typical Voltage<br><br>Maximum Current  | Self-Powered<br>Bus-Powered<br>Self-Powered<br>Bus-Powered  | 4.75<br>4.0     | 5.0<br>5.0<br>450<br>50                                | 5.25<br>5.25        | Volts<br><br>mA<br>mA   |
| <b>Analog Inputs</b><br>Typical input range<br><br>Resolution<br>Integral Linearity Error<br>Absolute Accuracy<br><br>Noise (Peak to Peak) | Single ended, LV<br>Differential, LV<br>Special, LV<br><br>Single-Ended<br>Differential<br>Special 0-3.6<br><br>Quick Sample off<br>Quick Sample on | 0<br>-2.44<br>0 | 12<br><br>± 0.05<br>± 0.13<br>± 0.25<br><br>± 1<br>± 2 | 2.44<br>2.44<br>3.6 | Volts<br>Volts<br>Volts<br>Volts<br>Bits<br>%<br>%<br>%<br><br>Counts<br>Counts |
| <b>Analog Outputs</b><br>Resolution<br>Absolute accuracy   | 5% to 95%   |                 | 10<br>± 5  |                     | Bits<br>%   |
| <b>Digital I/O, Timers, Counters</b><br>Low level input voltage<br>Output low voltage  | No load   | -0.3<br>2       | 3.3  | 0.8<br>5.8          | Volts<br>Volts<br>Volts   |

## **4.5. COMPUTER PROGRAM FOR CONTROL OF THE PUMP AND DISPLAYING THE MEASUREMENTS: PROFILAB**

The computer software used for data acquisition and control in our system is ProfiLab. User panels are designed with custom controls and whole program is compiled into a stand-alone executable file. [15]

The program, using to control our setup, is written by selecting an appropriate function block from library. Software includes the function block library which offers a huge number of components. There are four basic types of components:

- Control components: Logic components, analogue components, miscellaneous components.
- Front panel elements: Displays, control elements (switch/puss buttons etc.)
- Hardware components: Relay cards, serial port/printer port, multimeters, etc.
- Macros are a combination of all kinds of components.

The name of the stand-alone executable file used for our setup is “nukleerflow.exe”.

### **4.5.1. The Use of the Software Application**

The window given in Figure 3.16 appears on the screen when the executable file “nukleerflow” is run. Control of the pump is provided through this software. Pump starts by the use of start button (green button on the left) and stops with the stop button (red button on the left). With the five menus which are selective at the left corner of the window, the user is able to see calibration constants, results in table or graph format and list of data logger outputs. With the tools, appearing at the right corner, data can be saved, printed or extracted to the excel format.

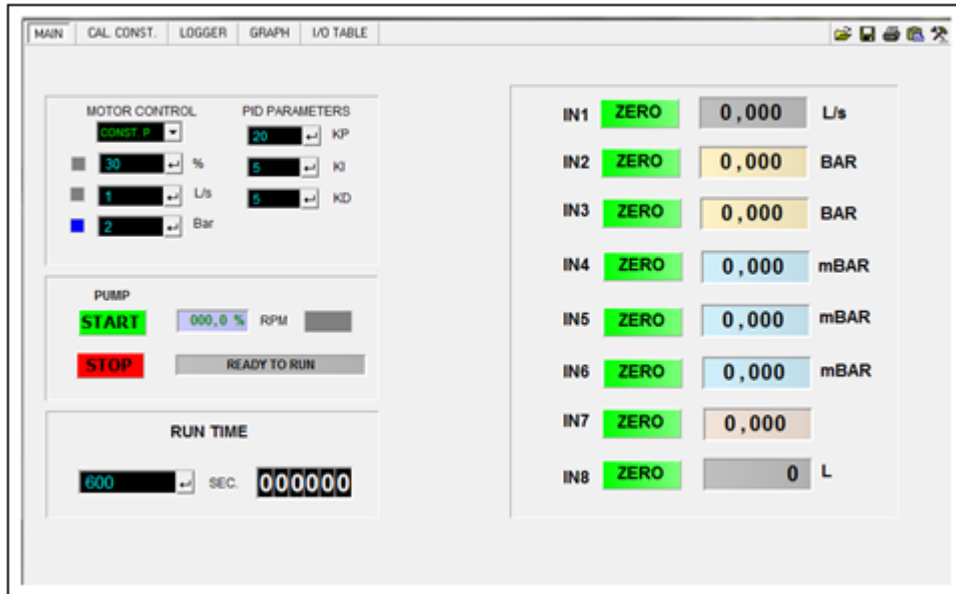


Figure 4.4. General view of software

**MAIN TAB:**

This menu contains main applications for the system run. PID parameters are the constants obtained from calibration constants. The right side includes the displays of the measurement devices. There are eight displays and each shows measurement of a different device. The list of displays and their data sources is given in Table 4.4.

Table 4.4. Displays and sources of data

| Display | Source   |
|---------|--|
| IN1     | Magnetic flow meter                              |
| IN2     | Pressure transmitter (at the outlet of the pump) |
| IN3     | Pressure transmitter (at the top of the setup)   |
| IN4     | Differential pressure sensor (0-5bars)           |
| IN5     | Differential pressure sensor (0-5bars)           |
| IN6     | Differential pressure sensor (0-1bars)           |
| IN7     | Empty  |
| IN8     | Water Meter                                      |

There are three choices for pump run techniques which are listed below the “motor control” title. “PUMP” displays show the pump revolution per minute with unit of percentage. It is a feedback mechanism for the user to control the pump when selection of the pump run technique is different from the manual one. To run the pump safely the rpm value must not be over the 85-90 percentages. Run time of the pump can also be entered while pump can be stopped at any time using the “stop” button.

When constant pressure technique is selected, pump gets feedback from the sensor placed at the outlet of the pump. By this way, pressure at the pump outlet adjusted and stayed constant by the software. To obtain the steady state pressure values, run time must be greater than 5 minutes. As it seen on the Figure 4.4, when this technique selected, a blue sign appears on the “motor control” section and desired pressure value is entered in the units of *bars*.

If the pump run technique is changed with constant Q, volumetric flow rate at the pump outlet is equal to the value entered by the user in the units of *liters per second*. Figure 4.5(a) shows the appearance of the “motor control” section after the selection of constant Q. An orange sign appears on the left side and desired value of volumetric flow rate can be entered by the user. The feedback of the pump is provided from magnetic flow meter. So, valves which let flow go through the magnetic flow meter must be full opened when this technique is selected.

The third pump run technique is the manual control of the pump. The motor of the pump is controlled manually by running at the specific value of the revolution of the motor in the units of *percentage*. The feedback mechanism is the pump itself. When this technique is selected, a green sign appears at the “motor control” section as shown in Figure 4.5(b).

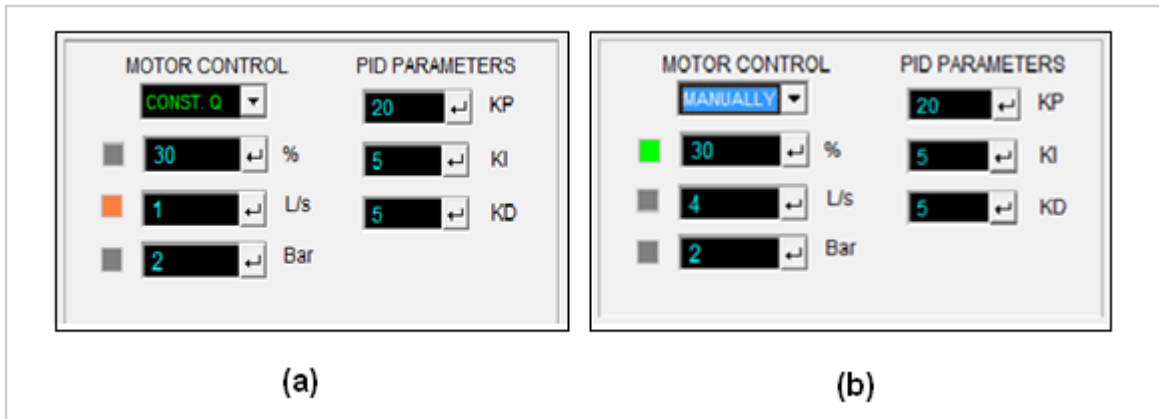


Figure 4.5. Pump run techniques: constant volumetric flow rate & manually control

**CALIBRATION CONSTANT TAB:**

The calibration constants of the sensors are entered with using this menu. The calculation of the calibration constants is given in the following section. This menu is only for entering the calculated values. The calibration constant window is shown in Figure 4.6.

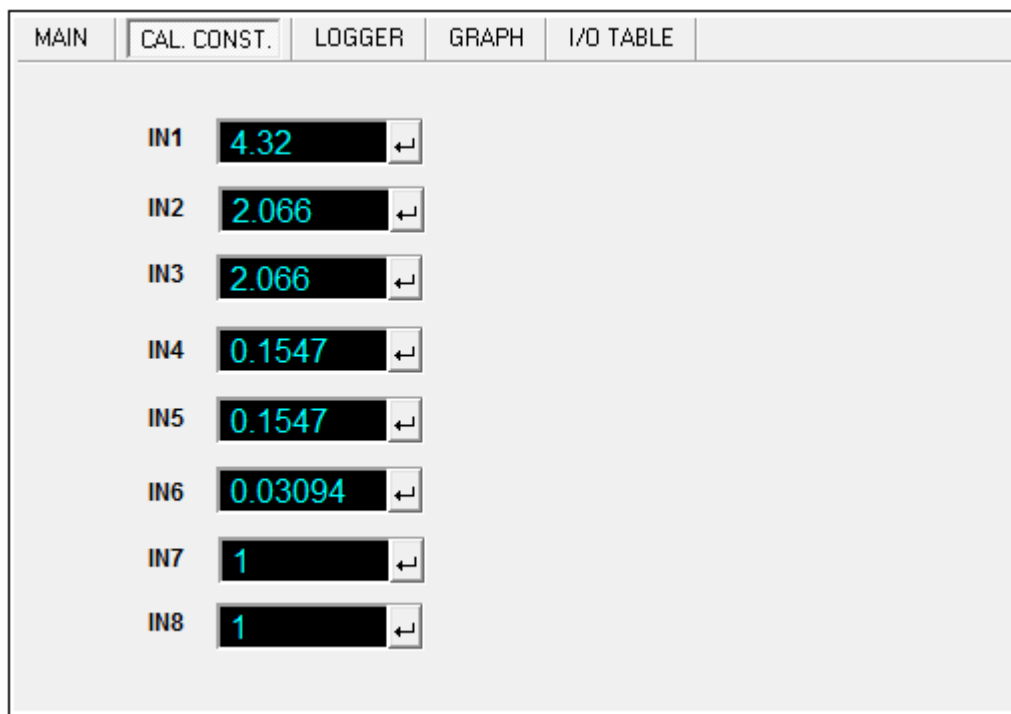


Figure 4.6. The calibration constants window



The calibration constant for Magnetic flow meter is 4.32, 2.066 for pressure transducers, 0.1547 for the differential pressure sensors whose measuring pressure range is between 0-5 bars, and 0.03094 for the differential pressure sensor whose measuring pressure range is between 0-1 bars and 1 for water meter.

**I/O TABLE TAB:**

This menu represents the specifications of data loggers and addresses the data loggers to the measurement devices. This window also shows calculation procedure of the calibration constants. Also calculation of PID parameters is explained in this window.

|      |             |        |       |           |
|------|-------------|--------|-------|-----------|
| MAIN | CAL. CONST. | LOGGER | GRAPH | I/O TABLE |
|------|-------------|--------|-------|-----------|

DATALOGGER LABJACK U3 LV  
DATALOGGER ADDRESS : 56  
TERMINATION RESISTORS : 121 OHMS ( 4 mA\*121ohm=0.484V@ ZERO INPUT )  
(20mA\*121ohm=2.42 V@ MAX. INPUT )  
CALCULATION CAL. CONST. : SENSOR MAX. OUT / (2.42-0.484)

| DATALOGGER | DESCRIPTION                                      |
|------------|--|
| FIO0       | IN1 : FLOWMETER 1 (4...20mA) (cal. const. =4.32) |
| FIO1       | IN2 : PRESSURE SENSOR 1 (0...4 BAR 4...20mA)     |
| FIO2       | IN3 : PRESSURE SENSOR 2 (0...4 BAR 4...20mA)     |
| FIO3       | IN4 : DIFF. PRE. SENSOR 1 (0...5 PSIA 4...20mA)  |
| FIO4       | IN5 : DIFF. PRE. SENSOR 1 (0...5 PSIA 4...20mA)  |
| FIO5       | IN6 : DIFF. PRE. SENSOR 1 (0...1 PSIA 4...20mA)  |
| FIO6       | IN7 :SPARE (4...20mA)                            |
| FIO7       | IN8 :COUNTER (PULSE) (FLOWMETER USED 1L/PULSE)   |
| CIO0       | EMERGENCY BUTTON INPUT                           |
| CIO3       | MOTOR START OUTPUT                               |
| DAC0       | MOTOR SPEED VALUE ANALOG OUT                     |

PID NOTES :  
 $Y = (K_P * X) + (K_I * \text{integral}(X) dt) + (K_D * dX/dt)$   
 $X = ( \text{Desired value} - \text{Actual value} ) = (X+) - (X-)$  TN = Integrator rate time constant  
KI =  $K_P / T_N$  KI =  $K_P/T_N$  KD =  $K_P \times T_V$  TV = Derivation rate time constant

Figure 4.7. I/O Window

### **LOGGER: (EXCEL)**

The logger section aims to make easier the data collection. With this option, the data can be recorded in excel format and it is easy to transform data to an excel file. There is opportunity to start and stop the data recording at any time and also the time step of the data recording is up to the user. There are ten columns, eight of them are addressed to the eight displays and last two are addressed to time and date of the experiment.

### **GRAPH:**

This tab lets the user to take data in graph format. The data of any selected display with respect to time is represented with the graphs. This section is useful to check the steady state behavior of the setup during conducting experiments.

## **5. PROCEDURES OF MEASUREMENTS AND ANALYSES**

Test procedures for the experiments can be classified into two groups according to the aim of the measurement. First type procedures are defined and described in the following section for flow rate measurements. Second type procedures include pressure drop measurement. Pressure drop measurement procedures are defined for each section of the experiment setup. Each section has different components and different pressure drop characteristics were included.

### **5.1. FLOW RATE MEASUREMENT PROCEDURES**

Flow rate measurement is performed via two volumetric flow rate measurement devices, magnetic flow meter and water meter. Magnetic flow meter and water meter are placed on the different branches of the setup. The experimental procedures are described as follows for each measurement technique.

#### **5.1.1. Measurements with the Magnetic Flow Meter**

The experimental procedure for measurements with the magnetic flow meter can be summarized with the steps listed below:

- *Gate valves (1), (3) and (8)* are opened while the all others are closed. Total rate of the flow goes through the magnetic flow meter.
- The pump revolution is set to a value and volumetric flow rate goes through the magnetic flow meter can be read from software display (*IN1*) or directly from the display on the magnetic flow meter in units of liters per second.
- The pressure value at the pump outlet is set to a value and with the same valve positions, volumetric flow rate can be recorded from displays in units of liters per second.
- Before recording the data, the 300 seconds run is necessary for the measurement devices reaches to the steady state conditions.

### 5.1.2. Measurements with the Water Meter

The experimental procedure for flow rate measurement with the water meter is performed by using following steps:

- *Gate valves (2), (4) and (8)* are opened while the rest is closed. Total rate of the flow now goes through the water meter.
- For a fixed value of the pump revolution, total volume of the fluid passes through the water meter can be read from software display (*IN8*) in the units of liters.
- For a fixed value of the pressure at the pump outlet, total volume of the fluid passes through the water meter can be recorded from software display (*IN8*) in the units of liters.
- Before recording the data, the 300 seconds run is necessary for the measurement devices reaches to the steady state conditions.
- Total volume of fluid passes through the water meter is recorded.
- The run time of each measurement (after 300 seconds) is also recorded to determine the volumetric flow rate in the units of liters per second.

### 5.2. PRESSURE DROP MEASUREMENT PROCEDURES

In this study, the experiments are described for the pressure drop measurements to investigate the friction loss coefficient, hydraulic loss coefficients of fittings, expansion coefficient and observation of parallel flow. For the pressure drop measurements, differential pressure measuring equipments are added to the setup. There are three differential pressure cells on the setup. Table 5.1 represents the name of the DP cell, range of measurement and their display numbers on the software which is used to read the measurements of the DP cells.

Table 5.1. Properties of the differential pressure measuring equipments

| DP cell | Measurement range (psia) | Measurement range (mbar) | Display |
|---------|--------------------------|--------------------------|---------|
| DP 1    | 0-5                      | 0-344                    | IN 4    |
| DP 2    | 0-5                      | 0-344                    | IN 5    |
| DP 3    | 0-1                      | 0-69                     | IN 6    |

### **5.2.1. Description of Experiments in Section 1**

In this section of the setup, head loss due to the friction is observed. There are three dimensionally equivalent pipes which are made of different materials, stainless steel, copper and PVC. Length and diameter of the pipes are 1.85 m and 3.2 cm respectively. The experimental procedure for Section 1 is followed for each pipe.

The standard procedure for determination of friction factor experimentally is based on measurement of the pressure drop through the pipe. The experimental procedure can be summarized with three basic steps. The first step is selection of the pipe material. The selected pipe is placed between flanges, carefully. System must be checked for any leak from system, especially from just placed pipe cuffs.

Measurement points are numbered for the simplicity of the experimental procedure definitions. The second step is placing the DP cell's high and low branches to the measurement points *measurement point 1*(pipe inlet) and *measurement point 2* (pipe outlet). For the various volumetric flow rates, pressure drop through the pipe is measured. Finally the friction loss coefficient is estimated by using the theory explained in Chapter 2.

### **5.2.2. Description of Experiments in Section 2**

The second section of the setup aims to observe flow in parallel pipes. There three parallel pipes on this section. In general, parallel flow is analyzed for parallel branches which lie at the same elevation. But the parallel flow included in this setup covers a number of flow resistance mechanisms such as gravity, area change, etc. The control of the flow is provided with globe valves which are placed at the entrance of each branch.

The experimental procedure for this section is based on pressure drop measurements on all branches individually. In addition to those measurements, overall pressure drop between inlet and outlet of the branching section. The aim of pressure drop measurement is to evaluate the volumetric flow rate in the each pipe to observe flow separation at the branch point.

Moreover, the experiments can be performed for previously stated pressure drop values. For a desired pressure drop values globe valve positions can be arranged. These kinds of experiments bring along the engineering judgment for practical applications.

### 5.2.3. Description of Experiments in Section 3

The main aim of the third section of the set up is to observe the pressure losses on fittings. The pressure drops on the 90° degree elbows are measured and hydraulic loss coefficients are determined. Also, there are other turn fittings, which are made by arranging the small pipes and elbows, such as C-shape bends and S-shape bends. C-shape bend is a fitting which used to change the direction of the flow to the opposite of the previous direction. On the other hand S-shape bend does not change the direction of the flow but its elevation. In addition to loss coefficients for turn fittings, the pressure gain due to pipe enlargement is examined. It is certain that friction losses on pipes and all fittings, included in this section, is also main contributor of the pressure loss along the section. The volumetric flow rate is remained constant during measurements. All pressure loss and gain contributors are taken into account for each measurement.

The definition of loss coefficient for elbows is given in Section 2.3. The values of the hydraulic loss coefficient are obtained by using the data of the pressure drop measurements. The loss coefficients for the elbows are obtained by performing sets of measurements between various measurements points placed on the section. Measurement points are selected in order to include various numbers of elbows between measurement points.

The effect of enlargement in the pipe diameter is observed by using pressure drop data between *the measurement points 16-17*. In order to maintain the constant volumetric flow rate an increase in cross sectional area of the pipe (or pipe diameter) means lower velocity. This relation is indicated with Eq.5.1.

$$Q = A_1V_1 = A_2V_2 \quad (5.1)$$

As  $A_2$  increases,  $V_2$  must be lower to maintain the same volumetric flow rate. This means that in the large diameter pipe the volume of fluid is moving more slowly and has less kinetic energy than it will have when it gets into the small diameter pipe. Pressure change in a straight pipe is related to the density of the fluid and velocity of the fluid in associated flow area. Therefore, the pressure difference can be written in the Eq.5.2:

$$P_2 - P_1 = \frac{V_1^2 - V_2^2}{2\rho} \quad (5.2)$$

If there is an increase in pipe diameter then  $A_2 > A_1$  and  $V_1 > V_2$ . Eventually, the change in pressure is positive. As a consequence, for an accurate measurement, the blue (low) branch of the DP cell is placed on the small diameter pipe while the red (high) one is placed on the large diameter pipe during the measurement.

As a last part of this section, a hydraulic loss coefficient determination for a gate valve is examined with pressure drop measurement between *measurement points 19-1*. Although the examined gate valve is not placed at the section 3, this experiment is included in this section to put the all hydraulic loss coefficient determination experiments on the same data sheet.

### 5.3. RELAP ANALYSES

RELAP which is a best-estimate code used for simulations of the nuclear reactor applications, was used to simulate the experiments. Eight of the experimental data were selected to simulate and results of the RELAP were compared with the results of the experiments. The selected experiments are listed in Table 5.2.

Table 5.2. Experiments selected for RELAP analyses

| Section number | Experiment simulated with RELAP   |
|----------------|---|
| 1              | <ul style="list-style-type: none"> <li>• Friction loss coefficient determination for the stainless steel pipe</li> <li>• Friction loss coefficient determination for the copper pipe</li> <li>• Friction loss coefficient determination for the PVC pipe</li> </ul> |
| 2              | <ul style="list-style-type: none"> <li>• Sampling 1</li> </ul>  |
| 3              | <ul style="list-style-type: none"> <li>• The 90° degree elbow (down)</li> <li>• The 90° degree elbow (up)</li> <li>• Gradual enlargement</li> </ul>   |

RELAP inputs were prepared for each section of the setup, individually. The appropriate components were used among the component library of RELAP. The components which were used in simulations are:

- Pipe
- Single junction
- Single volume
- Time dependent volume
- Single branch

The single volume and time dependent volume components were used to define the inlet and the outlet conditions of the modeled system. The pipe component was the most frequently used component for RELAP analyses of this study. The pipe component can be divided into number of volumes to obtain more accurate pressure drop analyses. Single junction components were used to link the two components which are, successively. The input file of RELAP includes input cards which define geometry, boundary and initial conditions of the components.

#### **5.4. REPEATABILITY ANALYSES**

To assess the repeatability of the experiments and the stability of the apparatus used to measure the differential pressure and flow rates, selected experiments were run six times. The selected experiments are the estimation of friction factor in the first section, the hydraulic loss coefficient determination of the 90<sup>0</sup> elbow (down) and the expansion coefficient determination in third section. In the estimation of the friction factor experiments, after each test, DP cell jacks were dismounted from the measurement points, water that fills the arms was evacuated, pipe was removed by opening the cuffs, and it was replaced again, DP cell jacks connected to the interested measurement points, DP cell arms were filled again and measurement is repeated. In this way, not only measurement uncertainty, but also non-reproducibility due to testing technique for the first section would be addressed. Figure 5.1 shows the estimated friction loss factors of six tests conducted for section 1 for the range of flows presented. The maximum difference is less than 4% at average velocities



between 2.1 and 3.1 m/s and the maximum difference is less than %2 at the average velocities larger than 3.1 m/s and less than %1 at the average velocities less than 2.1 m/s.

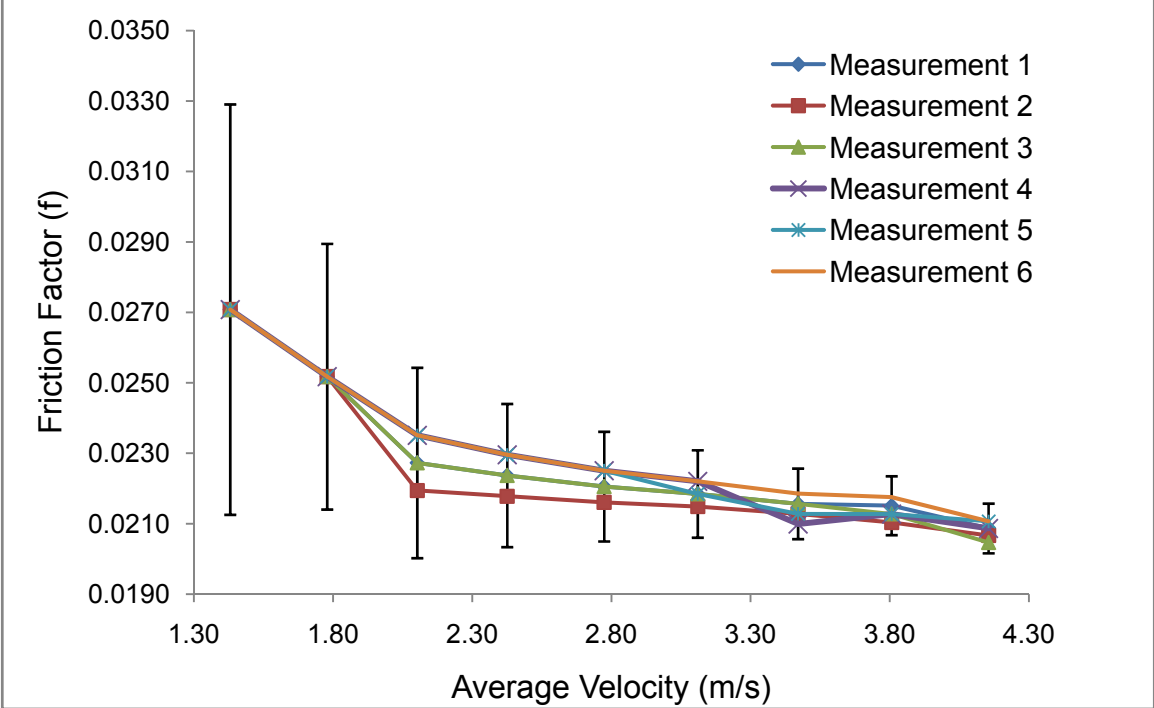


Figure 5.1. Repeatability of friction factor determination (copper pipe)

The 90° elbow in the third section was also tested six times for the repeatability analysis. After each test, DP cell jacks were disconnected from the measurement points, water that fills the arms was evacuated, filled and re-placed again and then the measurement was repeated. The repeatability of the experiments was tested by comparing hydraulic loss coefficient of the 90° elbow was assessed. Figure 5.2 illustrates K-values obtained from the six tests versus the average velocities. There is no difference at the average velocities less than 2.8 m/s. The maximum difference is less than 8% at average velocities greater than 2.8 m/s and the maximum difference is less than %12 at the average velocity of 4.1 m/s.

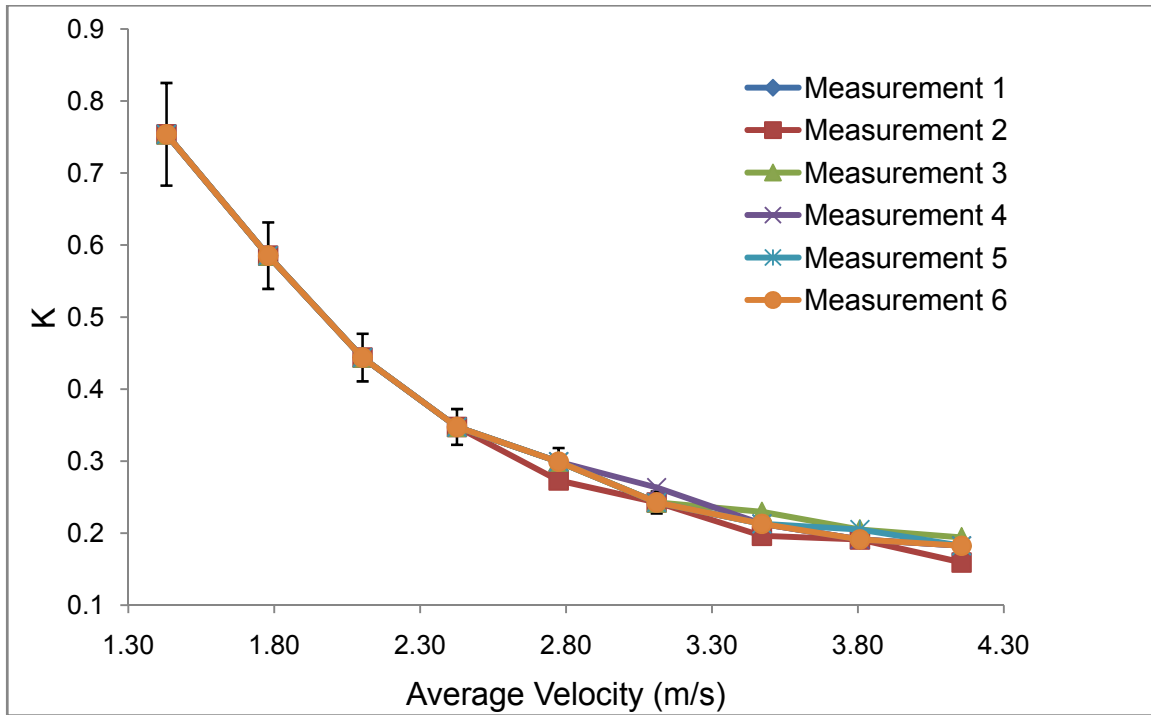


Figure 5.2. Repeatability of hydraulic loss coefficient of elbow (down)

The measurements used for analysis of the expansion coefficient (K-value) determination were performed six times for the repeatability analysis. After each test, DP cell jacks were disconnected from the measurement points, water filling the arms was evacuated, filled and re-placed again and then the measurement was repeated. The repeatability of the tests was checked by obtaining the expansion coefficient. Figure 5.3 illustrates K-values obtained from the six tests versus the average velocities. There is no difference at the average velocities 4.1 and 4.3 m/s. The maximum difference is less than 7% at average velocities less than 4.1 m/s and the maximum difference is less than %5 at the average velocities greater than 4.3 m/s.

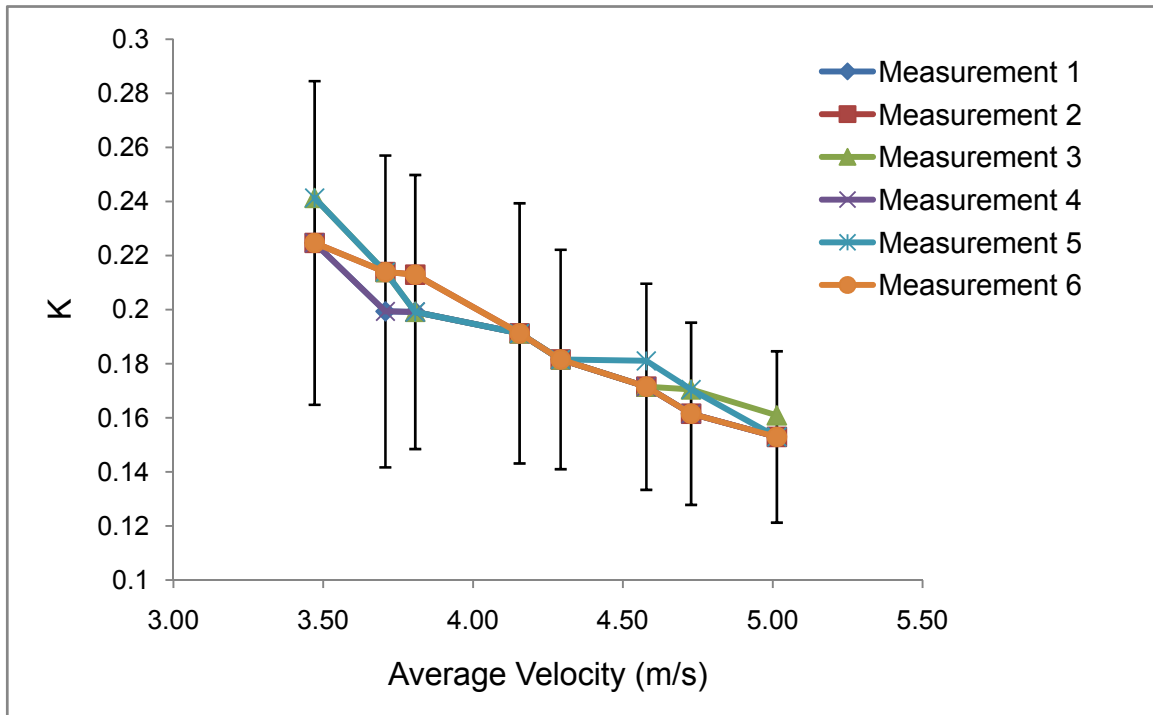


Figure 5.3. Repeatability of contraction coefficient

## 6. DATA AND RESULTS

### 6.1. FLOW RATE MEASUREMENT

There are two sets of data for the flow rate measurement part of the experiment. First data set is obtained with measurements of the magnetic flow meter and second data set is obtained by using the measurements of the water meter.

#### 6.1.1. Measurement with Magnetic Flow Meter

The measurement procedure for the magnetic flow meter is explained in section 4.1. The resultant data for this section can be subdivided into two groups by taking the pump run technique into account.

The first pump run technique is using fixed pump revolution values. Figure 6.1 shows the volumetric flow rate values versus change in pump revolution values in percentage. The volumetric flow rate linearly increases with increase pump revolution values.

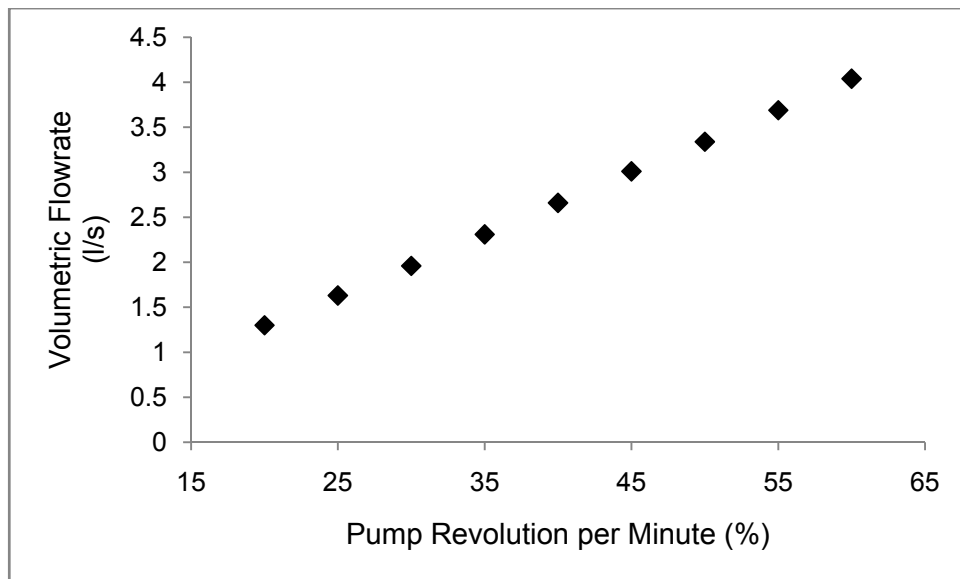


Figure 6.1. Magnetic Flow Meter: Volumetric Flow rate vs Pump RPM

The second pump run technique is fixing the pump outlet pressure. Figure 6.2 represents the result of the measurements according to change in pump outlet pressure. As the pump outlet pressure increases, the volumetric flow rate increases.

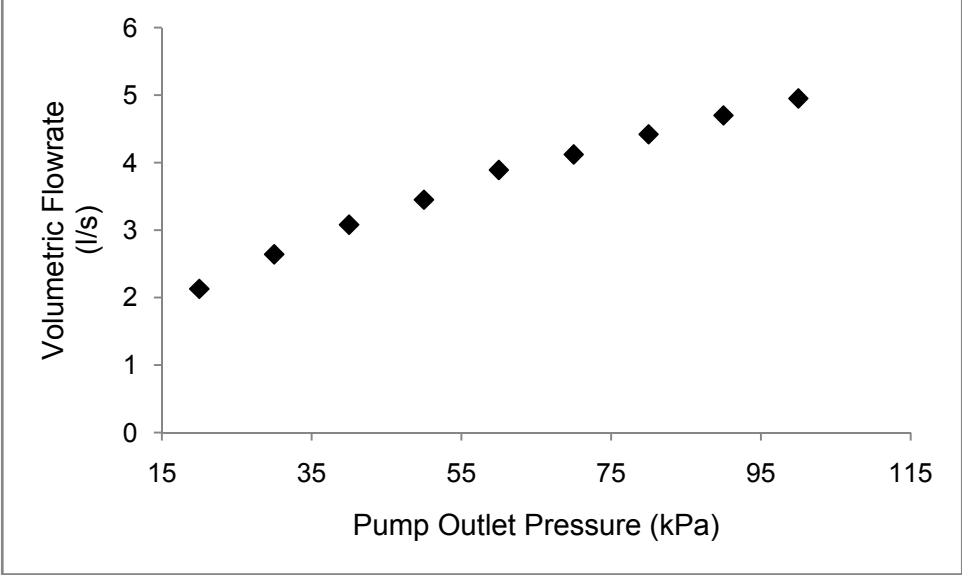


Figure 6.2. Magnetic Flow Meter: Volumetric Flow rate vs Pump Outlet Pressure

**6.1.2. Measurement with Water Meter**

The measurement procedure for the water meter is explained in section 4.1.2. The resultant data for this section can also be divided into two groups due to the for two pump run techniques as mentioned in the previous section.

In Figure 6.3, the volumetric flow rate values via change in pump revolution are presented. The data is obtained by measuring the total volume of fluid passes through the water meter in 100 seconds. As it can be seen from figure 6.3, the volumetric flow rate is linearly increasing with increase in pump revolution per minute.

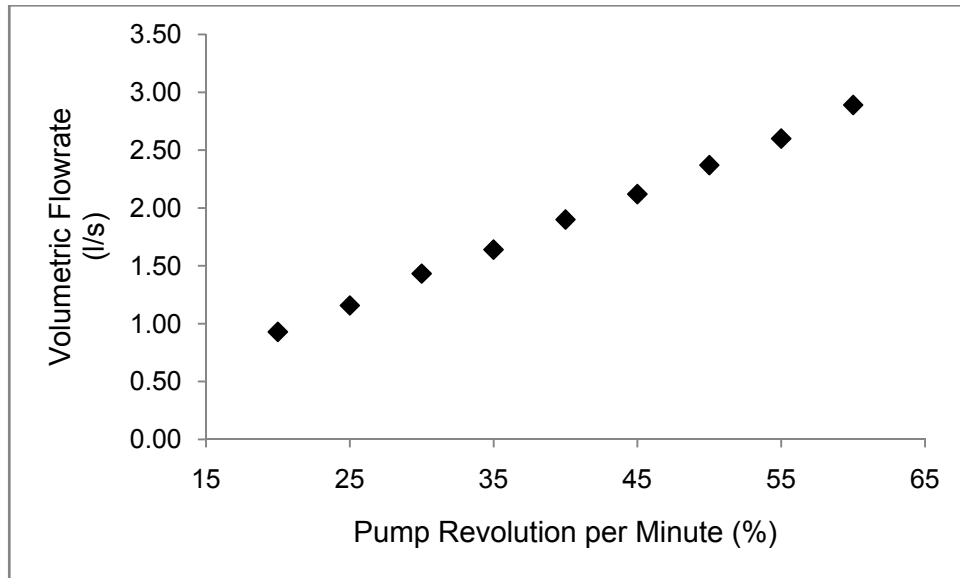


Figure 6.3. Water Meter: Volumetric Flow rate vs Pump RPM

Figure 6.4 shows the volumetric flow rate values via the pump outlet pressure.

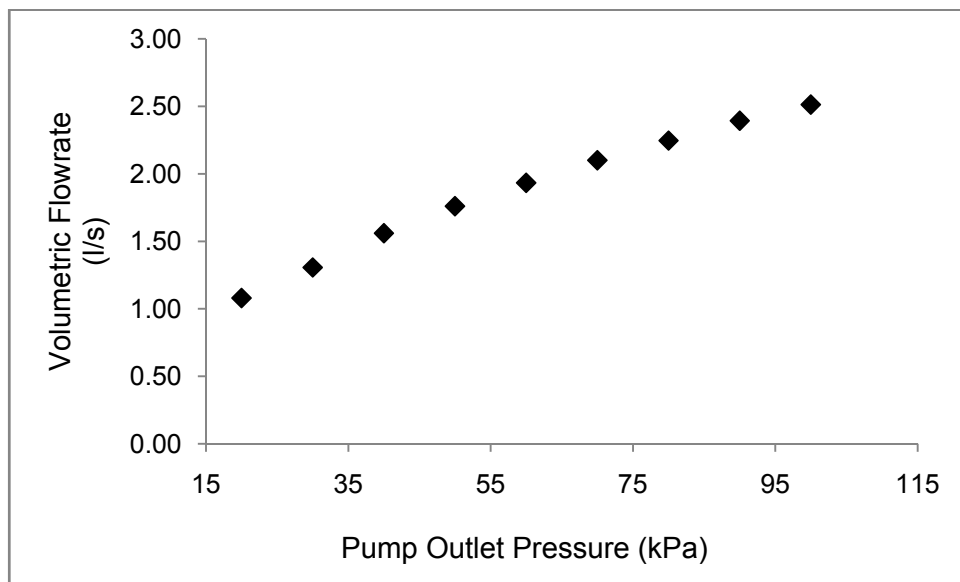


Figure 6.4. Water Meter: Volumetric Flow rate vs Pump Outlet Pressure

## 6.2. PRESSURE DROP MEASUREMENT

### 6.2.1. Section 1

In this section, the friction factors for pipes which have identical dimensions but made by different materials are obtained. The change in friction factor with the change in the

Reynolds number and roughness are analyzed. The theoretical information about friction factor is given in Chapter 2. In the light of the theory, it can be admitted that friction factor determination is strongly based on the pressure drop measurements. The experimental procedures for the pressure drop measurements in the first section are described in Chapter 5.

The friction factor behavior is reported as a function of Reynolds number in literature. Hence, the obtained friction factor values of each pipe, made by different materials, are given via the Reynolds number. In addition, comparison with literature has been made by using the Colebrook formula (Eq.2.39) which is widely used expression to estimate friction factor in pipes.

The error bars on the graphs shows the range of estimation error which arises from the measurement errors. The ranges of the errors are obtained by using error propagation rules and the detailed explanations of the measurement error analyses which are available in Appendix C.

#### **6.2.1.1. Stainless Steel Pipe**

The Moody Chart (Figure 2.13) shows the change in the friction factor as a function of Reynolds number and relative roughness values. According to this chart, the expected trend for the friction factor as a function of Reynolds number can be stated. The friction factor reduces, as the Reynolds number increases. The results of the friction factor determinations for the stainless steel pipe are represented in Figure 6.5. As shown in the figure, the expected trend for the friction factor as a function of Reynolds number is obtained. The results are also consistent with the results obtained by Colebrook formula. Colebrook friction factors for the same flow characteristics are all in the error range of the results obtained by the experiment. The friction factor values obtained in this study agree better with to the Colebrook results at Reynolds number of approximately 70000.

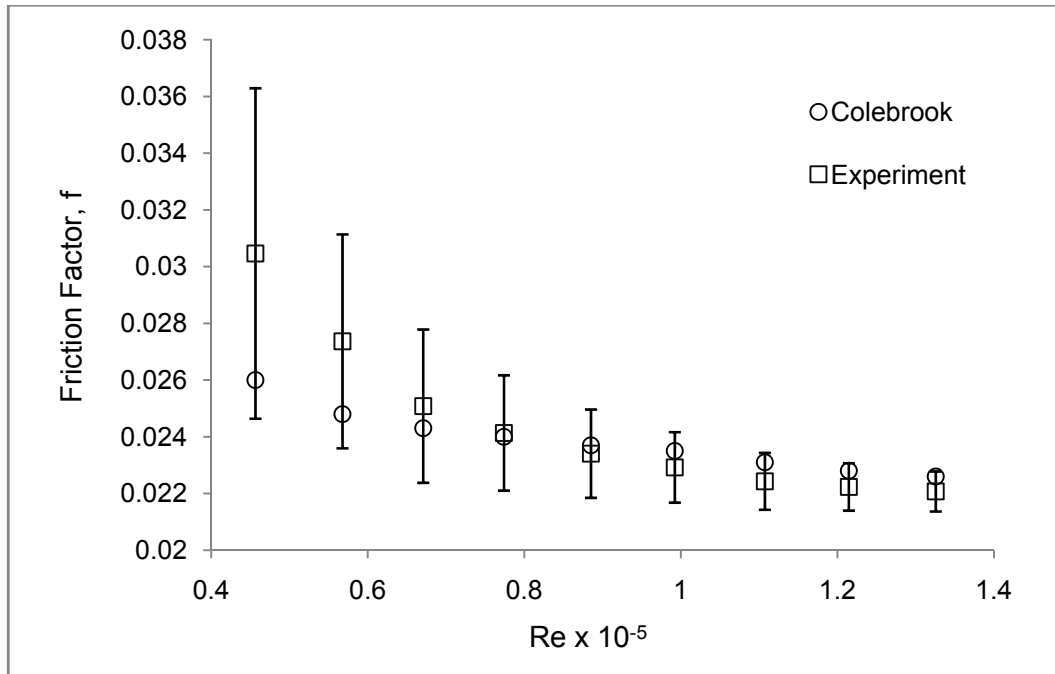


Figure 6.5. Section 1: Friction factor of the stainless steel pipe

### 6.2.1.2. Copper Pipe

The results of the friction factor determinations for the copper pipe are represented in Figure 6.6. It is clear from the figure that the expected trend for the friction factor as a function of Reynolds number is obtained. The results are consistent with the results obtained by Colebrook formula. Colebrook friction factors for the same flow characteristics are all in the error range of the results obtained by the experiment. The friction factor values become closer to the Colebrook results as the Reynolds number increases.



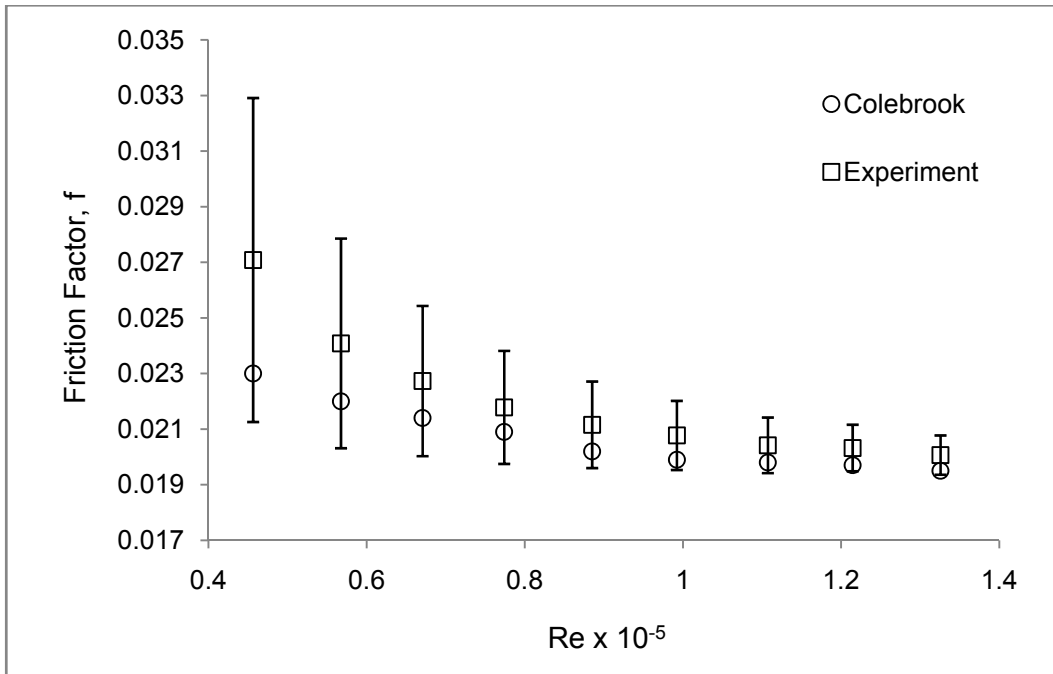


Figure 6.6. Section 1: Friction factor of the copper pipe

### 6.2.1.3. PVC Pipe

The results of the friction factor determinations for PVC pipe are represented in Figure 6.7. In the figure, the trend for the friction factor as a function of Reynolds number is compatible with the expected trend. The results are consistent with the results obtained by Colebrook formula. Colebrook friction factors for the same flow characteristics are all in the error range of the results obtained by the experiment. As the Reynolds number increases, the friction factor values become more coherent with the Colebrook friction factors.

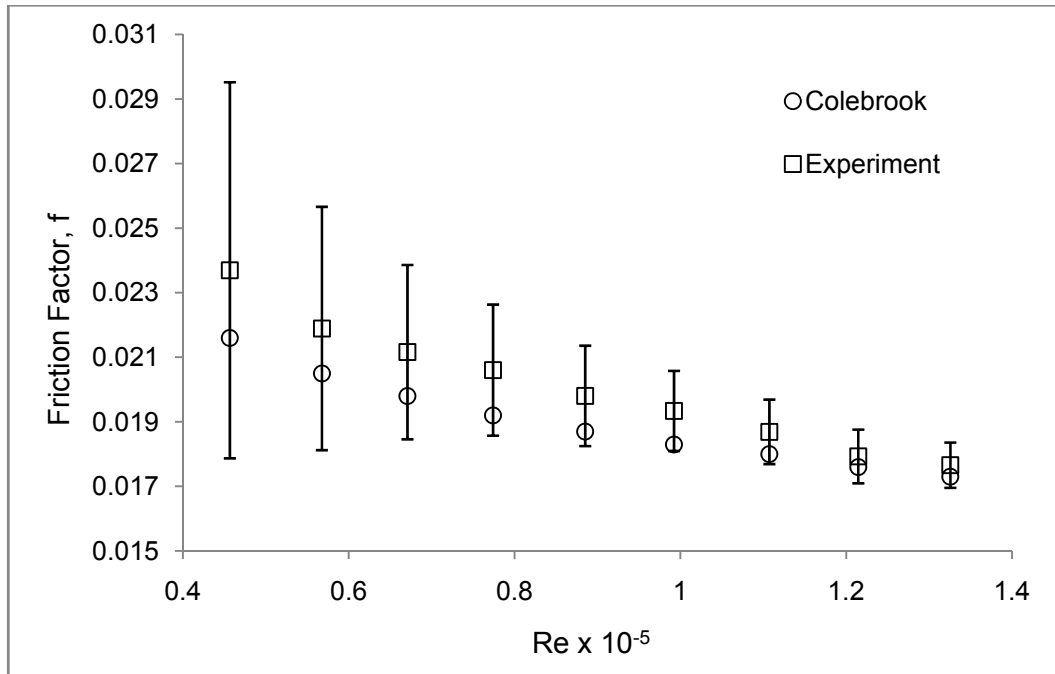


Figure 6.7. Section 1: Friction factor of the PVC pipe

#### 6.2.1.4. Effect of Roughness on the Friction Factor

The commercial stainless steel, copper and PVC pipes all have different roughness values. The standard roughness values for the stainless steel, copper and PVC pipes are given in Table 6.1. The stainless steel has the greatest roughness among the materials used in the setup. The roughness of the commercial stainless steel is three times greater than that of the copper and thirty times greater than that of the PVC pipe as presented in Table 6.1.

Table 6.1. Roughness of the pipes

| Pipe Material   | Roughness         |
|-----------------|-------------------|
| Stainless steel | 45 $\mu\text{m}$  |
| Copper          | 15 $\mu\text{m}$  |
| PVC             | 1.5 $\mu\text{m}$ |

Based on the roughness information given in Table 6.1, it can be commented that the stainless steel has the greatest friction factor and the friction factor of the PVC pipe is the smallest while friction factor of the copper at the middle of those two at the same

Reynolds number. Figure 6.8 shows the effect of roughness on friction factor. The values of friction factors for the stainless steel, copper and PVC pipes are compared in this figure. As the relative roughness decreases, the associated friction factor value decreases. The relative roughness values are used for comparison as in the Moody Chart (Figure 2.13). The results are consistent with the expectations. The greatest friction factor values are obtained for the stainless steel pipe and smallest values for the PVC pipe at the all Reynolds numbers. Moreover, it can be said that the trend of friction factor via Reynolds number becomes linearly decreasing profile as the relative roughness decreases. This result is compatible with the Moody Chart (Figure 2.13) for the Reynolds number range used for sampling.

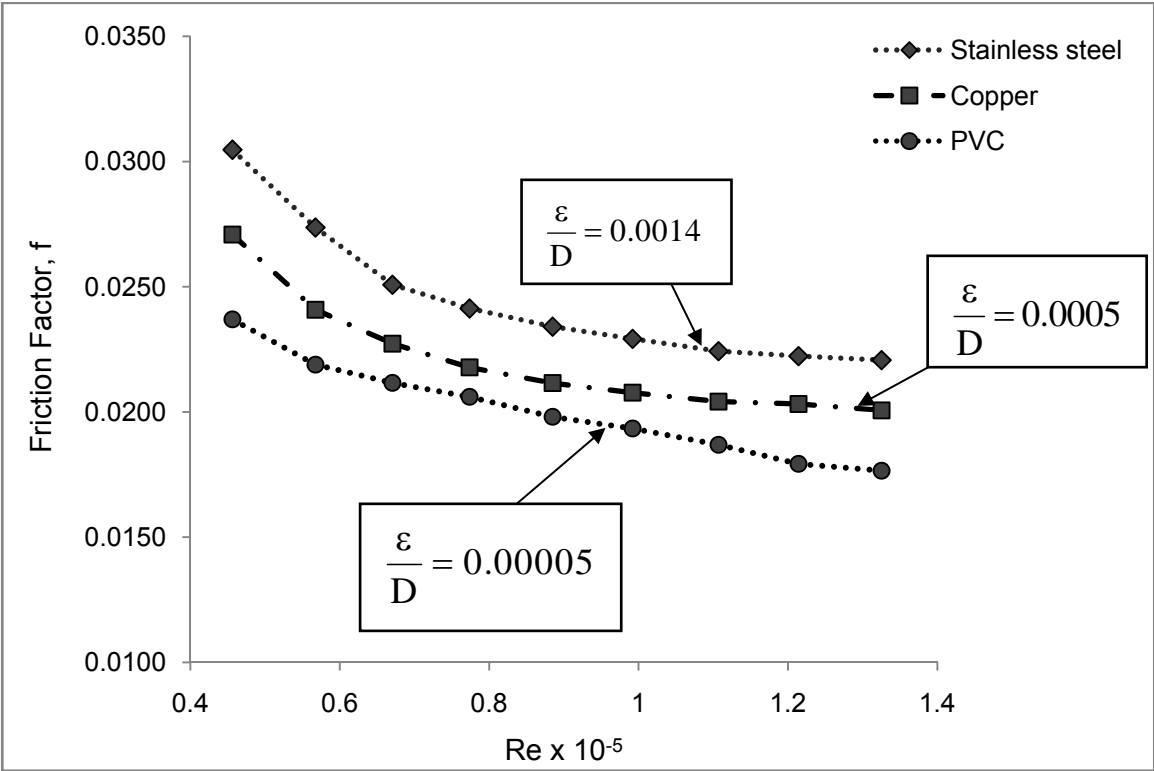


Figure 6.8. Friction Factor Chart

**6.2.2. Section 2**

The parallel flow is analyzed in this section. Flow is separated into three branches at some point and then merges after moving through 1 meter horizontal pipes that are parallel. Each branch has different diameters. The diameter of the upper branch (Branch 1) is 2.4 cm, of the middle branch (Branch 2) is 3.2 cm and of the lower part

(Branch 3) is 4.0 cm. The effect of flow area and gravity on flow separation can be observed. There are three globe valves are placed on branches to control the flow. Hence, there is great number of analyses which can be made for various globe valve opening fractions.

The theoretical information about parallel flow is given in Chapter 2. The basic theory behind the parallel flow is based on conservation of mass or in other terms volumetric flow rate. Volumetric flow rate at the inlet of the branch must be equal to the outlet of the branch. In this section, analyses are made for total volumetric flow rate estimation which based on estimation of volumetric flow rate in each branch. Volumetric flow rate in each branch is obtained by using pressure drop measurements through each branch. The experimental procedures for the pressure drop measurements in the parallel flow section are described in Chapter 5.

From a great number of measurements which include many combinations of the valve positions, selected sample results are presented here, and these results are marked as "*sampling*". In the first selected sampling, the globe valve of the upper branch and that of the lower branch are full opened while the globe valve of the middle branch is full closed. According to the pressure drop data on each branch, volumetric flow rate of each branch is obtained. Eventually, total volumetric flow rate is estimated. The estimated volumetric flow rate values are compared with the measurement results of magnetic flow meter. Figure 6.9 represents the results of the analysis for this sampling which is called "*sampling 1*". The estimated total volumetric flow rate values are in good agreement with the measurements.

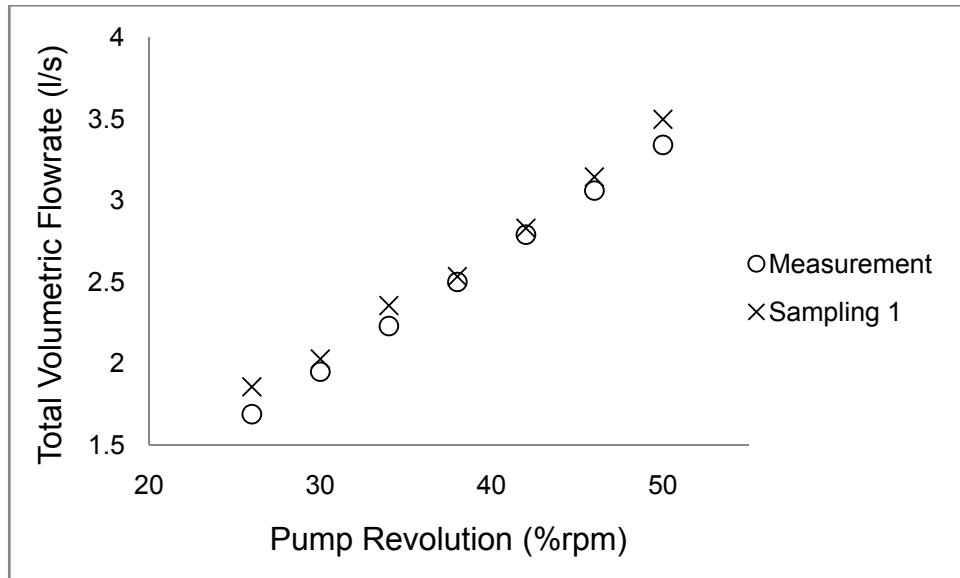


Figure 6.9. Estimated total volumetric flow rate for parallel flow sampling 1

In addition to estimation of the total volumetric flow rate, separation of the flow in branches is observed. Figure 6.10 shows the fractional volumetric flow rate in Branch 1 and 3. The fractional volumetric flow rate in Branch 1 is about %65 on average and in Branch 3 is about %35. At the branching point, substantial fraction of the total volumetric flow rate goes towards the Branch 1.

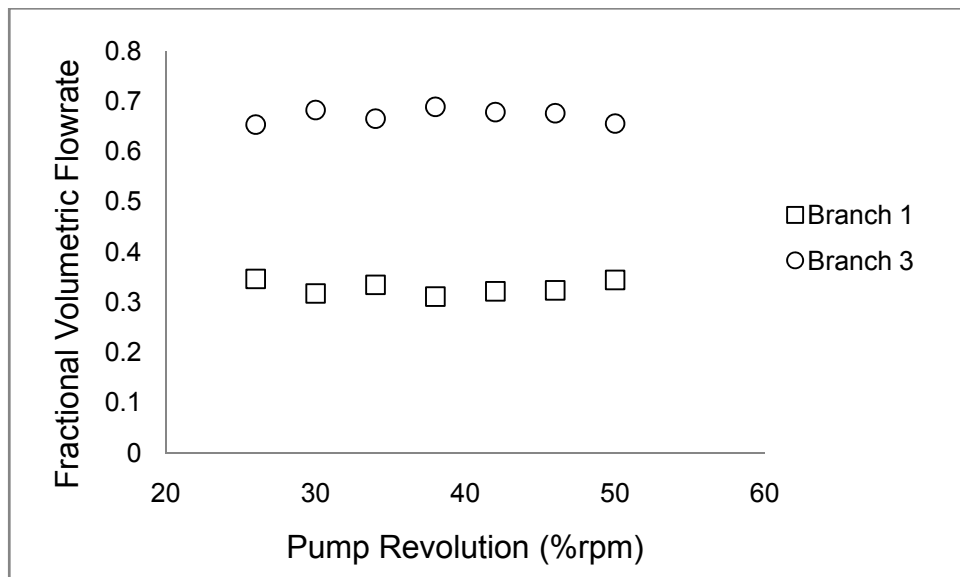


Figure 6.10. Fractional volumetric flow rates in branches for sampling 1

In the second sampling, the globe valve of the upper branch is fully opened and opening fraction of the globe valve at middle branch is 0.6 and the globe valve of the lower branch is fully closed. Figure 6.11 represents the results of the analysis for this sampling which is called “*sampling 2*”. The estimated total volumetric flow rate values are consistent with the measurements.

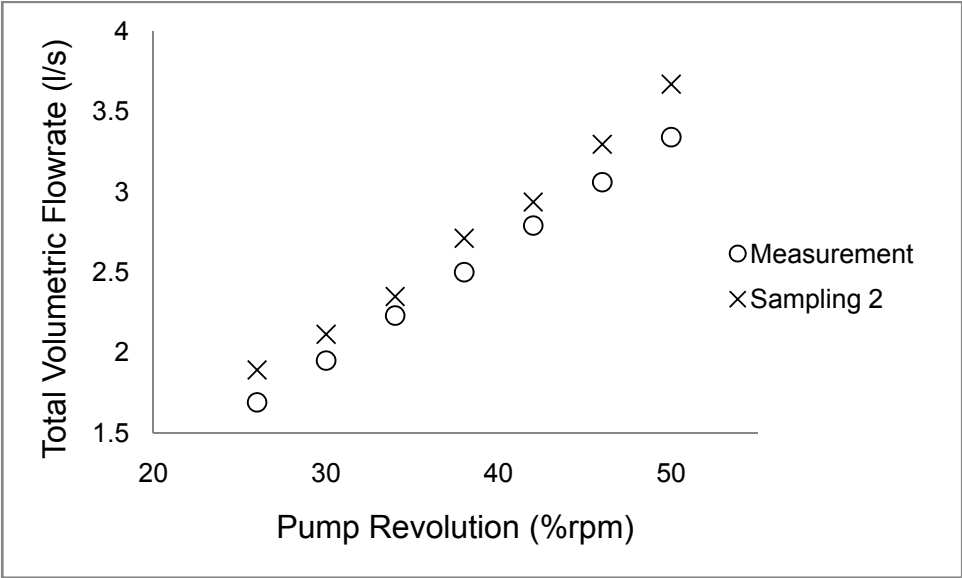


Figure 6.11. Estimated total volumetric flow rate for parallel flow sampling 2

Figure 6.12 shows the fractional volumetric flow rate in Branches 1 and 2. The fractional volumetric flow rate in Branch 1 is about %75 on average and in Branch 2 is about %25. At the branching point, substantial fraction of the total volumetric flow rate goes towards the Branch 1.

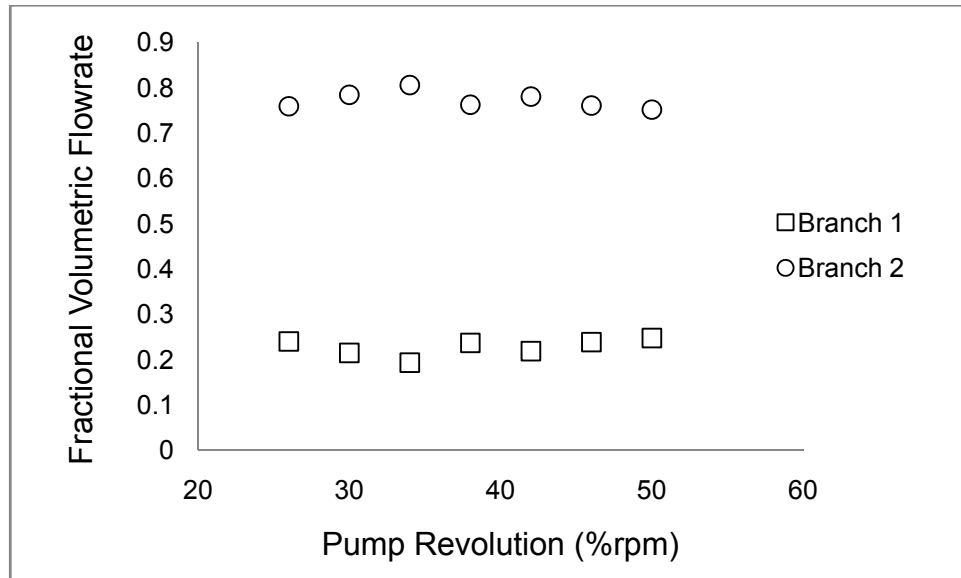


Figure 6.12. Fractional volumetric flow rates in branches for sampling 2

The elevation difference between Branch 1 and Branch 2 is 20 cm and between Branch 1 and Branch 3 is 40 cm. It is observed that the effect of flow area on the flow separation is more dominant than the effect of gravity.

### 6.2.3. Section 3

This section of the setup includes the determination of the hydraulic loss coefficients for various fittings. The examined fittings are 90° elbows, C-shape turn, S-shape turn, gradual expansion in pipe diameter and gate valve. The theoretical information about the hydraulic loss coefficients is given in Chapter 2. As in friction factor determination, hydraulic loss coefficient determination is directly related to the pressure drop measurements. The experimental procedures for the pressure drop measurements for this section are described in Chapter 5.

The hydraulic loss coefficient values are reported as a function of the Reynolds number in literature. Hence, the hydraulic loss coefficients are reported via Reynolds number and compared with the literature. For comparisons, results of Idelchik experiments [ref: no] are used because these results cover wide variety of fittings.

The error analyses for the hydraulic loss coefficients are based on measurement errors. The ranges of the errors are obtained by using error propagation rules and the

detailed explanations of the measurement error analyses are represented in Appendix C.

**6.2.3.1. Hydraulic Loss Coefficient of 90° Flanged Elbow (up):**

The second 90° elbow changes the direction of the flow from lower to higher elevation. As a result, the trend of the hydraulic loss coefficient varies. Figure 6.13 and Figure 6.14 represent the hydraulic loss coefficients. The hydraulic loss coefficient for this elbow increases significantly as the Reynolds number increases up to Reynolds number of 130000. From this point, increase in hydraulic loss coefficient slows down, obviously. Depending on the range of Reynolds number and relative roughness values, the trend in Figure 6.14 and 6.15 is consistent with the Idelchik data shown in Figure 2.15.

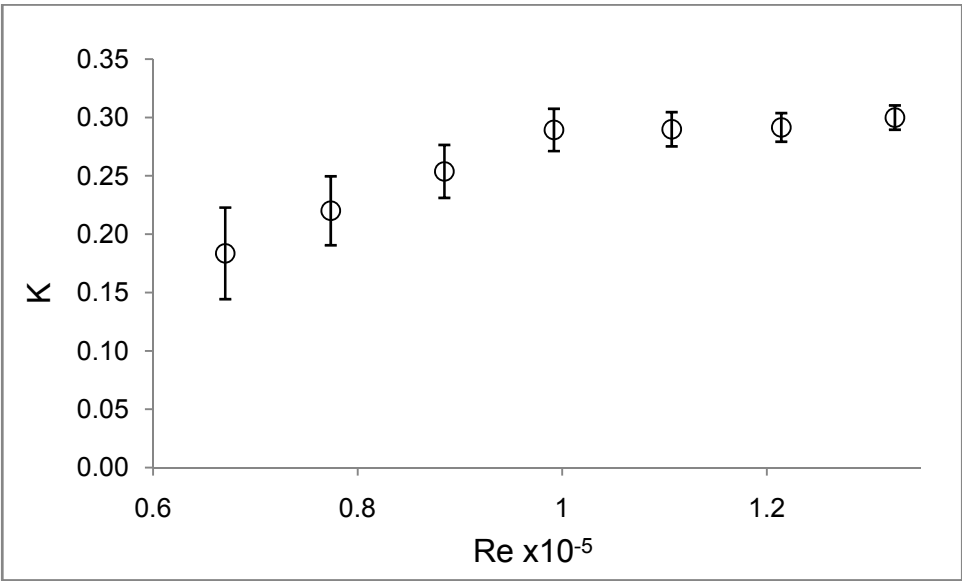


Figure 6.13. Hydraulic loss coefficients of the 90° elbow (up)

In Figure 6.14, the measurement error of the result for Reynolds number of 142000 is greater than that of the result for Reynolds number of 130000. This increase is caused by changing the pressure drop measurement equipment. DP 3 is used for measurements until the Reynolds number of 130000. But for greater values of the Reynolds number DP 3 is off the limit and DP 1 is used for further measurements. Eventually, this replacement affects the measurement errors.



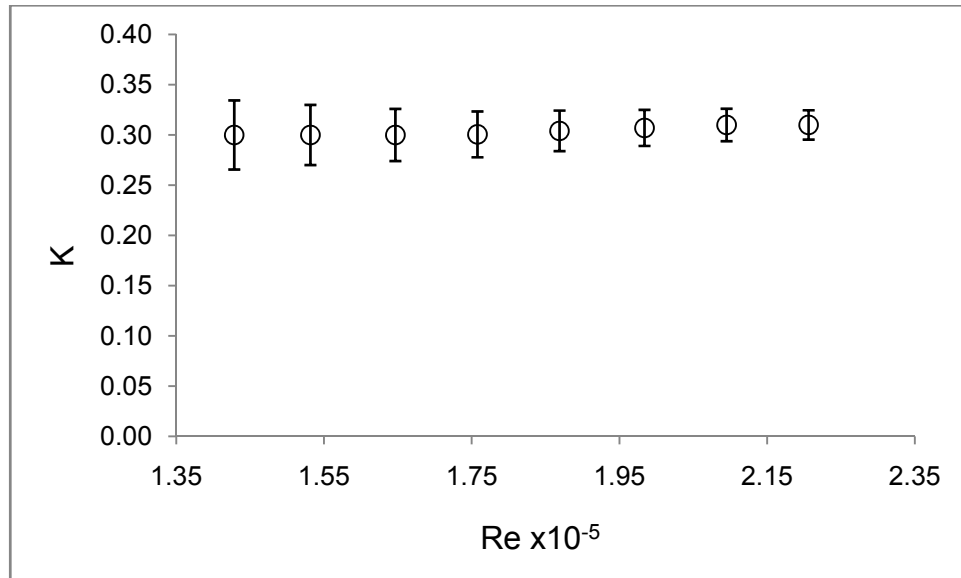


Figure 6.14. Hydraulic loss coefficients of the 90<sup>0</sup> elbow (up) (cont.)

#### 6.2.3.2. Hydraulic Loss Coefficient of 90<sup>0</sup> Flanged Elbow (down):

The 90<sup>0</sup> elbows are categorized into two groups depending on the flow orientation. The turning angle is 90 degree for the first one while direction of the flow is from upper point towards the lower point. Figure 6.15 represents the hydraulic loss coefficients of the 90<sup>0</sup> elbow. The hydraulic loss coefficient for this elbow decreases as the Reynolds number increases. The trend of the hydraulic loss coefficient is consistent with the experimental results of the Idelchik's experiment shown in Figure 2.17.

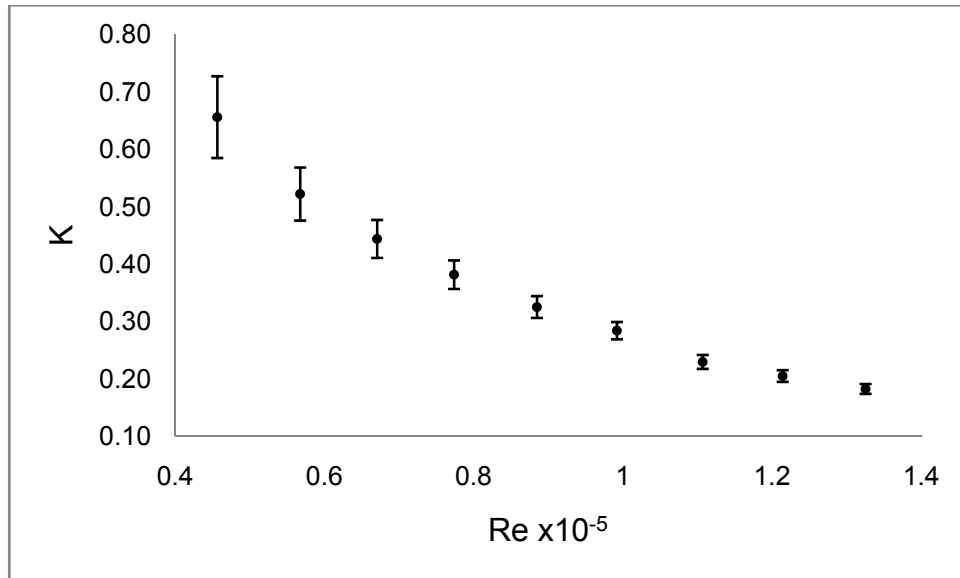


Figure 6.15. Hydraulic loss coefficients for 90° elbow (down)

### 6.2.3.3. Hydraulic Loss Coefficient of C-Shape Bend

The C-shape bend is a fitting that is used to change the direction of the flow 180°. Figure 6.16 represents the hydraulic loss coefficient of C-shape bend. The hydraulic loss coefficient for this elbow decreases as the Reynolds number increases. The trend of the hydraulic loss coefficient is coherent with the experimental results of the Idelchik's experiments on C-shape bends and these results are shown in Figure 2.19.

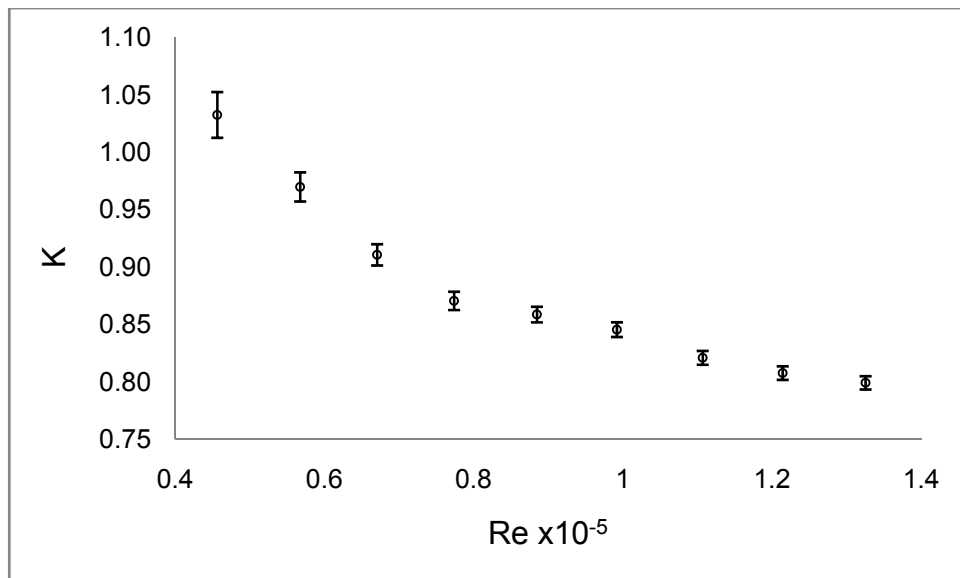


Figure 6.16. Hydraulic loss coefficients of C-shape bend

#### 6.2.3.4. Hydraulic Loss Coefficient of S-Shape Bend

The S-shape bend is a fitting that is used to change the elevation of the flow without changing its direction. Figure 6.17 shows the hydraulic loss coefficient of S-shape bend. The hydraulic loss coefficient for this elbow decreases as the Reynolds number increases. The trend of the hydraulic loss coefficient is coherent with the experimental results of the Idelchik experiment for S-shape bends (Figure 2.21).

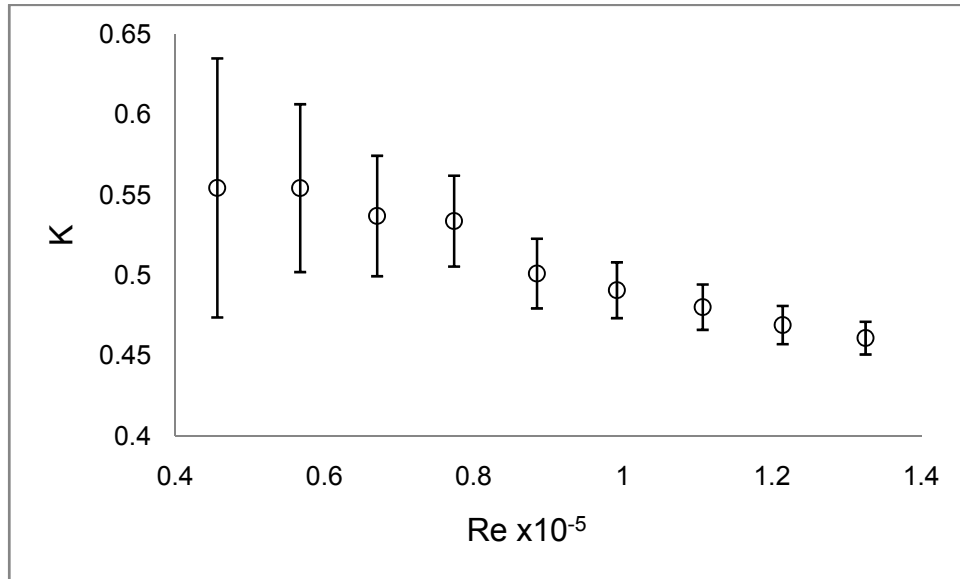


Figure 6.17. Hydraulic loss coefficients of S-shape bend

#### 6.2.3.5. Expansion Coefficient for Enlarging Pipe

The expansion coefficient of the gradually enlarging pipes can be categorized according to the diameter ratio of inlet to outlet and angle of enlargement. In the setup used for this study, the enlargement angle is  $60^{\circ}$  and outlet to inlet diameter ratio is 1.43. Figure 6.18 represents the expansion coefficient via Reynolds number. The expansion coefficient decreases as the Reynolds number increases. According to the Idelchik results, it can be inferred that the expansion coefficient decreases via increase in Reynolds number but it does not change significantly due to the small rise in Reynolds number. As presented in the Figure 6.18, the expansion coefficient does not change significantly although trend shows decreasing behavior. Thus, the estimated expansion coefficient values are consistent with the results of Idelchick's experiments.

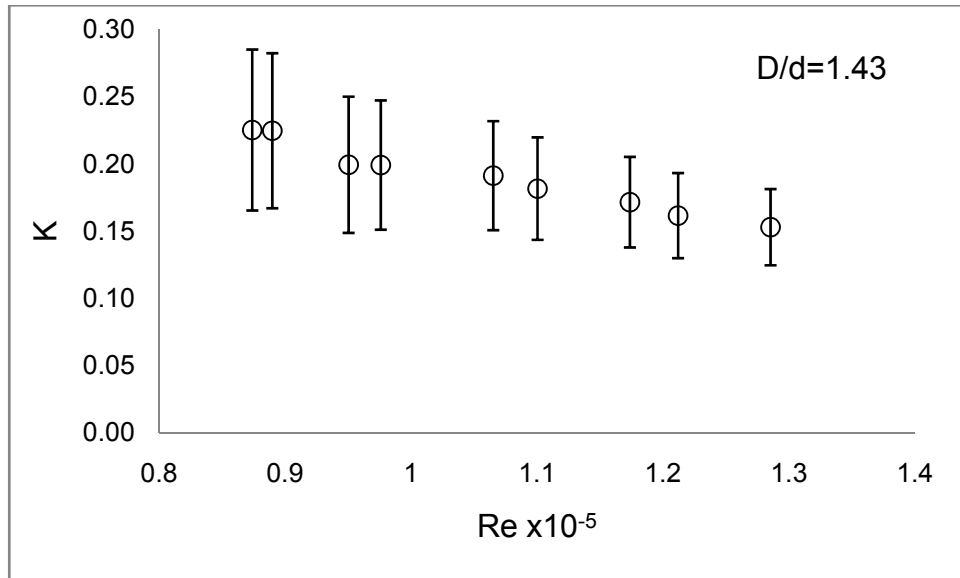


Figure 6.18. Expansion coefficients of gradually enlarging pipe

#### 6.2.3.6. Hydraulic Loss Coefficient of Gate Valve

The hydraulic loss coefficients for the gate valve are represented in Figure 6.19. The hydraulic loss coefficient for the gate valve decreases as the Reynolds number increases. The trend in change of the hydraulic loss coefficient is consistent with the experimental data in common literature for the gate valves.

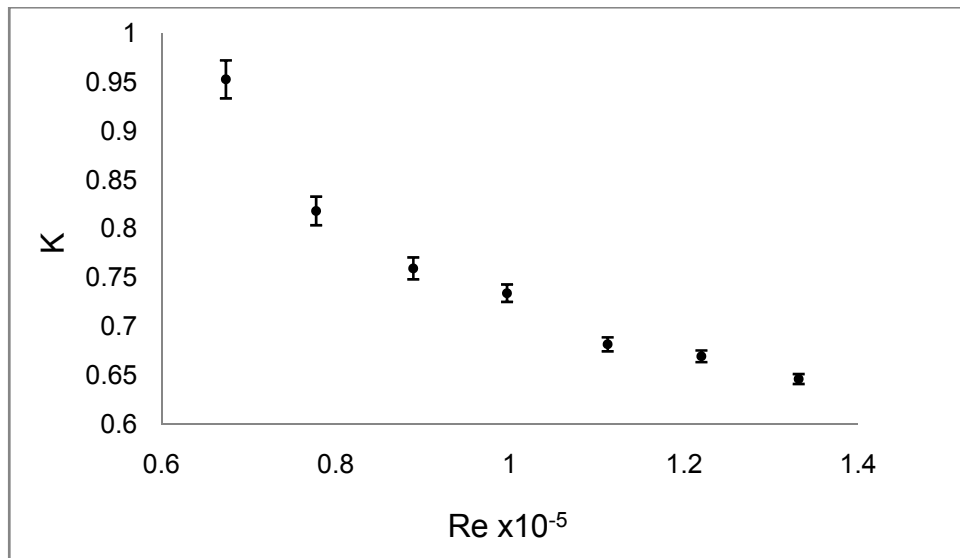


Figure 6.19. Hydraulic loss coefficients of gate valve

## **6.3. RELAP SIMULATIONS OF TEST SECTIONS**

In RELAP analyses, the input cards were prepared for each component. Input files were used to simulate the selected experiments in each section. These results are compared with the experimental data on the graphics. Results of the analyses are reported in this section in the order of the sections of the setup.

### **6.3.1. Section 1**

In the first section, three RELAP analyses were performed. The pipes on which the pressure drop measurement experiments were performed were modeled and divided into 50 volumes for the analyses. Runs for three hundred seconds were performed for the same volumetric flow rates as in the experiments and friction factor estimation was performed for the associated pressure drop values through the measurement section. The analyses were performed for stainless steel, copper and PVC pipes.

#### **6.3.1.1. Stainless Steel Pipe**

The first RELAP analysis was performed for the stainless steel pipe. Total length of the pipe is 1.85 meter as indicated before and it was divided into 50 volumes for the RELAP analyses. Roughness of 45 $\mu$ m was used for this pipe. Results of the RELAP analyses along with the experimental data are represented in Figure 6.20. These results are consistent with the results of the experiments performed for the stainless steel pipe as can be seen in the figure. As the Reynolds number increases the friction factor is decreases and all results are in the error range of the experimental data.

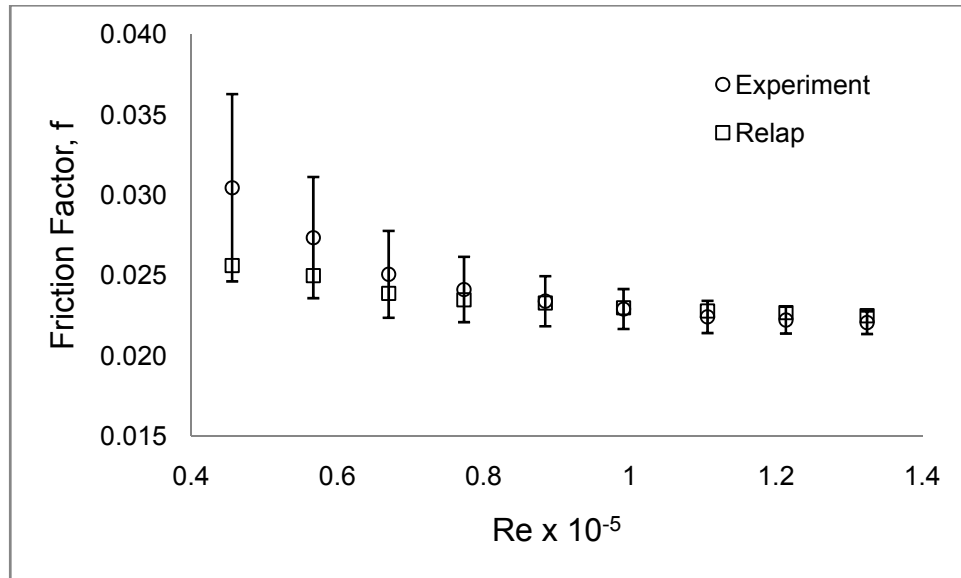


Figure 6.20. Results of RELAP analyses for the estimation of friction factor of the stainless steel pipe

#### 6.3.1.2. Copper Pipe

The second RELAP analysis was performed for the copper pipe. This pipe was also divided into 50 volumes for the RELAP analyses. Roughness of 15 $\mu$ m was used for this pipe. Results of the RELAP analyses are represented in Figure 6.21. This figure shows that the results of the RELAP analyses are consistent with the results of the experiments performed for the copper pipe. The friction factor values decrease due to the increase in the Reynolds number. As can be seen from the figure, all results are in the error range of the experimental results.

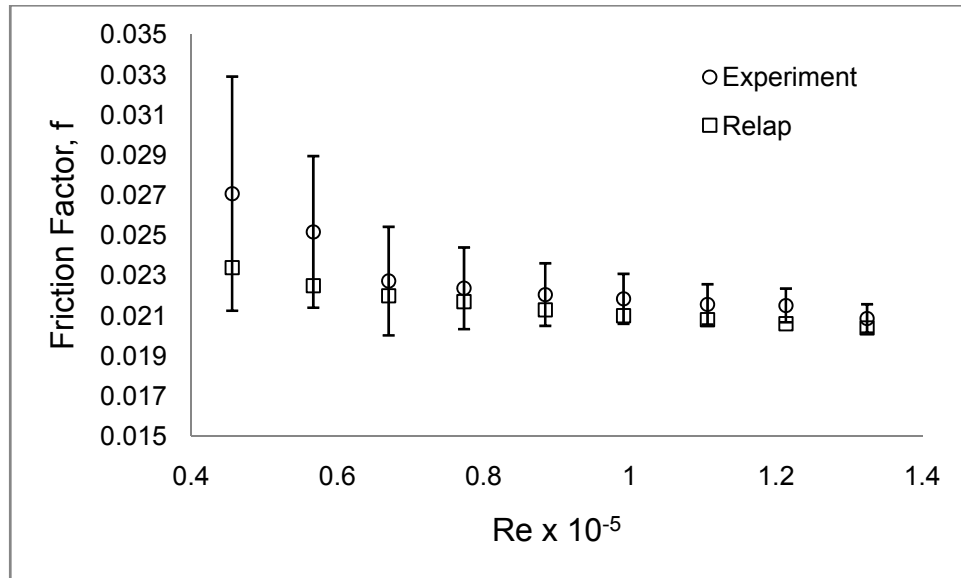


Figure 6.21. Results of RELAP analyses for the estimation of friction factor of the copper pipe

### 6.3.1.3. PVC Pipe

The third and the last RELAP analysis for section one was performed for the copper pipe. Volume number of 50 is used for more accurate estimation of the pressure drop through the pipe. Roughness of 1.5 $\mu$ m was used for the PVC pipe. Results of the RELAP analyses are represented in Figure 6.22. According to this figure, the results of the RELAP analyses are consistent with the results of the experiments performed for the copper pipe. All results are in the range of measurement errors.

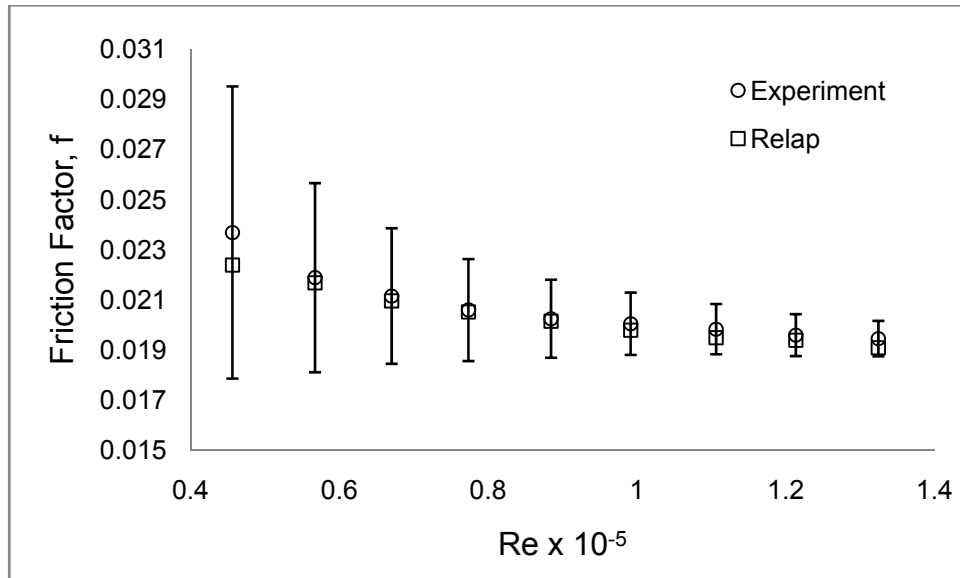


Figure 6.22. Results of RELAP analyses for the estimation of friction factor of the PVC pipe

### 6.3.2. Section 2

RELAP analyses for this section were performed by complete modeling of the section. Sampling 1 is simulated with RELAP. As in the experimental procedure, pressure drop along the pipes are determined and volumetric flow rate values are estimated. Figure 6.23 represents the result of total volumetric flow rate estimations.

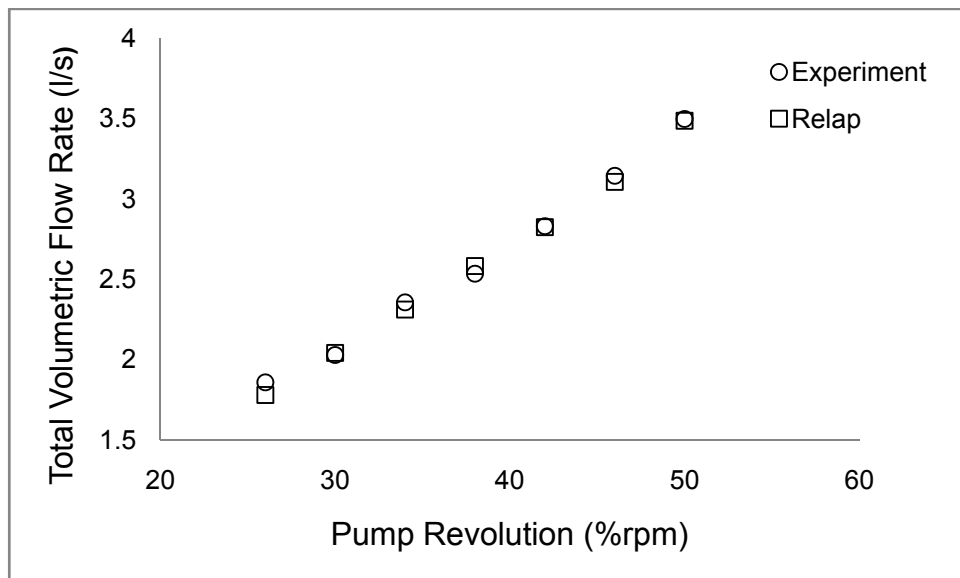


Figure 6.23. Estimated total volumetric flow rate (RELAP)



Figure 6.23 shows that computational results which uses RELAP simulation data are in good agreement with the experimental results.

### 6.3.3. Section 3

RELAP analyses for Section 3, were performed for selected fittings which were the 90° elbow (down), the 90° elbow (up) and the gradually enlarging pipe. Section 3 was modeled with RELAP completely and results were obtained for each fitting. The results of RELAP analyses were compared with the experimental results.

#### 6.3.3.1. Determination of the Loss coefficient of the 90° elbow (down)

The RELAP analyses for the 90° elbow (down) were performed for various flow rates. The results of calculations and experimental data for the loss coefficient were compared. Figure 6.24 represents the results of the analyses. This figure shows that the results of the RELAP analysis are in good agreement with the experimental results.

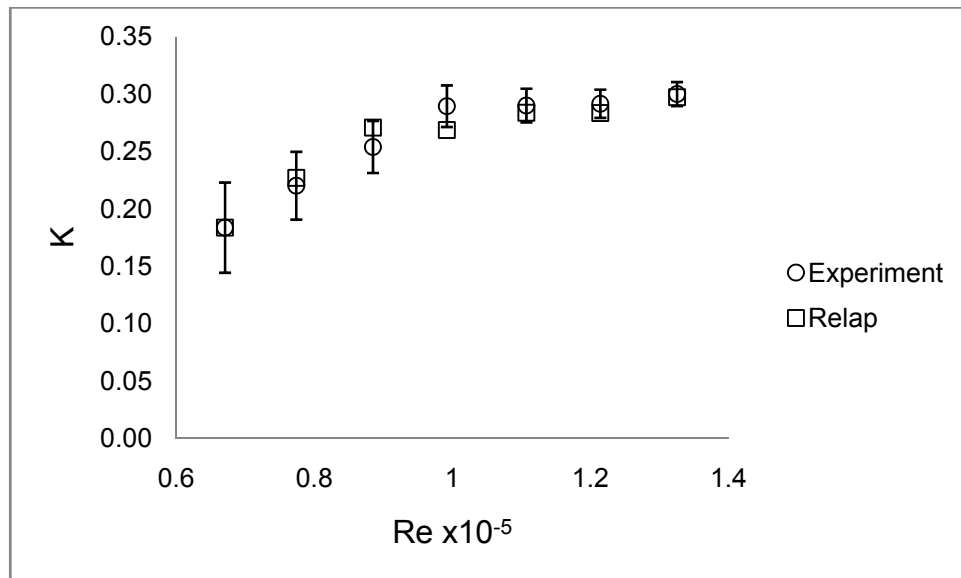


Figure 6.24. Results of RELAP analyses for the hydraulic loss coefficient determination of the 90°elbow (down)

#### 6.3.3.2. Determination of the Loss Coefficient of the 90° elbow (up)

The RELAP analyses for the 90° elbow (up) were performed for various flow rates. The results were compared with the experimental results. Figure 6.25 represents the

results of the analyses. This figure shows that the results of the RELAP analysis are consistent with the experimental data.

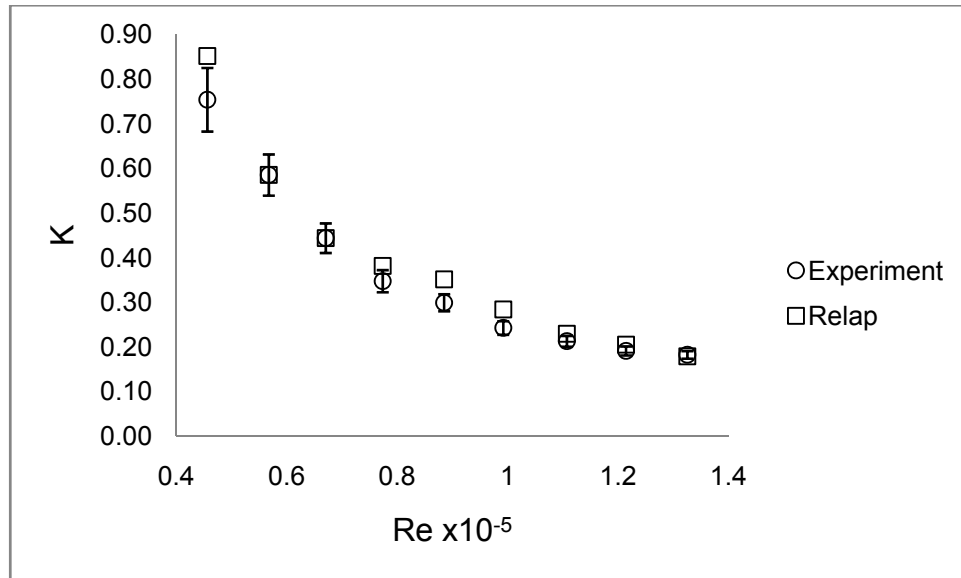


Figure 6.25. Results of RELAP analyses for the hydraulic loss coefficient determination of the 90° elbow (up)

### 6.3.3.3. Determination of the Loss Coefficient of the Gradual Enlargement

The RELAP analyses were performed for the gradually enlarging pipe. The results were compared with the experimental data. Figure 6.26 represents the results of the analyses. This figure shows that the results of the RELAP analysis are consistent with the experimental results. Although the hydraulic loss coefficient values obtained by the RELAP analyses over the experimental results, behavior of the hydraulic loss coefficient due to change in Reynolds number is in good agreement with the experimental data. Experimental results and RELAP analyses results are both consistent with the results of the Idelchik's experiments.

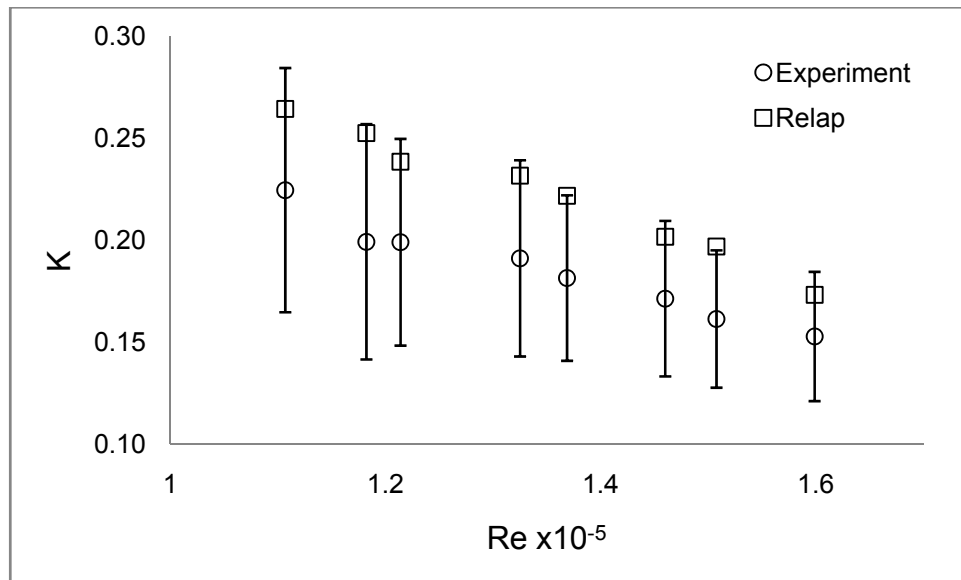


Figure 6.26. Results of RELAP analyses for the hydraulic loss coefficient determination of the gradual enlargement

## 6.4. EXPERIMENT MANUALS

The main aim of this study was to build an experimental setup which will be used for educational purposes in the Thermal-Hydraulics Laboratory. Preparation of the experiment manuals which will be used in the lab sessions was also included in this study. A great number of experiments were performed for each section of the experiment. The experiments were stated and appropriate experimental parameters were determined. Eventually, proper manuals were prepared.

The experiments were divided into four groups and four manuals were prepared. The experiments which will be performed in the lab sessions are:

- Experiment #1: Familiarization with the fluid mechanics experiments and flow rate measurement techniques
- Experiment #2: Friction loss for flow in a straight pipe
- Experiment #3: Determination of the hydraulic loss coefficients of fittings
- Experiment #4: Parallel flow

The Experiment #1 aims to provide familiarization with the use of the setup and flow rate measurement techniques. The Experiment #2 includes the estimation of the friction factors for stainless steel, copper and PVC pipes. The purpose of the Experiment #3 is to determine the hydraulic loss coefficients of the various fittings which are elbows, s-shape bend, c-shape bend, gate valve and enlargement in flow area. Experiment #4 is prepared to analyze the parallel flow. The prepared manuals of these four experiments are given in Appendix D.

## 7. CONCLUSIONS

The main purposes of this study were to design and construct an experimental setup which included basic fluid mechanics applications, to conduct and simulate the associated experiments. This thesis had been completed by following basic steps which were design and sizing of the setup, conducting experiments and simulation of the experiments.

In the design and sizing of the setup, FLOWNEX which is a computational fluid dynamics (CFD) code for macro systems was used. The selection of the theoretical information which has been covered in the setup, the appropriate material selection for the construction, sizing of the setup which is conditional to the selected material includes determination of the dimensions of the setup and sizing of the pump and the selection of the measurement techniques were all within the scope of design and sizing step.

Flow in pipes has a wide range of application in nuclear power plants. Hence, flow characteristics, hydraulic loss coefficients, gain terms and etc. have great importance in analyses of the nuclear power plants. In extensive meaning, flow in pipes was selected as the theory which the experimental setup was based on. The basic fluid mechanic applications such as friction factor estimation, the hydraulic loss coefficients determination for fittings and observation of the parallel flow were included in the setup.

Stainless steel was selected as a material for the frame of the setup. The main reason for this selection was that it is the most widely used material in nuclear power plants. In addition to stainless steel, copper and PVC pipes were also used in the setup to observe the effect of material on friction loss term.

FLOWNEX analyses were performed to state the appropriate dimensions and the pump characteristics. The working range of flow rate was decided with these analyses, and for determination of the pump characteristics a code which had been developed for this study was used.

When the pump characteristics had been determined, the measurement techniques were selected and specifications of the measurement devices were assigned. There were two types of flow meter selected which were a magnetic flow meter and a multi-jet flow meter. Differential pressure measuring devices (DP cells), Bourdon type manometer and a pressure transmitter were chosen for pressure measurements.

When setup had been constructed, experiments were performed. The setup was completely computer controlled so to learn the use of the setup, basic practices were performed at the beginning of this study. Then, experiment matrices were begun to be assigned. For each section of the setup and each component in the sections great number of experiments were performed. Thus, the experimental parameters were stated and final experiments were conducted. Experimental data were obtained for each case and compared with the data available in literature. Experimental data were found to be consistent with data in the literature.

In the last part of this study, simulations of the experiments were performed using RELAP (Reactor Leak and Excursion Program) which is a best estimate code used to simulate nuclear power plants. Results of the simulations were compared with the experimental data. The results were in good agreement with the experimental data.

In conclusion, an experimental setup which will be used in the undergraduate education was designed and constructed. Satisfactory results were obtained from the experiments and simulations performed with RELAP. The documents will be required to perform experiments, i.e. experiment manuals were prepared.

## REFERENCES

1. Duncan, W.J, Thom, A.S., Young, A.D., 1990, Mechanics of Fluids (2nd Ed.), Chapman and Hall Inc, NY,USA
2. Cheng, D., Heywood, N., 1984, Flow in pipes. I. Flow of homogenous fluids, Physics in Technology, Vol. 15,pp. 244-251
3. Massey, B.S., 1989, Mechanics of Fluids (6th Ed.), T.J. Press Ltd , NY, USA
4. Munson, B.R., Young, D.F, Okiishi, T.H., 2002, Fundamentals of Fluid Mechanics ( 4th Ed.), John Wiley&Sons, NY,USA
5. Çengel, Y., Cimbala, J.M., 2008, Akışkanlar Mekaniği Temelleri ve Uygulamaları, İzmir Güven Kitapevi, Türkiye
6. Bird R.B., Stewart, W.E., Lightfoot, E.N., 1960, Transport Phenomena ,John Wiley&Sons, NY, USA
7. Moody, L.F., 1944, Friction Factors for Pipe Flow, Transaction of the A.S.M.E., November, pp. 671-684
8. Kinsky, R., 1989, Applied Fluid Mechanics, Mc Graw-Hill Book Company, NY, USA
9. Ding,C., Carlson, L., Ellis, C., Mohseni, O., 2005, Pressure Loss Coefficients of 6,8 and 10 inch Steel Pipe Fittings, St. Anthony Falls Lab, University of Minnesota, Minnesota, (unpublished)
10. Idelchick,I.E., Fried, E., 1989, Flow Resistance- A Design Guide for Engineers, Taylor & Francis, Philadelphia
11. User Manual of the Differential Pressure Measuring Device, Dwyer Inst.
12. User Manual of the Electromagnetic Flow Measuring System, Promag 30, Endress & Hauser
13. User Manual of the Pump, Multivert 16, WILO, 2009
14. User Manual of the DAQ system, Labjack, 2009
15. <http://www.audon.co.uk/profilab.html>, ProfilLAB, 2010
16. User Manual of FLOWNEX, 2009
17. User Manual of RELAP, 2009

18. Grabe, M., 2005, Measurement Uncertainties in Science and Technology, Springer, NY, USA
19. Knoll, G., 2000, Radiation Detection and Measurement (3<sup>rd</sup> Ed.), John Wiley & Sons, Ny, pp. 86-92
20. Feisel, L.D., Rosa, A.J., 2005, The Role of the Laboratory in Undergraduate Engineering Education, Journal of Engineering Education, pp. 121-130
21. Eriksson, B., 1997, Experimental Studies in Fluid Mechanics, Project 036/92, Department of Energy and Environmental Technology, Karlstad University, Sweden, (unpublished)



# APPENDIX

## APPENDIX A. FLOWNEX [16]

### A.1. GENERAL INFORMATION

FLOWNEX is a system computational fluid dynamics (CFD) code. Based on the network approach, users can perform detailed calculations on design and analysis. The optimization of wide range of thermal fluid systems can also be performed. It solves the flow, pressure, and temperature distribution in thermal fluid networks and provides the engineer/designer with the essential information on the interaction between network components and on the behavior of complex systems. Graphical User Interface is used to create or edit networks and to prepare input data for the networks. Networks are created by placing and connecting elements and nodes of elements. Nodes are used to connect elements and to present boundaries for a network.

FLOWNEX is used for many applications in a variety of industries, today. For instance, to model many applications in mining, aircraft or power generation industries, FLOWNEX can be used. In addition to these applications, FLOWNEX is also used for educational purposes. It can be used for the academic training as simulators to create a virtual equivalent of the real life thermal hydraulic systems.

#### A.1.1. Solver Properties

FLOWNEX solves networks quickly and accurately by using a very fast and stable implicit solver. The advantage of this is eliminating the excessive time step restriction imposed on explicit codes. A steady state network of 1000 elements and 100 nodes typically is simulated in less than 3 seconds.

FLOWNEX uses dynamic memory allocation. Thus, very large and small networks can be solved on a personal computer without re-dimensioning the code for every run. There are a number of error and warning messages to debug the computational process correctly. Long pipes can be subdivided into small divisions for which flow is

simulated. This provides more accurate and more detailed analysis on pressure or temperature distribution through the pipe.

### **A.1.2. List of applications that can be modeled with FLOWNEX**

There are a lot of theoretical problem and engineering applications which can be modeled with FLOWNEX. Some of them are:

- Steady-state and transient flows
- Incompressible, compressible and two-phase flows
- Laminar and turbulent flows
- Heat transfer
- Complex heat exchangers
- Turbo machinery

Extended thermal fluid networks in various industries have been simulated and designed with FLOWNEX, such as modeling of pebble bed modular reactor (PBMR) (power generation industry), heat recovery systems on mines and compressed air networks (mining industry), fuel distribution systems on aircrafts (aircraft industry).

### **A.1.3. Fluids in FLOWNEX**

FLOWNEX includes several standard fluids in its default fluid library. Also any fluid or mixture of fluids can be defined and added to the fluid library. Gases and liquids (single and two-phase), gas mixtures, buoyancy driven flows, gravitational effects in liquid and gas flows can be modeled with FLOWNEX. There are also fluid models in FLOWNEX. The constant or pressure and temperature dependent density options for liquids, rigid column theory or elastic theory for liquids, ideal gasses, non-ideal gasses are included in these models.

### **A.1.4. Components in FLOWNEX**

FLOWNEX provides models for several components. Brief list of components is given below:

- Junction
- Reservoir

- Bend
- Basic pipes
- Pipe
- Resistive duct
- Phantom element
- Heat transfer element
- Node
- Compressor
- Turbine
- Fan or pump
- Heat exchangers
- Valves
- Restrictors
- Control elements

#### **A.1.5. Advanced heat transfer capabilities of FLOWNEX**

FLOWNEX offers a number of advantages for heat transfer problems. These are:

- A Heat transfer element consists of a number of material layers, each of which can be divided into a number of increments. Heat transfer elements can have both thermal resistance and thermal inertia and can be connected to flow elements or nodes.
- Heat transfer elements also include variable heat transfer area in the radial direction and axial heat transfer and radiation heat transfer between the end surfaces of two heat transfer elements. There is also the option to allow radiation and convection heat transfer from the end surface of a heat transfer element to ambient conditions.

#### **A.2. GOVERNING EQUATIONS**

The analysis of thermal-fluid networks is based on the numerical solutions of the governing equations of fluid dynamics and heat transfer. FLOWNEX solves the differential equations for mass, momentum, and energy conservation to obtain the mass flow, pressure and temperature distributions throughout a network.

Three conservation laws are applied for solution.

- Conservation of mass
- Conservation of momentum
- Conservation of energy

These laws are described in the form of partial differential equations. A solution algorithm is developed for the solution of the coupled equations which are constituted with these differential equations. The most essential data for the solution includes the boundary and initial conditions of the problem.

For description and construction of the equations, the reference frame selection is decisive. There are two popular reference frames commonly used, Lagrangian and Eulerian reference frames. Lagrangian reference frame considers fixed mass control volume moving one location to another along a stream line while Eulerian reference frame considers a stationary fixed-volume control volume in which fluid crosses the control surface. In modeling thermal-fluid systems Eulerian reference frame is more suitable.

FLOWNEX uses the basic conservation laws for analysis. By applying these laws, associated equations for mass, momentum and energy conservation equations are generated. These conservation equations are discussed in following sections.

The steps of solution procedure in FLOWNEX can be summarized as follows:

1. Guess initial node pressures
2. Calculate mass flows using  $\Delta p - Q$  relationships
3. Test for continuity at all nodes
4. Adjust pressure to ensure continuity at all nodes
5. Update mass flows using updated pressures
6. Repeat (1) through (5) until solution converges
7. Solve the energy equation
8. Repeat (1) through (7) until solution converges
9. Move to next time step and repeat from (1) to (8) (for transient simulations)

### A.2.1. Mass Equation in FLOWNEX (1-Dimensional)

The general presentation of mass conservation equation in one dimensional coordinate system is given in Eq.A.1.

$$\frac{\partial \rho}{\partial t} + \frac{\partial(\rho V)}{\partial x} = 0 \quad (\text{A.1})$$

In the Eq.A.1,  $V$  is the flow velocity in  $x$ -direction (direction of flow),  $\rho$  is the fluid density. This equation is appropriate for the problems in which density or velocity of the fluid is time dependent.

This equation is written for a control volume and control volume is three dimensional. Because the variables change only in the direction of flow and value at a given point is considered to be the average value across the cross-sectional area of the control volume, one-dimensional assumption can hold for the defined control volume.

If the flow is steady state, then equation A.2.1 can be written in the form of Eq.A.2.

$$\frac{\partial(\rho V)}{\partial x} = 0 \quad (\text{A.2})$$

Further simplification is possible for incompressible (constant  $\rho$ ) fluids. Then Eq.A.2 takes the following form:

$$\frac{\partial V}{\partial x} = 0 \quad (\text{A.3})$$

### A.2.2. Momentum Equation in FLOWNEX (1-Dimensional)

The general presentation of momentum conservation equation for one-dimensional flow in a pipe flow is given in Eq.A.4.

$$\frac{\partial(\rho V)}{\partial t} + \frac{\partial(\rho V^2)}{\partial x} = -\frac{\partial p}{\partial x} - \rho g \frac{\partial z}{\partial x} - \frac{f \rho |V| V}{2D} \quad (\text{A.4})$$

The first term at the left hand side of the Eq.A.4 is time derivative for transient flow while the second term is convective term. First term at the right hand side is pressure gradient source term, the second terms is the body force due to gravity and the third

term represents the friction force due to shear stress. In the third term,  $f$  is the friction factor and  $D$  is the diameter of the pipe.

For incompressible flow the convective term in Eq.A.4 can be written in terms of kinetic energy. The resulted equation, Eq.A.5, can be written as follows.

$$\rho \frac{\partial V}{\partial t} + \frac{\partial p}{\partial x} + \frac{1}{2} \frac{\partial(\rho V^2)}{\partial x} + \rho g \frac{\partial z}{\partial x} = - \frac{f \rho |V| V}{2D} \quad (\text{A.5})$$

The summation of the second, third and fourth term at the left hand side of the Eq.A.5, can be defined as stagnation pressure which is given with Eq.A.6.

$$p_0 = \left( p + \frac{1}{2} \rho V^2 + \rho g z \right) \quad (\text{A.6})$$

If Eq.A.6 is put into the Eq.A.5 and flow is steady state then Eq.A.5 can be written as follows.

$$\frac{\partial p_0}{\partial x} = - \frac{f \rho |V| V}{2D} \quad (\text{A.7})$$

Finally, one-dimensional momentum conservation equation for a pipe with length of  $L$  and diameter of  $D$  for steady state incompressible flow forms as given in Eq. A.8.

$$\Delta p_0 = - \frac{f L \rho |V| V}{2D} \quad (\text{A.8})$$

### A.2.3. Energy Equation in FLOWNEX (1-Dimensional)

The general presentation of energy conservation equation for one-dimensional flow in terms of the specific stagnation enthalpy,  $h_0$ , is given in Eq.A.9.

$$\frac{\partial(\rho(h_0 + gz) - p)}{\partial t} + \frac{\partial(\rho V(h_0 + gz))}{\partial x} = \dot{Q}_H - \dot{W} \quad (\text{A.9})$$

The stagnation enthalpy is defined as:

$$h_0 = h + \frac{1}{2} V^2 \quad (\text{A.10})$$

The height and gravitational acceleration are time independent. With this information and using the mass conservation equation and making some arrangements in Eq.A.9, the energy conservation equation which is solved in FLOWNEX for  $h_o$  is obtained (Eq.A.11).

$$\frac{\partial(\rho h_o)}{\partial t} - \frac{\partial p}{\partial t} + \frac{\partial(\rho V h_o)}{\partial x} + \rho V \frac{\partial(gz)}{\partial x} = \dot{Q}_H - \dot{W} \quad (\text{A.11})$$

## **APPENDIX B. RELAP (Reactor Excursion and Leak Analysis Program) [17]**

### **B.1. GENERAL INFORMATION**

The light water reactor (LWR) transient analysis code, RELAP5/MOD3, was developed at the Idaho National Engineering Laboratory (INEL) for the U.S. Nuclear Regulatory Commission (NRC). RELAP5/MOD3 has been used as the basis for a nuclear plant analyzer. Specific applications have included simulations of transients in LWR systems such as loss of coolant, anticipated transients without scram (ATWS), and operational transients such as loss of feed-water, loss of offsite power, station blackout, and turbine trip. RELAP5/MOD3 is a highly generic code that, in addition to calculating the behavior of a reactor coolant system during a transient, can be used for simulation of a wide variety of hydraulic and thermal transients in both nuclear and nonnuclear systems involving mixtures of steam, water, non-condensable, and solute.

The RELAP5/MOD3 code is based on a non-homogeneous and non-equilibrium model for the two phase system that is solved by a fast, partially implicit numerical scheme to permit economical calculation of system transients.

The code includes many generic component models from which general systems can be simulated. The component models include pumps, valves, pipes, heat releasing or absorbing structures, reactor point kinetics, electric heaters, jet pumps, turbines, separators, accumulators, and control system components. In addition, special process models are included to simulate the effects such as form loss, flow at an abrupt area change, branching, choked flow, boron tracking, and non-condensable gas transport.

The system mathematical models are coupled into an efficient code structure. The code includes extensive input checking capability to help the user discover input errors and inconsistencies. Also included are free-format input, restart, renodalization, and variable output edit features.

The RELAP5/MOD3 hydrodynamic model is a one-dimensional, transient, two-fluid model for flow of a two-phase steam-water mixture that can contain non-condensable



components in the steam phase and/or a soluble component in the water phase. The RELAP5/MOD3 hydrodynamic model contains several options for invoking simpler hydrodynamic models. These include homogeneous flow, thermal equilibrium, and frictionless flow models. These options can be used independently or in combination.

The two-fluid equations of motion that are used as the basis for the RELAP5/MOD3 hydrodynamic model are formulated in terms of volume and time-averaged parameters of the flow. Phenomena that depend upon transverse gradients, such as friction and heat transfer, are formulated in terms of the bulk properties using empirical transfer coefficient formulations. In situations where transverse gradients cannot be represented within the framework of empirical transfer coefficients, such as subcooled boiling, additional models specially developed for the particular situation are employed. The system model is solved numerically using a semi-implicit finite-difference technique. The user can select an option for solving the system model using a nearly implicit finite-difference technique, which allows violation of the material Courant limit. This option is suitable for steady-state calculations and for slowly varying, quasi-steady transient calculations.

## **B.2. GOVERNING EQUATIONS**

The RELAP5/MOD3 thermal-hydraulic model solves eight field equations for eight primary dependent variables. The primary dependent variables are pressure ( $P$ ), phasic specific internal energies ( $U_g, U_f$ ), vapor volume fraction (void fraction) ( $\alpha_g$ ), phasic velocities ( $v_g, v_f$ ), non-condensable quality ( $X_n$ ), and boron density ( $\rho_b$ ). The independent variables are time ( $t$ ) and distance ( $x$ ). Non-condensable quality is defined as the ratio of the non-condensable gas mass to the total gaseous phase mass. The secondary dependent variables used in the equations are phasic densities ( $\rho_f, \rho_g$ ), phasic temperatures ( $T_g, T_f$ ), saturation temperature ( $T_s$ ), and non-condensable mass fraction in non-condensable gas phase ( $X_{ni}$ ) for the  $i$ -th non-condensable species.

The basic two-fluid differential equations that form the basis for the hydrodynamic model are next presented. This discussion will be followed by the development of a convenient form of the differential equations that is used as the basis for the numerical solution scheme.

The basic field equations for the two-fluid non-equilibrium model consist of two phasic continuity equations, two phasic momentum equations, and two phasic energy equations. The equations are recorded in differential stream tube form with time and one space dimension as independent variables and in terms of time and volume-average dependent variables. A short summary of the conservation equations for mass, momentum and energy is given in follows. Further data is available in RELAP5/MOD3 Code Manual Volume-I [referans no].

### **B.2.1. Mass Equation in RELAP**

The mass continuity equations which are used in RELAP are derived from the one-dimensional phasic mass equations and they can be presented with Eq.B.1 and Eq.B.2.

$$\frac{\partial}{\partial t}(\alpha_g \rho_g) + \frac{1}{A} \frac{\partial}{\partial x}(\alpha_g \rho_g v_g A) = \Gamma_g \quad (\text{B.1})$$

$$\frac{\partial}{\partial t}(\alpha_f \rho_f) + \frac{1}{A} \frac{\partial}{\partial x}(\alpha_f \rho_f v_f A) = \Gamma_f \quad (\text{B.2})$$

In Eq.B.1 and Eq.B.2,  $\alpha$  is the volume fraction of the phase,  $\rho$  is the phase density,  $v$  is the phasic velocity and  $\Gamma$  is the volumetric mass exchange rate.

### **B.2.2. Momentum Equation in RELAP**

The phasic conservation of momentum equations are used in an expanded form and in terms of momenta per unit volume using the phasic primitive variables  $v_g$  and  $v_f$ . The spatial variation of momentum term is expressed in terms of  $v_g^2$  and  $v_f^2$ . This form has the desirable feature that the momentum equation reduces to Bernoulli's equations for steady, incompressible, and frictionless flow. A guiding principle used in the development of the RELAP5/MOD3 momentum formulation is that momentum

effects are secondary to mass and energy conservation in reactor safety analysis and a less exact formulation (compared to mass and energy conservation) is acceptable especially since nuclear reactor flows are dominated by large sources and sinks of momentum. A primary reason for use of the expanded form is that it is more convenient for development of the numerical scheme. The momentum equations for each phase come from the one-dimensional phasic momentum equations. Eq.B.3 and Eq.B.4 are momentum balance equations for vapor phase and liquid phase, respectively.

$$\alpha_g \rho_g A \frac{\partial v_g}{\partial t} + \frac{1}{2} \alpha_g \rho_g A \frac{\partial v_g^2}{\partial x} = -\alpha_g A \frac{\partial P}{\partial x} + \alpha_g \rho_g B_x A - (\alpha_g \rho_g A) FWG(v_g) + \Gamma_g A (v_{gI} - v_g) - (\alpha_g \rho_g A) FIG(v_g - v_f) - C \alpha_g \alpha_f \rho_m A \left[ \frac{\partial(v_g - v_f)}{\partial t} + v_f \frac{\partial v_g}{\partial x} - v_g \frac{\partial v_f}{\partial x} \right] \quad (B.3)$$

$$\alpha_f \rho_f A \frac{\partial v_f}{\partial t} + \frac{1}{2} \alpha_f \rho_f A \frac{\partial v_f^2}{\partial x} = -\alpha_f A \frac{\partial P}{\partial x} + \alpha_f \rho_f B_x A - (\alpha_f \rho_f A) FWF(v_f) - \Gamma_g A (v_{fI} - v_f) - (\alpha_f \rho_f A) FIF(v_f - v_g) - C \alpha_f \alpha_g \rho_m A \left[ \frac{\partial(v_g - v_f)}{\partial t} + v_g \frac{\partial v_f}{\partial x} - v_f \frac{\partial v_g}{\partial x} \right] \quad (B.4)$$

The force terms on the right sides are, respectively, the pressure gradient, the body force (i.e., gravity and pump head), and wall friction, momentum transfer due to interface mass transfer, interface frictional drag, and force due to virtual mass. The terms FWG and FWF are part of the wall frictional drag, which are linear in velocity, and are products of the friction coefficient, the frictional reference area per unit volume, and the magnitude of the fluid bulk velocity. The interfacial velocity in the interface momentum transfer term is the unit momentum with which phase appearance or disappearance occurs. The coefficients FIG and FIF are parts of the interface frictional drag, which is linear in relative velocity, and are products of the interface friction coefficients, the frictional reference area per unit volume, and the magnitude of interface relative velocity.

### B.2.3. Energy Equation in RELAP

The energy equations which are used in RELAP come from the one-dimensional phasic energy equations and they can be presented with Eq.B.5 and Equation B.6.

$$\begin{aligned} \frac{\partial(\alpha_g \rho_g U_g)}{\partial t} + \frac{1}{A}(\alpha_g \rho_g U_g v_g A) = -P \frac{\partial \alpha_g}{\partial t} - \frac{P}{A} \frac{\partial}{\partial x}(\alpha_g v_g A) \\ + Q_{wg} + Q_{ig} + \Gamma_{ig} h_g^* + \Gamma_w h_g' + DISS_g \end{aligned} \quad (B.5)$$

$$\begin{aligned} \frac{\partial(\alpha_f \rho_f U_f)}{\partial t} + \frac{1}{A}(\alpha_f \rho_f U_f v_f A) = -P \frac{\partial \alpha_f}{\partial t} - \frac{P}{A} \frac{\partial}{\partial x}(\alpha_f v_f A) \\ + Q_{wf} + Q_{if} + \Gamma_{if} h_f^* - \Gamma_w h_f' + DISS_f \end{aligned} \quad (B.6)$$

In the phasic energy equations,  $Q_{wg}$  and  $Q_{wf}$  are the phasic wall heat transfer rates per unit volume. The phasic enthalpies,  $h_f^*$  and  $h_g^*$ , associated with bulk interface mass transfer defined as the interface energy jump conditions at the liquid-vapor interface are satisfied.  $DISS_g$  and  $DISS_f$  are the phasic energy dissipation terms and are the sums of wall friction and pump effects.

## APPENDIX C. THE MEASUREMENT ERROR ANALYSIS

The error is a property of testing that depends on all contributing measurements. The error analysis is essential part of any scientific experiment [18]. The error analysis was performed for the estimation of hydraulic loss coefficients of fittings and friction loss coefficients of pipes. The determination of errors is related with the measurement of all parameters affecting the K-values as described in Section 2.3 at this thesis.

Pressure and flow rate were measured by using the DP cells and the magnetic flow meters. The measurement errors associated with the measurement devices are assigned by the manufacturer. The measurement error is 0.1% in full scale for DP cell measurements. [11]

Table C.1. Measurement errors of the DP cells

| DP cell | Measurement Range (psia) | Measurement Range (mbar) | Measurement Error (%F.S.) | Error (mbar) |
|---------|--------------------------|--------------------------|---------------------------|--------------|
| DP 1    | 0-5                      | 0-344                    | 1                         | $\pm 3.44$   |
| DP 2    | 0-5                      | 0-344                    | 1                         | $\pm 3.44$   |
| DP 3    | 0-1                      | 0-69                     | 1                         | $\pm 0.69$   |

Although the DP cell measurement error is constant for all range of the measurements, the error of the volumetric flow rate measurement varies due to the flow rate. The error values assigned by the manufacturer for the working range of the experiments performed in this study are given in Figure C.1. [12]. The figure indicates that as the flow rate increases, percentage error in the measurement becomes greater.

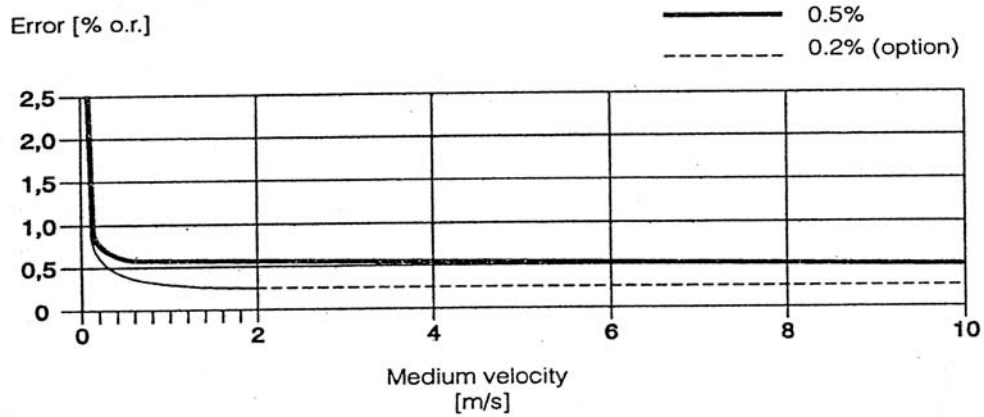


Figure C.1. Percentage errors in flow rate measurement [12]

The measurement errors associated with the measurement devices are both assigned by the manufacturer. Because of the derivation of loss coefficients depends on flow rate and pressure drop measurements, the effect of measurement errors on the loss coefficient determination are analyzed with the standard error propagation rules. [19]

For the friction loss coefficient determinations, Eq.C.1 is used.

$$f = \frac{2 * \Delta P}{\frac{L}{D} \rho V^2} \quad (C.1)$$

To determine the error in the estimate of the friction loss error dividing rules for dividing are used (Eq.C.2).

$$\sigma_f = C_1 \sqrt{\frac{\partial^2 f}{\partial \Delta P^2} \sigma_{\Delta P}^2 + \frac{\partial^2 f}{\partial (V^2)^2} \sigma_{v^2}^2} \quad (C.2)$$

In the above equation,  $C_1$  is a constant term and comes from the friction loss coefficient determination given with Eq.C.1,  $C_1 = \frac{2}{(\frac{L}{D})\rho}$ . As it can be seen from

Eq.C.2, two measurement errors affect the friction loss coefficient determination. First of all, error associated with the square of the average flow velocity must be

determined. For this reason, error multiplication rule is applied and Eq.C.3 is obtained.

$$\sigma_{V^2} = \sqrt{V^2\sigma_V^2 + V^2\sigma_V^2} = \sqrt{2}V\sigma_V \quad (\text{C.3})$$

Here,  $V$  is the average flow velocity in the units of meter per second.  $\sigma_V$  is the error in the average flow velocity and it is obtained by using the volumetric flow rate (l/s) measurement errors assigned by the manufacturer.

The error in pressure drop measurement contributes to the error in friction loss coefficient, also. The pressure drop measurement error value directly participates in the calculations.

For the hydraulic loss coefficient of fittings determinations, Eq.2.33 is used. The term  $h_f$  is the head loss on fittings and it can be determined by using the Bernoulli Equation as given below:

$$h_l = \frac{P_1 - P_2}{\gamma} + \frac{V_1^2}{2g} - \frac{V_2^2}{2g} - \sum f \frac{L}{D} \frac{V_i^2}{2g} + (z_1 - z_2) \quad (\text{C.4})$$

To explain the error analysis for this part, a symbolic representation of this equation can be written as in Eq.C.5.

$$h_l = h_1 + h_2 - h_3 \quad (\text{C.5})$$

$h_1$  shows the total head loss on the system,  $h_2$  shows the head loss due to velocity change and  $h_3$  shows the head loss due to friction. The elevation change is not considered in error analysis because errors due to length measurements are neglected.

Error of the value of head loss on fittings can be found by using the Eq.C.6.

$$\sigma_{h_l} = \sqrt{\sigma_{h_1}^2 + \sigma_{h_2}^2 + \sigma_{h_3}^2} \quad (\text{C.6})$$

If Eq.C.4 is put into the Eq.2.33, following equation is obtained for hydraulic loss coefficient:

$$K_L = \frac{h_l}{V^2 / 2g} \quad (C.7)$$

The error of the hydraulic loss coefficient of a fitting can be determined by applying the error dividing propagation rule to the error of head loss on fitting and the error of velocity square. Final equation can be written in the form of Eq.C.8.

$$\sigma_K = C_2 \sqrt{\frac{\partial^2 K}{\partial h_l^2} \sigma_{h_l}^2 + \frac{\partial^2 K}{\partial (V^2)^2} \sigma_{h_l}^2} \quad (C.8)$$

In Eq.C.8  $\partial(V^2)^2$  is the error in square of the average velocity of the fluid which is given with Eq.C.3 and  $C_2$  is a constant which equals to  $2g$ .



## **APPENDIX D. THE EXPERIMENT MANUALS**

### **D.1. MANUAL FOR EXPERIMENT #1**

#### **THERMAL HYDRAULICS LABORATORY**

#### **EXPERIMENT #1**

#### **FAMILIARIZATION WITH THE FLUID MECHANICS EXPERIMENTS AND FLOW RATE MEASUREMENT TECHNIQUES**

##### **PURPOSE:**

The aims of this experiment are:

- To familiarize the student with the widely used equipments of fluid mechanics measurements
- To examine and compare the flow rate measurement techniques

##### **INTRODUCTION**

We have an experimental setup for pressure measurements in pipes and fittings. This experimental setup includes various techniques on flow rate and pressure measurements. This experiment aims to familiarize the student with the experimental setup to perform the further experiments such as pressure drop measurement which will be performed in incoming lab sessions.

Experiment #1 includes examples of motor control options for the pump run techniques and flow rate measurements. In the first part of the experiment motor control options will be examined. Working principles of each option will be discussed. In the second part, flow rate measurement devices are going to be examined. Basic theoretical information is summarized in the following section.

##### **THEORY**

**MAGNETIC FLOW METER:**

This device is technically a velocity type water meter. It uses magnetic properties to determine the water flow velocity. One of the attractive properties of the magnetic flow meters is that they do not obstruct the flow. Thus, the pressure drop across the

magnetic flow meter is equal to the pressure drop through a pipe. The operation of a magnetic flow meter is based on Faraday's law of induction. A magnetic field is applied to the metering tube, which results in a potential difference proportional to the flow velocity perpendicular to the flow direction. A voltage is induced when a conductor moves through a magnetic field. The liquid serves as the conductor. Applied voltage is directly proportional to the flow velocity and is fed to the measuring amplifier by a pair of electrodes. Across the cross-section of the pipe the flow volume is calculated. A schematic presentation of a magnetic flow meter is given in Figure 1. In the figure,  $U_e$  is the induced voltage and it is equal to the product of magnetic induction ( $B$ ), distance between electrodes ( $L$ ) and flow velocity ( $v$ ) [1].

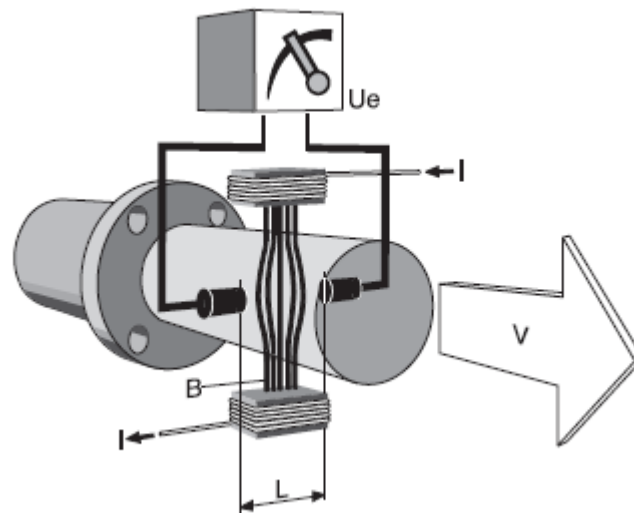


Figure 1. Working Principle of MFM

(Ref: Figure2.27 from M.S. thesis of Veda Duman,2010)

#### WATER METER: (TYPICAL MULTIJET FLOW METER)

The multi-jet fluid flow meter shows the total volume of fluid that goes through it.

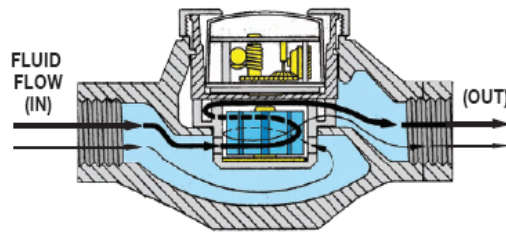


Figure 2. Multi-jet Flow meter

(Ref: Figure2.25b from M.S. thesis of Veda Duman)

Multi-jet flow meters are very accurate in small sizes. They have an impeller which is placed horizontally on a vertical shaft. They use multiple parts surrounding an internal chamber, to create a jet of water against an impeller (Figure 2). Rotation speed of the impeller is proportional to the flow velocity. Multi-jet meters generally have bronze alloy bodies and outer casings, with internal measuring parts made from thermoplastics and stainless steel. Multi-jet meters are very accurate in low flow rates and they provide long-term flow measurement.

### **EXPERIMENTAL PROCEDURE**

#### **NOTE:**

- Before the experiment, read the “WARNINGS” at the last page, carefully.
- Valve numbers are shown on Figure 3.

#### **Part 1: Familiarization with the motor control options**

1. Turn the control key to position “1” on the fuse box, it is behind the setup. (If LEDs on the box do not light then ask your assistant to check the plug.)
2. Plug the USB connection to the computer.
3. Open the controller program “nukleerflow.exe” (it is on the desktop)
4. First run (MANUAL CONTROL : MAGNETIC FLOW METER LINE):
  - a. Valves 1,3,8 : full open
  - b. Valves 2,4,5,6,7: full closed
  - c. Motor control : Manual

- d. % rpm: 50
  - e. Run time: 600 seconds
  - f. Push the start button
  - g. After the 300 seconds read and record the volumetric flow rate from the display on the MAGNETIC FLOW METER
  - h. Read and record the volumetric flow rate from display IN1 on program window. Compare it with the previous step (step g).
5. Second run (CONSTANT VOLUMETRIC FLOW RATE: MAGNETIC FLOW METER LINE)
- a. Valves positions remains as in the step 4.
  - b. Motor control: Constant Q
  - c.  $Q=2.0$  l/s
  - d. Run time: 600 seconds
  - e. At the "LOGGER" tab on program window enter the data rate as 1 data/second
  - f. Push the start button
  - g. Observe the flow rate (IN1) on LOGGER and discuss the behavior.
  - h. Record this data to an excel file and plot the time vs volumetric flow rate graph and discuss by yourself on your report.**

**Question 1: Is this setup running for a constant Q?**

6. Third run (CONSTANT PUMP OUTLET PRESSURE: MAGNETIC FLOWRATE)
- a. Valves positions remains as in the step 4.
  - b. Motor control: Constant P
  - c.  $P= 2$ bars
  - d. Run time: 600 seconds
  - e. At the "LOGGER" tab on program window enter the data rate as 1 data/second

- f. Push the start button
- g. Observe the pump outlet pressure (IN2) on LOGGER and discuss the behavior.
- h. Record this data to an excel file and plot the time vs pump outlet pressure graph and discuss by yourself on your report.**

**Question 2: Is this setup running for a constant P?**

**Part 2: Flow rate measurement**

**1. MAGNETIC FLOW METER:**

- a. Valves positions remains as in the step 4.
- b. Motor control: Manual
- c. Run time: 600 seconds
- d. Push the start button
- e. Observe the flow rate on IN1 display on the MAIN WINDOW
- f. Fill the table below with at least 300 second runs:

| RPM(%) | Volumetric flow rate (l/s) |
|--------|----------------------------|
| 25     |                            |
| 30     |                            |
| 35     |                            |
| 40     |                            |
| 45     |                            |

**In the report:**

- 1. Plot the RPM vs Volumetric flow rate graph.**
- 2. Plot the RPM vs Average velocity in the pipe (m/s) graph.**  
**(Pipe diameter=4cm)**

### 3. Discuss your results

#### 2. WATER METER:

- a. Valves 2,4,8 : full open
- b. Valves 1,3,5,6,7: full closed
- c. Motor control: Manual
- d. Run time: 600 seconds
- e. Push the start button
- f. Observe the flow rate on IN8 display on the MAIN WINDOW
- g. Record your measurement and time and fill the table below :

| RPM(%) | First measurement |      | Second measurement |      | Volumetric flow rate (l/s) |
|--------|-------------------|------|--------------------|------|----------------------------|
|        | IN8               | time | IN8                | time |                            |
| 25     |                   |      |                    |      |                            |
| 30     |                   |      |                    |      |                            |
| 35     |                   |      |                    |      |                            |
| 40     |                   |      |                    |      |                            |
| 45     |                   |      |                    |      |                            |

#### In the report:

1. Plot the RPM vs volumetric flow rate graph.
2. Discuss your results

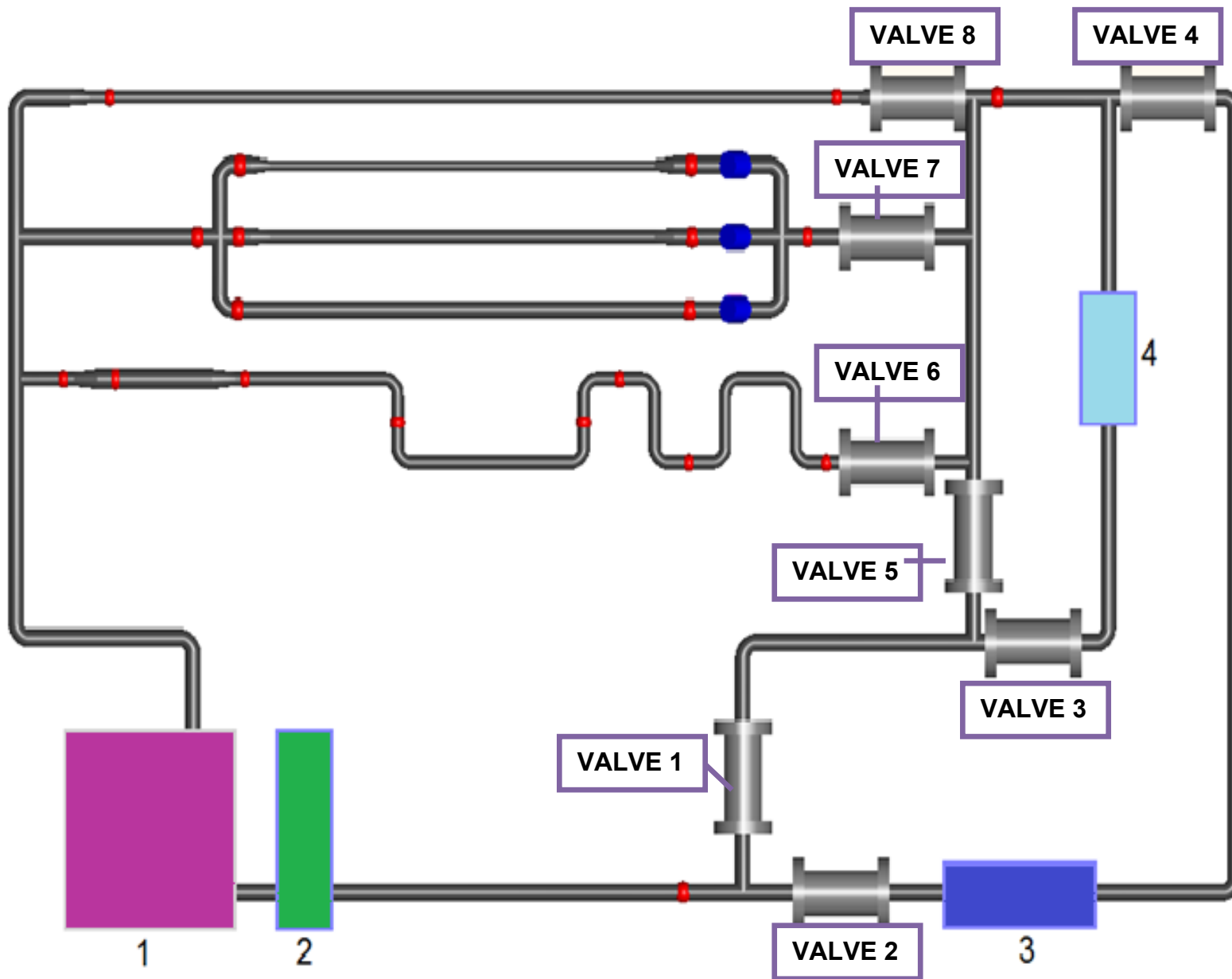


Figure 3. Experimental Setup

**WARNINGS:**

**!DO NOT touch the three- phase plug at any time of the experiment.**

**! DO NOT close the “nukleerflow.exe” at any time of the experiment.**

**!DO NOT change calibration constants on the “nukleerflow.exe”.**

**!!IF THE CONSTANT Q MOTOR CONTROL OPTION IS USED, DO NOT close the valves 1 and 3.**

**!!AT THE END OF THE EXPERIMENT:**

- **Stop the pump**
- **Exit the “nukleerflow.exe”. After pushing the exit button, wait until program to close itself. It takes a few minutes.**
- **Unplug the USB connection**
- **Switch off the key on the fuse box.**

**REFERENCES:**

1. “A Comprehensive Experimental and Computational Analysis of Pressure Drop in Pipes and Fittings”, Veda Duman, M.S. Thesis, 2010



## **D.2. MANUAL FOR EXPERIMENT #2**

### **THERMAL HYDRAULICS LABORATORY**

#### **EXPERIMENT #2**

#### **FRICITION LOSS FOR FLOW IN A STRAIGHT PIPE**

##### **PURPOSE:**

The aims of this experiment are:

- To measure pressure drop through a straight pipe by using DP cells.
- To obtain the friction factors of different materials
- To investigate the Reynolds number and roughness dependence of friction factor

##### **INTRODUCTION**

This experiments aims to obtain the friction factors for the copper, stainless steel, and PVC pipes by measuring pressure drop through a straight pipe. Differential pressure measurement devices, DP cells, will be used for the measurements.

Experiment #2 includes measurements of pressure drop to obtain friction coefficients. Friction factor of each pipe is going to be investigated for various volumetric flow rates. The Reynolds number dependency of the friction is going to be observed. In addition, by using pipes, made by different materials, roughness dependency of the friction factor is also going to be observed and discussed. Finally, a chart which shows the friction factors as a function of Reynolds number and roughness is going to be obtained (Similar to Moody Chart [1]).

##### **THEORY [1]**

While fluid is flowing through a pipe, some forces become effective on the fluid. The major forces acting on the fluid are pressure forces, forces acted by system components, gravitational force and viscous friction forces. One of the most important events occurring because of fluid motion into the pipe is pressure drop across the pipe. Pressure drop across the pipe strongly depends on the friction between fluid

and the pipe wall. The frictional resistance to which fluid is subjected as it flows along a pipe results in a continuous loss of energy or total head of the fluid. This information is formulated with Darcy-Weisbach formula (Eq.1) which was demonstrated by Weisbach and Darcy introduced the term relative roughness for friction determination later.

$$h_f = f \frac{L V^2}{D 2g} \quad (\text{Eq.1})$$

Here,  $h_f$  is the loss of head due to friction, L and D are the length and internal diameter of the pipe and V the mean velocity of flow. The factor  $f$  is the friction factor and it is a dimensionless quantity. It depends on the Reynolds number and relative roughness which is defined as roughness to the diameter of the pipe ratio.

In the early 1880's, Osborne Reynolds (1842-1912) run a number of experiments to investigate the laws of resistance in pipes. He observed the changes in flow according to the changes in fluid velocity. He concluded his studies by introducing the flow type determination laws which are based on the critical values of a number called Reynolds Number (Eq.2).

$$\text{Re} = \frac{\rho V_{\text{avg}} D}{\mu} \quad (\text{Eq.2})$$

In this equation,  $\rho$ ,  $V_{\text{avg}}$ , D and  $\mu$  are the density of fluid, average velocity of fluid in the pipe, circular pipe diameter and dynamic viscosity of fluid, respectively.

The object of this experiment is to estimate the friction factor for pipes which made by different materials. The aim of using the different material made pipes is to investigate the friction factor values for various relative roughness values. Darcy-Weisbach equation is used to determine friction factor. For this reason, pressure drop across the pipe is going to be measured and head loss due to friction is obtained. The other essential information for investigation of flow is average velocity of fluid flows through the pipe and it is measured with the magnetic flow meter.

**Table1.** Technical data for pipes:

| <b><u>Pipe</u></b>            | <b><u>Roughness</u></b> | <b><u>Length</u></b> | <b><u>Diameter</u></b> |
|-------------------------------|-------------------------|----------------------|------------------------|
| <b><u>Stainless steel</u></b> | 45 $\mu\text{m}$        | 1.85 m               | 3.2 cm                 |
| <b><u>Copper</u></b>          | 15 $\mu\text{m}$        | 1.85 m               | 3.2 cm                 |
| <b><u>PVC</u></b>             | 1.5 $\mu\text{m}$       | 1.85 m               | 3.2 cm                 |

### **EXPERIMENTAL PROCEDURE**

#### **NOTE:**

- Before the experiment, read the “WARNINGS” at the last page, carefully.
  - Valve numbers are shown on Figure 1.
7. Turn the control key to position “1” on the fuse box, it is behind the setup. (If LEDs on the box do not light then ask your assistant to check the plug.)
  8. Plug the USB connection to the computer.
  9. Open the controller program “nukleerflow.exe” (it is on the desktop)
  10. Valves 1,5,8 : full open
  11. Valves 2,3,4,6,7: full closed
  12. Dp1 is used for measurements: Put HIGH arm to the point which will be at the higher pressure (pipe inlet), and LOW arm to the lower pressure point (pipe outlet)
  13. Motor control : Manual
  14. Run time: 600 seconds
  15. Push the start button
  16. After the 300 seconds read and record the pressure drop from the display IN4 on program window. Fill the table below:

17. Fill the table below for steel pipe:

| %rpm [1] | Q(l/s) [1] | V(m/s) | Re | $\Delta P$ (mbar) | f |
|----------|------------|--------|----|-------------------|---|
| 30       | 1.95       |        |    |                   |   |
| 34       | 2.23       |        |    |                   |   |
| 38       | 2.5        |        |    |                   |   |
| 42       | 2.79       |        |    |                   |   |
| 46       | 3.06       |        |    |                   |   |
| 50       | 3.34       |        |    |                   |   |

**In the report:**

**a. Plot the graph of f vs Reynolds number for the stainless steel pipe**

**b. Discuss your results**

18. Replace the stainless steel pipe with copper pipe and repeat the procedure steps from 7 to 10.

19. Fill the table for the copper pipe:

| %rpm [1] | Q(l/s) [1] | V(m/s) | Re | $\Delta P$ (mbar) | f |
|----------|------------|--------|----|-------------------|---|
| 30       | 1.95       |        |    |                   |   |
| 34       | 2.23       |        |    |                   |   |
| 38       | 2.5        |        |    |                   |   |
| 42       | 2.79       |        |    |                   |   |
| 46       | 3.06       |        |    |                   |   |
| 50       | 3.34       |        |    |                   |   |

**In the report:**

- a. Plot the graph of  $f$  vs Reynolds number for the copper pipe
- b. Discuss your results.

20. Replace the copper pipe with PVC pipe and repeat the procedure steps from 7 to 10.

21. Fill the table for the PVC pipe:

| %rpm [1] | Q(l/s) [1] | V(m/s) | Re | $\Delta P$ (mbar) | f |
|----------|------------|--------|----|-------------------|---|
| 30       | 1.95       |        |    |                   |   |
| 34       | 2.23       |        |    |                   |   |
| 38       | 2.5        |        |    |                   |   |
| 42       | 2.79       |        |    |                   |   |
| 46       | 3.06       |        |    |                   |   |
| 50       | 3.34       |        |    |                   |   |

**In the report:**

1. Plot the graph of  $f$  vs Reynolds number for the PVC pipe
2. Discuss your results.
3. Compare the friction factors of the stainless steel, copper and PVC pipes and discuss the effect of roughness on friction factor.



**WARNINGS:**

**!DO NOT touch the three- phase plug at any time of the experiment.**

**! DO NOT close the “nukleerflow.exe” at any time of the experiment.**

**!DO NOT change calibration constants on the “nukleerflow.exe”.**

**!!IF THE CONSTANT Q MOTOR CONTROL OPTION IS USED, DO NOT close the valves 1 and 3.**

**!!AT THE END OF THE EXPERIMENT:**

- **Stop the pump**
- **Exit the “nukleerflow.exe”. After pushing the exit button, wait until program to close itself. It takes a few minutes.**
- **Unplug the USB connection**
- **Switch off the key on the fuse box.**

**REFERENCES:**

1. “A Comprehensive Experimental and Computational Analysis of Pressure Drop in Pipes and Fittings”, Veda Duman, M.S. Thesis, 2010

## **D.3. MANUAL FOR EXPERIMENT #3**

### **THERMAL HYDRAULICS LABORATORY**

#### **EXPERIMENT #3**

#### **DETERMINATION OF HYDRAULIC LOSS COEFFICIENTS OF FITTINGS**

##### **PURPOSE**

The aims of this experiment are:

- To measure pressure drop through fittings
- To obtain the hydraulic loss coefficients of fittings
- To investigate the effect of the Reynolds number on the hydraulic loss coefficients of fittings

##### **INTRODUCTION**

This experiment aims to obtain the hydraulic loss coefficients of fittings by measuring pressure drop through the fittings. Differential pressure measurement devices, DP cells, will be used for measurements.

Experiment #3 includes measurements of pressure drop to obtain hydraulic loss coefficients. Hydraulic loss coefficient of each fitting is going to be investigated for the various volumetric flow rates. The fittings that will be examined in this experiment are:

- 90 degree elbow (up)
- 90 degree elbow (down)
- S-shape turn
- Gradual enlargement in flow area
- Gate valve

Measurements will be performed for each fitting and behavior of their hydraulic loss coefficient versus Reynolds number will be observed.



## **THEORY[1]**

One of the basic and most common problems in fluid mechanics is the estimation of pressure loss. For more accurate estimations, components of a flow circuit must be analyzed with detailed experiments. One of the most essential information for pressure loss estimations is hydraulic loss coefficients of the components. To generalize the hydraulic loss coefficient of the each component, huge numbers of experiments has been performed. Today, the experiments for estimation of hydraulic loss coefficients are still performed in the industrial applications to obtain more accurate results which are required to provide the persistence of the operations rather than using catalogued values.

For an incompressible fluid flowing through a pipe, the following equations, which are derived from mass balance equation (Eq.1) and momentum balance equation (Eq.2), are applied.

$$Q = V_1 A_1 = V_2 A_2 \quad (\text{Eq.1})$$

$$z_1 + \frac{p_1}{\gamma} + \frac{V_1^2}{2g} = z_2 + \frac{p_2}{\gamma} + \frac{V_2^2}{2g} + h_f + h_l \quad (\text{Eq.2})$$

Eq.1 is called as continuity equation while Eq.2 is known as Bernoulli's Equation.

In Eq.2, total pressure loss on the circuit has number of agents. The contributors of the pressure loss in a pipe circuit can be categorized in three groups:

- a) That is created by the effect of viscous resistances throughout the total length of the circuit. (Experiment #1)
- b) That is created by the local effects such as bends, valves and enlargement in flow area.
- c) That is created by the effect of gravity.

Hydraulic loss coefficient of bends:

The head loss due to the bend is given by the following expression:

$$h_b = K_{bend} \frac{V^2}{2g} \quad (\text{Eq.3})$$

$K_{bend}$  is the hydraulic loss coefficient which depends on the bend radius/ pipe radius ratio and angle of the bend. It should be noted that the head loss defined with Eq.3 does not only includes effect of turning but also effect of friction loss.

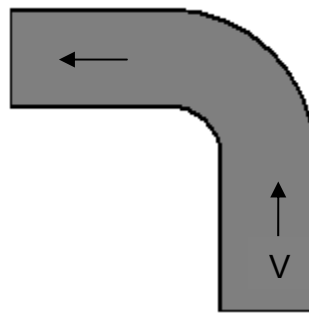


Figure 1. Flow in 90 degree elbow (up) [1]

Hydraulic loss coefficient of gate valves:

The head loss due to the valve is given by the following expression:

$$h_v = K_{valve} \frac{V^2}{2g} \quad (\text{Eq.3})$$

$K_{valve}$  is the hydraulic loss coefficient which depends on type of valve and fraction of opening.

Pressure drop on enlarging pipes and expansion coefficient determination:

The pressure difference due to the slowly enlarging flow area is given by the following expression:

$$\Delta p = K_{exp} \frac{V^2}{2} \rho \quad (\text{Eq.4})$$

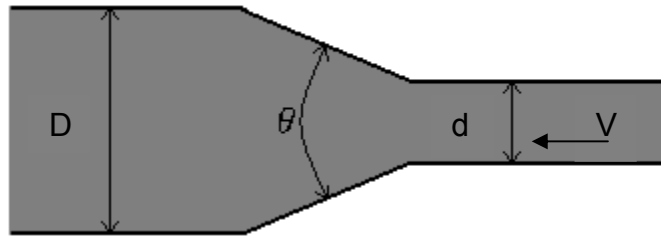


Figure 2. Flow in slowly enlarging pipe [1]

In order to maintain the constant volumetric flowrate an increase in cross sectional area of the pipe (or pipe diameter) means lower velocity according to the Eq.1. As  $A_2$  increases,  $v_2$  must be lower to maintain the same volumetric flowrate. This means that in the large diameter pipe the volume of fluid is moving more slowly and has less kinetic energy than it will have when it gets into the small diameter pipe. [1]

Pressure change in a straight pipe is related to the density of the fluid and velocity of the fluid in associated flow area. Therefore, with using Eq.2, the pressure difference can be written as follows:

$$P_2 - P_1 = \frac{v_1^2 - v_2^2}{2\rho} \quad (\text{Eq.5})$$

If there is an increase in pipe diameter then  $A_2 > A_1$  and  $v_1 > v_2$ . Eventually, the change in pressure is positive [1].

### **EXPERIMENTAL PROCEDURE**

#### **NOTE:**

- Before the experiment, read the “WARNINGS” at the last page, carefully.
- Valve and measurement point numbers are shown on Figure 3.

22. Turn the control key to position “1” on the fuse box, it is behind the setup. (If LEDs on the box do not light then ask your assistant to check the plug.)

23. Plug the USB connection to the computer.
24. Open the controller program “nukleerflow.exe” (it is on the desktop)
25. Valves 1,5,6: full open
26. Valves 2,3,4,7,8: full closed

**Part 1. Hydraulic loss coefficient of a 90 degree elbow (down)**

1. Dp3 is used for measurements: Put HIGH arm to the point which will be at the higher pressure (measurement point 13) and LOW arm to the lower pressure point (measurement point 14).
2. Motor control : Manual
3. Run time: 600 seconds
4. Push the start button
5. After the 300 seconds read and record the pressure drop from the display IN6 on program window. Fill the table below:

| %rpm [1] | Q(l/s) [1] | V(m/s) | Re | $\Delta P$ (mbar) | K |
|----------|------------|--------|----|-------------------|---|
| 30       | 1.95       |        |    |                   |   |
| 34       | 2.23       |        |    |                   |   |
| 38       | 2.5        |        |    |                   |   |
| 42       | 2.79       |        |    |                   |   |
| 46       | 3.06       |        |    |                   |   |
| 50       | 3.34       |        |    |                   |   |

**In the report:**

- a. Plot the graph of K vs Reynolds number
- b. Discuss your results

**Part 2. Hydraulic loss coefficient of a 90 degree elbow (up)**

1. Dp3 is used for measurements: Put HIGH arm to the point which will be at the higher pressure (measurement point 15) and LOW arm to the lower pressure point (measurement point 16).
2. Repeat the same procedure with the previous measurement.
3. Fill the table below:

| %rpm [1] | Q(l/s) [1] | V(m/s) | Re | $\Delta P$ (mbar) | K |
|----------|------------|--------|----|-------------------|---|
| 30       | 1.95       |        |    |                   |   |
| 34       | 2.23       |        |    |                   |   |
| 38       | 2.5        |        |    |                   |   |
| 42       | 2.79       |        |    |                   |   |
| 46       | 3.06       |        |    |                   |   |
| 50       | 3.34       |        |    |                   |   |

**In the report:**

- a. Plot the graph of K vs Reynolds number
- b. Discuss your results.

**Part 3. Hydraulic loss coefficient of S-shape turn**

1. Dp3 is used for measurements: Put HIGH arm to the point which will be at the higher pressure (measurement point 12) and LOW arm to the lower pressure point (measurement point 13).
2. Repeat the same procedure with the previous measurement.

3. Fill the table below:

| %rpm [1] | Q(l/s) [1] | V(m/s) | Re | $\Delta P$ (mbar) | K |
|----------|------------|--------|----|-------------------|---|
| 30       | 1.95       |        |    |                   |   |
| 34       | 2.23       |        |    |                   |   |
| 38       | 2.5        |        |    |                   |   |
| 42       | 2.79       |        |    |                   |   |
| 46       | 3.06       |        |    |                   |   |
| 50       | 3.34       |        |    |                   |   |

**In the report:**

- a. Plot the graph of K vs Reynolds number.
- b. Discuss your results.

**Part 4. Expansion coefficient for Gradual Enlargement in Flow Area (60 degree)**

1. Dp2 is used for measurements: Put HIGH arm to the point which will be at the higher pressure (measurement point 16) and LOW arm to the lower pressure point (measurement point 17).
2. Motor control : Manual
3. Run time: 600 seconds
4. Push the start button
5. After the 300 seconds read and record the pressure drop from the display IN5 on program window. Fill the table below:

| %rpm [1] | Q(l/s) [1] | V(m/s) | Re | $\Delta P$ (mbar) | K(exp) |
|----------|------------|--------|----|-------------------|--------|
| 50       | 3.34       |        |    |                   |        |
| 52       | 3.45       |        |    |                   |        |
| 55       | 3.68       |        |    |                   |        |
| 57       | 3.8        |        |    |                   |        |
| 60       | 4.03       |        |    |                   |        |

**In the report:**

- a. Plot the graph of  $K_{exp}$  vs Reynolds number.
- b. Discuss your results.

**Part 4. Hydraulic Loss Coefficient of a Gate Valve**

1. Valves 2,4,8: full open
2. Valves 1,3,5,6,7: full closed
3. Dp2 is used for measurements: Put HIGH arm to the point which will be at the higher pressure (measurement point 19) and LOW arm to the lower pressure point (measurement point 1).
4. Motor control : Manual
5. Run time: 600 seconds
6. Push the start button
7. After the 300 seconds read and record the pressure drop from the display IN5 on program window. Fill the table below:

| %rpm [1] | Q(l/s) [1] | V(m/s) | Re | $\Delta P$ (mbar) | K |
|----------|------------|--------|----|-------------------|---|
| 30       | 1.95       |        |    |                   |   |
| 34       | 2.23       |        |    |                   |   |
| 38       | 2.5        |        |    |                   |   |
| 42       | 2.79       |        |    |                   |   |
| 46       | 3.06       |        |    |                   |   |
| 50       | 3.34       |        |    |                   |   |

**In the report:**

- a. Plot the graph of K vs Reynolds number.
- b. Discuss your results.

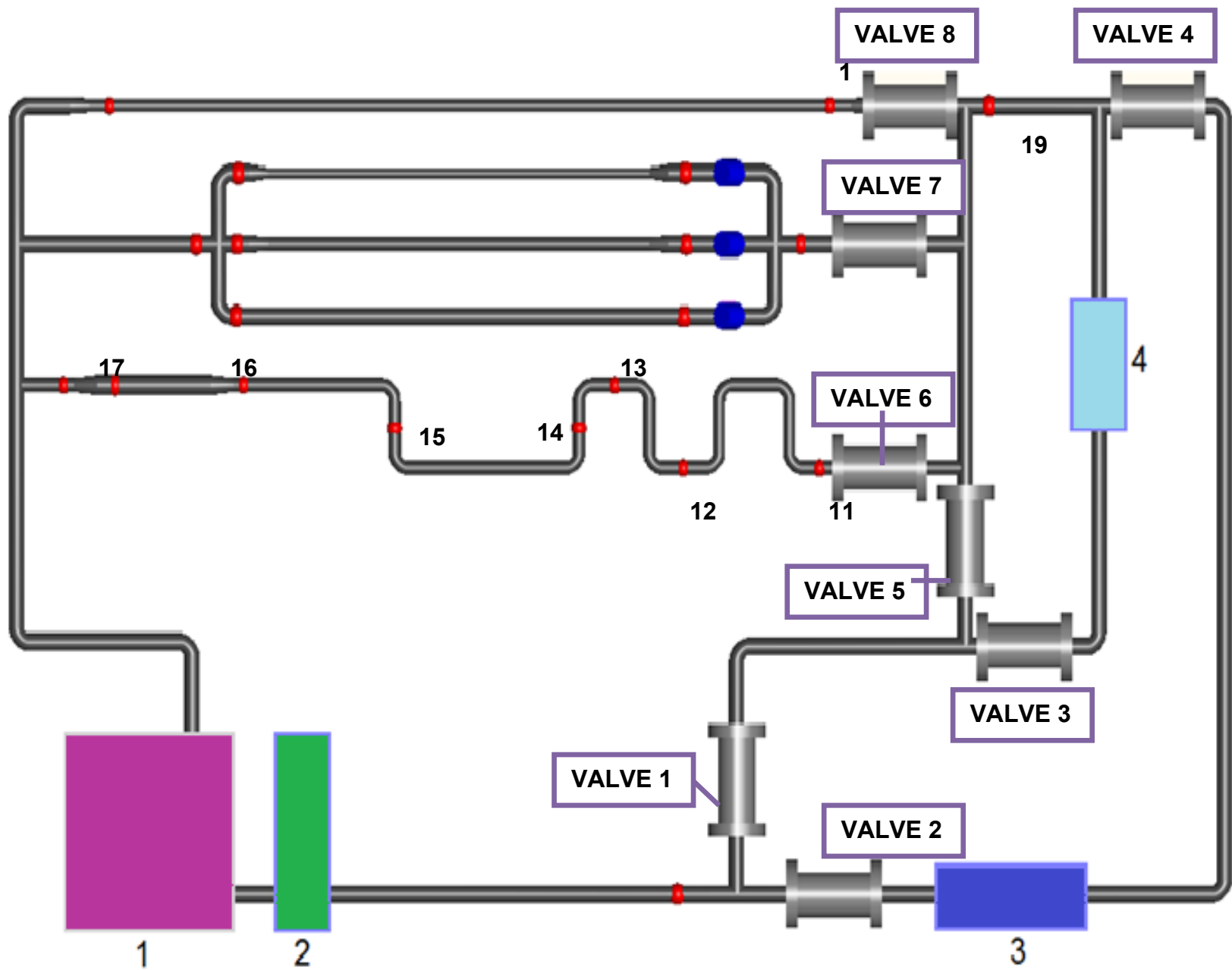


Figure 3. Experimental Setup



**WARNINGS:**

**!DO NOT touch the three- phase plug at any time of the experiment.**

**! DO NOT close the “nukleerflow.exe” at any time of the experiment.**

**!DO NOT change calibration constants on the “nukleerflow.exe”.**

**!IF THE CONSTANT Q MOTOR CONTROL OPTION IS USED, DO NOT close the valves 1 and 3.**

**!!AT THE END OF THE EXPERIMENT:**

- **Stop the pump**
- **Exit the “nukleerflow.exe”. After pushing the exit button, wait until program to close itself. It takes a few minutes.**
- **Unplug the USB connection**
- **Switch off the key on the fuse box.**

**REFERENCES:**

1. “A Comprehensive Experimental and Computational Analysis of Pressure Drop in Pipes and Fittings”, Veda Duman, M.S. Thesis, 2010

## **D.4. MANUAL FOR EXPERIMENT #4**

### **THERMAL HYDRAULICS LABORATORY**

#### **EXPERIMENT #4**

#### **PARALLEL FLOW**

##### **PURPOSE**

The aims of this experiment are:

- To analyze the parallel flow
- To observe the flow separation at the branch
- To investigate the effect of gravity and pipe diameter on flow separation

##### **INTRODUCTION**

This experiment aims to observe parallel flow in branching horizontally parallel pipes. Each pipe has different diameters and elevation. Globe valves are placed on each branch to manipulate the flow separation direct the flow to make different observations.

Experiment #4 includes measurements of pressure drop through each parallel pipe. Also overall pressure drop will be measured through the section. Pressure drop through each pipe and on the branching section are going to be observed and flow separation ratios are going to be investigated.

First of all, after pressure drop on each pipe is measured, they are used to obtain the volumetric flow rate values on each pipe. By this way, the total volumetric flow rate is going to be found and compared with the total volumetric flow rate which is measured by the magnetic flow meter. In addition, fractional volumetric flow rate values on each pipe will be determined and separation of the flow will be observed.

In conclusion, the effects of difference in pipe diameters and gravity on flow separation will be examined and discussed.

## THEORY [1]

The flow through parallel pipes is a common application among flow systems. The parallel flow can be defined as the flow which divides and subsequently merges again when three or more pipes are connected as shown in Figure 1.

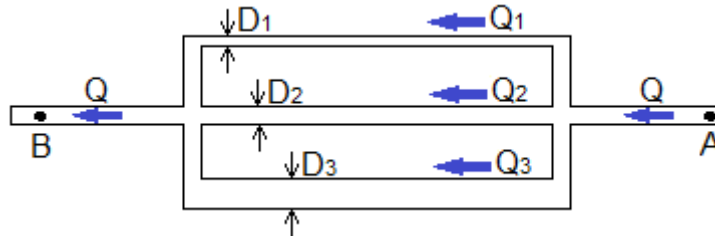


Figure 1. Flow through parallel pipes [1]

As shown on the figure, the sum of volumetric flow rates at each parallel line is equal to the total volumetric flow rate. Therefore continuity equation for this flow can be represented with Equation 1.

$$Q_A = Q_B = Q_1 + Q_2 + Q_3 \quad (\text{Eq.1})$$

The separation of volumetric flow rate depends on the flow area of the each parallel pipe and elevation of pipes because of the effect of gravity.

The steady state energy equation (Bernoulli's equation), between points A and B, may be rewritten as given below;

$$\frac{p_A}{\gamma} + \frac{V_A^2}{2g} + z_A - h_f = \frac{p_B}{\gamma} + \frac{V_B^2}{2g} + z_B \quad (\text{Eq.2.})$$

The head loss due to friction and pipe fitting elements are included in  $h_f$ .

## **EXPERIMENTAL PROCEDURE**

### **NOTE:**

- Before the experiment, read the “WARNINGS” at the last page, carefully.
  - Valve and measurement point numbers are shown on Figure 2.
27. Turn the control key to position “1” on the fuse box, it is behind the setup. (If LEDs on the box do not light then ask your assistant to check the plug.)
28. Plug the USB connection to the computer.
29. Open the controller program “nukleerflow.exe” (it is on the desktop)
30. Valves 1,5,7: full open
31. Valves 2,3,4,6,8: full closed

### **Part 1. Natural separation 1:**

6. Globe valve 2 is full closed while others are full opened.
7. DP 1, DP 2 and DP 3 are used for measurements:

|                    | DP 1 | DP 2 | DP 3 |
|--------------------|------|------|------|
| Branch             | 1    | All  | 3    |
| Measurement Points | 4-5  | 3-10 | 8-9  |

8. Motor control : Manual
9. Run time: 600 seconds
10. Push the start button
11. After the 300 seconds read and record the pressure drop values. Fill the table below:

| %rpm [1] | Q(l/s) [1] | $\Delta P$ 1 (mbar) | $\Delta P$ 3 (mbar) | $\Delta P$ 2(mbar) | $Q_t$ |
|----------|------------|---------------------|---------------------|--------------------|-------|
| 30       | 1.95       |                     |                     |                    |       |
| 34       | 2.23       |                     |                     |                    |       |
| 38       | 2.5        |                     |                     |                    |       |
| 42       | 2.79       |                     |                     |                    |       |
| 46       | 3.06       |                     |                     |                    |       |
| 50       | 3.34       |                     |                     |                    |       |

**In the report:**

**a. Fill the table below:**

| Q(l/s) [1] | Q 1 (mbar) | Q 3 (mbar) | $Q_t$ | F1 (Q1/ $Q_t$ ) | F3 (Q3/ $Q_t$ ) |
|------------|------------|------------|-------|-----------------|-----------------|
| 1.95       |            |            |       |                 |                 |
| 2.23       |            |            |       |                 |                 |
| 2.5        |            |            |       |                 |                 |
| 2.79       |            |            |       |                 |                 |
| 3.06       |            |            |       |                 |                 |
| 3.34       |            |            |       |                 |                 |

**b. Plot the graph of Q vs  $Q_{total}$**

**c. Plot the graph of F1 and F3 vs inlet velocity**

**d. Discuss your results. Which branch that flow is strongly prefer?**

**What are the reasons of that?**

**Part 2. Natural separation 2:**

1. Globe valve 3 is full closed while others are full opened.
2. DP 1, DP 2 and DP 3 are used for measurements:

|                    | DP 1 | DP 2 | DP 3 |
|--------------------|------|------|------|
| Branch             | 1    | All  | 2    |
| Measurement Points | 4-5  | 3-10 | 6-7  |

3. Motor control : Manual
4. Run time: 600 seconds
5. Push the start button
6. After the 300 seconds read and record the pressure drop values. Fill the table below:

| %rpm [1] | Q(l/s) [1] | $\Delta P$ 1 (mbar) | $\Delta P$ 3 (mbar) | $\Delta P$ 2(mbar) | $Q_t$ |
|----------|------------|---------------------|---------------------|--------------------|-------|
| 30       | 1.95       |                     |                     |                    |       |
| 34       | 2.23       |                     |                     |                    |       |
| 38       | 2.5        |                     |                     |                    |       |
| 42       | 2.79       |                     |                     |                    |       |
| 46       | 3.06       |                     |                     |                    |       |
| 50       | 3.34       |                     |                     |                    |       |

**In the report:**

**a. Fill the table below:**

| Q (l/s) [1] | Q <sub>1</sub> (mbar) | Q <sub>3</sub> (mbar) | Q <sub>t</sub> | F1 (Q <sub>1</sub> / Q <sub>t</sub> ) | F2 (Q <sub>2</sub> / Q <sub>t</sub> ) |
|-------------|-----------------------|-----------------------|----------------|---------------------------------------|---------------------------------------|
| 1.95        |                       |                       |                |                                       |                                       |
| 2.23        |                       |                       |                |                                       |                                       |
| 2.5         |                       |                       |                |                                       |                                       |
| 2.79        |                       |                       |                |                                       |                                       |
| 3.06        |                       |                       |                |                                       |                                       |
| 3.34        |                       |                       |                |                                       |                                       |

**c. Plot the graph of Q vs Q<sub>total</sub>**

**d. Plot the graph of F1 and F3 vs inlet velocity**

**e. Discuss your results. Which branch that flow is strongly prefer? Explain why.**

**Part 2. Effect of globe valves:**

1. Globe valve 3 is full closed while globe valve 1 is full opened and globe valve 2 is fraction of opening 0.6.
2. Dp1, DP2 and DP3 are used for measurements:

|                    | DP 1 | DP 2 | DP 3 |
|--------------------|------|------|------|
| Branch             | 1    | All  | 2    |
| Measurement Points | 4-5  | 3-10 | 6-7  |

3. Motor control : Manual
4. Run time: 600 seconds
5. Push the start button

6. After the 300 seconds read and record the pressure drop values. Fill the table below:

| %rpm [1] | Q(l/s) [1] | $\Delta P$ 1<br>(mbar) | $\Delta P$ 3<br>(mbar) | $\Delta P$ 2(mbar) | $Q_t$ |
|----------|------------|------------------------|------------------------|--------------------|-------|
| 30       | 1.95       |                        |                        |                    |       |
| 34       | 2.23       |                        |                        |                    |       |
| 38       | 2.5        |                        |                        |                    |       |
| 42       | 2.79       |                        |                        |                    |       |
| 46       | 3.06       |                        |                        |                    |       |
| 50       | 3.34       |                        |                        |                    |       |

**In the report:**

a. Fill the table below:

| Q(l/s) [1] | Q 1<br>(mbar) | Q 3<br>(mbar) | $Q_t$ | F1<br>( $Q_1 / Q_t$ ) | F2<br>( $Q_2 / Q_t$ ) |
|------------|---------------|---------------|-------|-----------------------|-----------------------|
| 1.95       |               |               |       |                       |                       |
| 2.23       |               |               |       |                       |                       |
| 2.5        |               |               |       |                       |                       |
| 2.79       |               |               |       |                       |                       |
| 3.06       |               |               |       |                       |                       |
| 3.34       |               |               |       |                       |                       |

- b. Plot the graph of Q vs  $Q_{total}$
- c. Plot the graph of F1 and F3 vs inlet velocity
- d. Compare the results with the results of the previous part.
- e. Discuss your results. Which branch that flow is strongly prefer? Explain why.



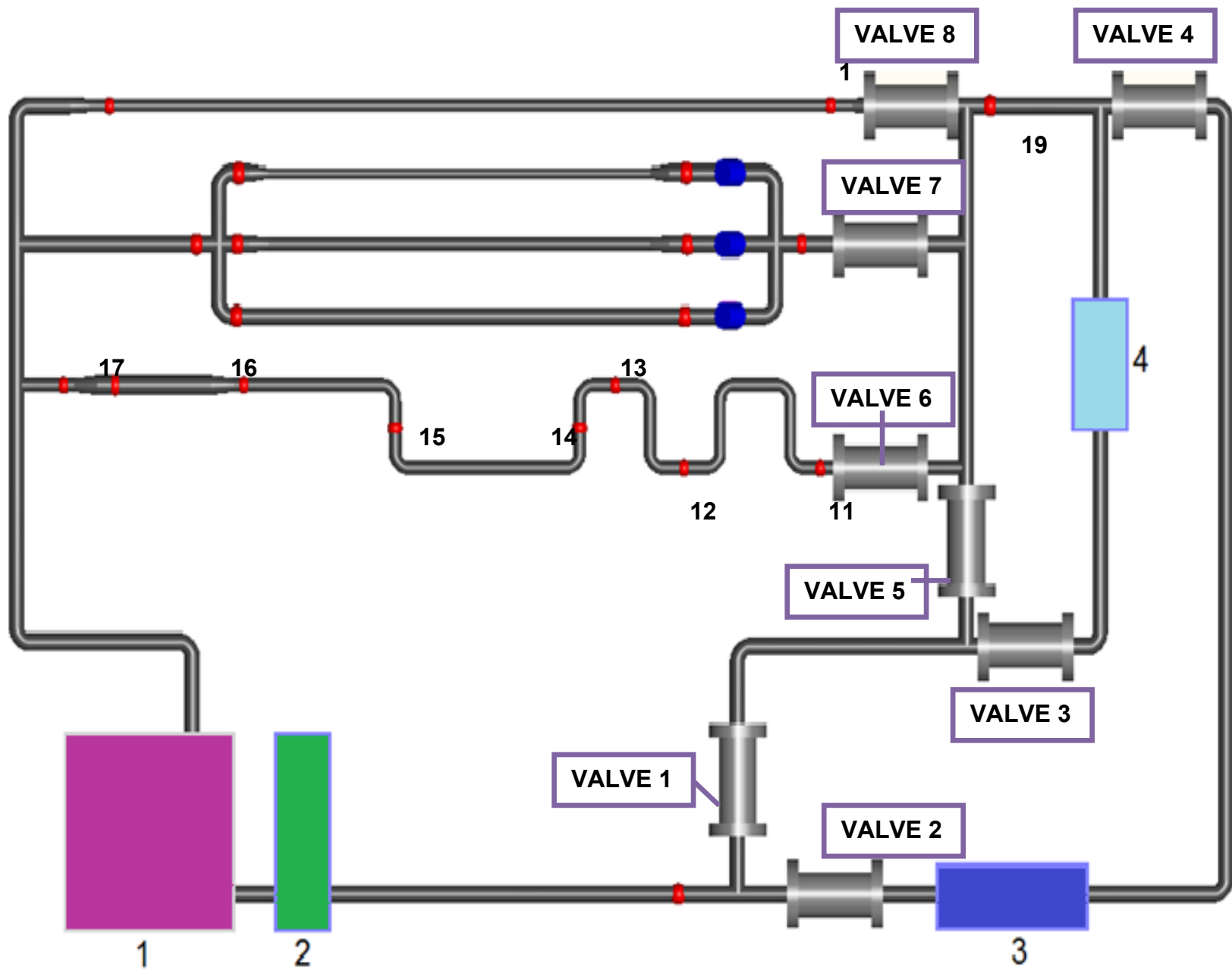


Figure 2. Experimental Setup

**WARNINGS:**

**!DO NOT touch the three- phase plug at any time of the experiment.**

**! DO NOT close the “nukleerflow.exe” at any time of the experiment.**

**!DO NOT change calibration constants on the “nukleerflow.exe”.**

**!IF THE CONSTANT Q MOTOR CONTROL OPTION IS USED, DO NOT close the valves 1 and 3.**

**!!AT THE END OF THE EXPERIMENT:**

- **Stop the pump**
- **Exit the “nukleerflow.exe”. After pushing the exit button, wait until program to close itself. It takes a few minutes.**
- **Unplug the USB connection**
- **Switch off the key on the fuse box.**

**REFERENCES:**

1. “A Comprehensive Experimental and Computational Analysis of Pressure Drop in Pipes and Fittings”, Veda Duman, M.S. Thesis, 2010

## **RESUME**

Name & Surname: Veda DUMAN

Birth Place: Ankara

Date of Birth: 21.02.1984

Marital Status: Single

Education & Academic Carrier:

High School, Ankara Atatürk Anatolian High School, 1998-2002

Undergraduate: Hacettepe University, Department of Nuclear Engineering, 2002-2007

Foreign Language: English

Experience:

2007-.... Research & Teaching Assistant at Hacettepe University, Department of Nuclear Engineering